Applied Catalysis B: Environment and Energy 345 (2024) 123663

Contents lists available at ScienceDirect

Applied Catalysis B: Environment and Energy

journal homepage: www.elsevier.com/locate/apcatb

Tandem catalysis for CO_2 conversion to higher alcohols: A review

Yiming He[a,1], Fabian H. Müller[b,1], Regina Palkovits[b,c], Feng Zeng[a,*], Chalachew Mebrahtu[b,*]

[a] State Key Laboratory of Materials-Oriented Chemical Engineering, College of Chemical Engineering, Nanjing Tech University, Nanjing 211816, Jiangsu, China
[b] Institute for Technical and Macromolecular Chemistry, RWTH Aachen University, Worringerweg 2, 52074 Aachen, Germany
[c] Institute for Sustainable Hydrogen Economy, Forschungszentrum Jülich, Am Brainergy Park 1, 52428 Jülich, Germany

ARTICLE INFO

Keywords:
Tandem catalysis
CO_2 conversion
Higher alcohols
Indirect pathways

ABSTRACT

In recent years, due to the substantial emission of CO_2, global warming has become more severe, and there is an urgent need to develop technologies to reduce greenhouse gas CO_2 emissions. Converting CO_2 into higher alcohols is a promising process, as it not only produces valuable chemicals but also utilizes CO_2 as feedstock. Currently, most reported catalytic approaches are based on direct hydrogenation of CO_2 to synthesize higher alcohols. However, the synthesis of higher alcohols involves multiple steps, requiring catalysts with multiple functional sites and their synergistic interactions are crucial. Nevertheless, controlling catalysts at the nanoscale poses challenges, hindering the design of efficient multi-site catalysts. An alternative approach worth considering is to perform a tandem of multiple well-established catalytic reactions (e.g., methanol synthesis, CO_2-Fischer-Tropsch-Synthesis, RWGS, syngas conversion, olefin hydration, etc.) to indirectly achieve the conversion of CO_2 into higher alcohols, instead of direct CO_2 hydrogenation. Therefore, in this review, these alternative strategies of higher alcohols synthesis are discussed, and their potential is evaluated. First, thermodynamic analysis, the selective adjustment strategies, and the current challenges faced for direct CO_2 hydrogenation are introduced. Then, physical integration of multiple catalysts as a feasible strategy to endow the catalyst with multifunctional properties is discussed. Subsequently, several feasible routes of CO_2 conversion into higher alcohols and the advanced catalysts employed for each pathway are summarized. Finally, merits and limitations of the different approaches are provided, emphasizing the great potential the tandem reaction strategy holds for the efficient synthesis of higher alcohols by CO_2 conversion.

1. Introduction

The excessive use of fossil fuels since the beginning of the industrial revolution in the early 19th century has led to steadily increasing anthropological emissions of greenhouse gases, such as carbon dioxide (CO_2). This increase of the atmospheric CO_2-concentration is strongly correlated to the rise of the global average temperature over the last century [1–4]. In order to curb further increases of CO_2 emissions, different countries have proposed different strategies. China, for example, has adopted the so-called "double carbon" strategy, in which the country strives to reach peak CO_2-emissions by 2030 and aims to achieve carbon neutrality by 2060 [5]. Similarly, the European Union strives to reach carbon neutrality by the middle of the 21st century [6, 7]. To mitigate and reduce CO_2 emissions, various methods of CO_2 fixation have attracted wide interest from researchers. This includes, among others, CO_2 capture, storage, and utilization technologies (CCS and CCU, respectively), which play a crucial role in mitigating the greenhouse effect [8]. Here, CO_2 utilization technologies enable the valorization of CO_2 into valuable chemicals while simultaneously reducing CO_2 emissions effectively.

The conversion of CO_2 into valuable chemicals by its hydrogenation has been extensively studied. Until recently, C_1-products such as methane, formic acid, methanol, or carbon monoxide (CO) have been the focal point of CO_2 hydrogenation research [9–12]. However, the focus started to shift towards the synthesis of C_{2+}-products, e.g., higher alcohols (HA), as they provide several advantages over C_1-products. For example, higher alcohols can either directly serve as fuels themselves or can be employed as fuel additives to increase the fuels' octane number and thus improve combustion properties [13,14]. Compared to methanol, ethanol exhibits lower corrosion potential, a lower vapor pressure, better solubility with liquid hydrocarbons, improved water tolerance, and higher overall energy density [15]. Apart from transport sector

* Corresponding authors.
E-mail addresses: zeng@njtech.edu.cn (F. Zeng), asmelash@itmc.rwth-aachen.de (C. Mebrahtu).
[1] These authors have contributed equally to this work.

https://doi.org/10.1016/j.apcatb.2023.123663
Received 27 October 2023; Received in revised form 17 December 2023; Accepted 23 December 2023
Available online 2 January 2024

applications, higher alcohols are widely used as raw materials or intermediates to produce surfactants, solvents, detergents, antiseptics, cosmetics, and pharmaceuticals [16]. Moreover, the low-temperature synthesis of higher alcohols is thermodynamically more favorable than methanol synthesis (MS) due to its lower Gibbs free energy of reaction and a larger equilibrium constant value (Chapter 2, Table 1, entry 3 to 6) [17]. Currently, higher alcohols are produced either by fermentation of corn and sugar cane or by hydration of alkenes.[18–20] While the former sparks ethics-controversies (food vs. fuel), the latter still relies heavily on fossil feedstocks. In addition, synthesis gas (syngas) conversion to higher alcohols and the hydrogenation of acetic acid based on methanol carbonylation to higher alcohols have also been realized in small-scale applications [21–23]. Consequently, the use of CO_2 as an abundant feedstock for higher alcohol synthesis (HAS) represents a very promising approach for replacing fossil fuels and potential food sources in the production of various chemicals.

Currently, the majority of research reports focus on the direct hydrogenation of CO_2 to higher alcohols, i.e., the conversion of CO_2 over a single (possibly multifunctional) catalyst. To achieve high CO_2 conversion and selectivity to higher alcohols, selective catalysts must possess various functionalities such as CO_2 activation, adsorption ability of intermediates, modulation of surface-active species, carbon chain growth, and low selectivity to by-products. In recent years, a wide variety of such catalysts have been developed for the synthesis of higher alcohols from CO_2 hydrogenation [24,25], including noble metal-based [26–32], Mo-based [33–36], Cu-based [37–41], and Co-based [42–47] systems. In this endeavor, various strategies were employed to modulate the product selectivity: (i) strong metal-support interaction (SMSI) on metal oxide supports [46,48–50], (ii) the utilization of highly tunable nano-frameworks such as metal organic frameworks (MOFs), covalent organic frameworks (COFs), or porous organic polymers (POPs)[41, 51–53], (iii) the adjustment of catalyst nanostructures to alter their product selectivity [26,27,44,54,55], or (iv) modification of the catalyst selectivity by adjusting the crystal phases of the oxide support [45,56, 57].

Until now, a multitude of reviews have provided insightful overviews on the current state of research in the direct hydrogenation of CO_2 to higher alcohols [24,25,58,59,60]. However, most of the current catalysts suffer from insufficient CO_2 conversion, poor stability, low selectivity, or yield of higher alcohols. In addition, a deep mechanistic understanding of these catalysts is often scarce due to their complex metal-promoter-support structure. Hence, it's believed that catalyst design for the synthesis of higher alcohols by CO_2 hydrogenation may be simplified by decoupling the complex multi-step reaction mechanism into multiple, well-researched individual reactions [58,61–63]. Generally, the coupling of relatively mature processes such as reverse water gas shift (RWGS)[64–66], CO_2-Fischer-Tropsch-Synthesis (FTS) to olefins [67–70], methanol synthesis [12,71–73], CO_2 hydrogenation to acetic acid [74–76], syngas conversion [77–79], olefins hydration or hydroformylation [80–84], and acetic acid to higher alcohols reaction [84–87], may consolidate the understanding of reaction mechanisms and thus benefit the design of multifunctional materials in the future.

Therefore, in this review, a systematic discussion of the above-mentioned aspects is provided. The review starts by presenting the thermodynamics and first mechanistic insights of HAS from CO_2 hydrogenation. Here, common challenges in HAS such as the suppression of hydrocarbon-formation or sufficient C-C-coupling activity are addressed. Subsequently, an overview of catalyst systems for the direct CO_2 hydrogenation to higher alcohols is provided. This chapter is divided into (i) Rh-based catalysts, (ii) Cu-based catalysts, (iii) Co-based catalysts, and (iv) Mo-based catalysts. Then the review focuses on a multitude of pathways to synthesize HAS via an indirect conversion of CO_2 through the integration of various reactions in series. Here, the basic reactions of a possible tandem catalyst system are introduced before combining them into an integrated process for HAS. The various routes for CO_2-based synthesis of higher alcohols shown in Scheme 1 are therefore the core of this review. In summary, we believe that this review will help to further deepen mechanistic understanding of higher alcohols synthesis as well as inspire the development of novel strategies in future catalyst design.

2. Thermodynamics and mechanistic insights

To overcome the above-mentioned challenges, careful considerations of the thermodynamic equilibrium can provide valuable information.[88–91]. Basic thermodynamic parameters of chemical reactions such as the standard Gibbs free energy change ($\Delta G_{298\ K}$), the standard enthalpy change ($\Delta H_{298\ K}$), and the standard equilibrium constant ($K_{298\ K}$), may lead to guiding suggestions in catalyst design. Jia et al. performed a thorough thermodynamic analysis of the CO_2 hydrogenation to higher alcohols [17]. Table 1 displays the aforementioned thermodynamic parameters for the most important reactions of the process. Accordingly, at 298 K, methane is the thermodynamically favorable product due to its low standard Gibbs free energy change (−113.5 kJ/mol) and the highest reaction equilibrium constant (7.79×10^{19}). Its vast excess over competing reactions such as carbon monoxide (CO) or alcohol formation indicates the irreversibleness of hydrocarbon formation under the present conditions. The prevention of excessive CO_2 reduction to methane is therefore one key challenge and efficient catalysts must hold a high kinetic barrier for CH_4 formation. In our previous study, we found that lowering the temperature, increasing the pressure, and raising the H_2/CO_2 ratio can thermodynamically reduce methane formation [88]. Thermodynamically, lower temperatures inhibit the endothermic formation of carbon monoxide via the RWGS (Entry 2) reaction while alcohols formation favors lower reaction temperatures. Higher pressures generally favor the contractive alcohol formation over the isovolumetric RWGS reaction. Consequently, the key challenge in the formation of higher alcohols is to balance energy-demanding CO_2 activation and C-C-bond coupling against competing reactions e.g., CO_2 methanation, methanol formation, and the RWGS reaction. Based on the above analysis, the greatest challenge is to design catalysts with the ability to simultaneously activate CO_2 and

Table 1
$\Delta G_{298\ K}$, $\Delta H_{298\ K}$, and $K_{298\ K}$ of main reactions in the synthesis of higher alcohols by CO_2 hydrogenation.[17].

Entry	Reaction formula	$\Delta G_{298\ K}$ [a] (kJ/mol)	$\Delta H_{298\ K}$ [b] (kJ/mol)	$K_{298\ K}$ [c]
1	$CO_2 + 4\ H_2 \rightleftharpoons CH_4 + 2\ H_2O$	− 113.5	− 165.0	7.79×10^{19}
2	$CO_2 + H_2 \rightleftharpoons CO + H_2O$	28.6	41.2	9.67×10^{-6}
3	$CO_2 + 3\ H_2 \rightleftharpoons CH_3OH + H_2O$	3.5	− 49.3	2.45×10^{-1}
4	$CO_2 + 3\ H_2 \rightleftharpoons \frac{1}{2}C_2H_5OH + \frac{3}{2}H_2O$	− 32.4	− 86.7	4.70×10^{5}
5	$CO_2 + 3\ H_2 \rightleftharpoons \frac{1}{3}\text{n-}C_3H_7OH + \frac{5}{3}H_2O$	− 39.9	− 94.6	9.82×10^{6}
6	$CO_2 + 3\ H_2 \rightleftharpoons \frac{1}{4}\text{n-}C_4H_9OH + \frac{7}{4}H_2O$	− 43.2	− 98.3	3.73×10^{7}

[a] Standard Gibbs free energy change;
[b] standard enthalpy change;
[c] standard equilibrium constant.

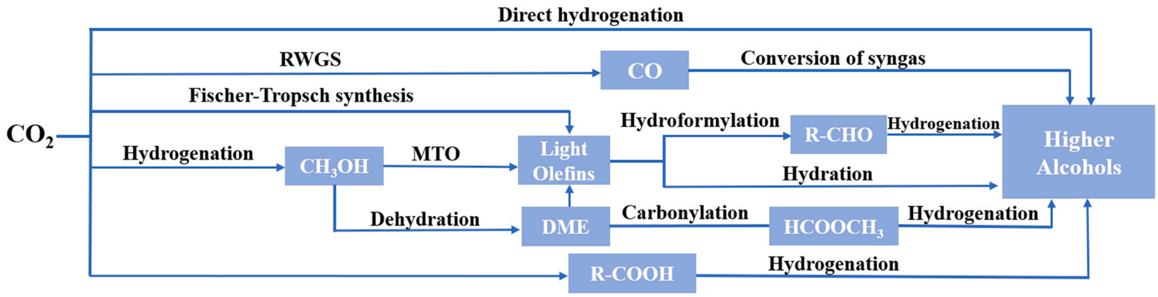

Scheme 1. Different pathways for CO_2-based higher alcohols synthesis.

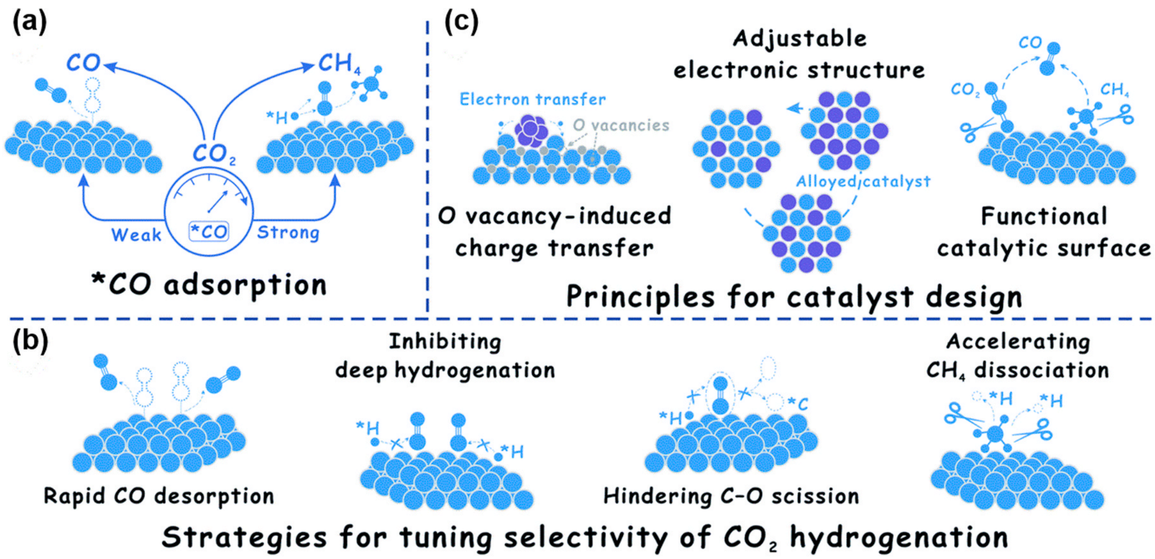

Fig. 1. (a-c) Strategies for tuning the selectivity of CO_2 hydrogenation.
Reprinted with permission from Ref. [96].

grow carbon chains as well as avoid excessive hydrogenation to hydrocarbons.

As indicated in Table 1, the CO_2 hydrogenation reaction system comprises a wide variety of reactants, intermediates, and products, Fig. 1 gives an overview of these species. The main products from CO_2 activation are CO from the RWGS reaction and CH_4 from CO_2 methanation (Table 1 Entry 1 and 2). In the next step, CO can couple with intermediates such as $*CH_x$, $*CH_xO$, *HCOO, etc. to form C_{2+} oxygenated compounds (e.g., aldehydes, alcohols, carboxylic acids, etc.), but can also be dissociated to CH_x to form long chain hydrocarbons. For example, Cu-based systems often display relatively high activity in the RWGS reaction. Simultaneously, Cu-based systems show only weak CO-adsorption and therefore only rarely exhibit excessive reduction to hydrocarbons [92,93]. Co, Fe, Ni, and some other metals, on the other hand, are more prone to break C-O bonds, ultimately leading to methanation [94,95]. This vividly illustrates the importance of tailored active sites for controlling product selectivity. Wang et al. summarized the strategies for tuning the product selectivity in CO_2 hydrogenation, as shown in Fig. 1(a) [96]. The authors concluded that the adsorption strength of *CO intermediates is a key factor, which directly determines whether CO continues to participate in the reaction or terminates to form methane. Fig. 1(c) shows the formation of oxygen vacancies on easily reducible metal oxide supports during the construction of SMSI. The oxygen vacancies play an important role in the activation of CO_2 and can modulate metal-*CO interactions to adjust the product selectivity. According to the authors, as depicted in Fig. 1(b), the catalyst design principles should meet: (i) accelerated CO adsorption to avoid dissociation to CH_x, (ii) inhibition of deep hydrogenation to hydrocarbons, (iii) prevention C-O bond-breakage and (iv) accelerated dissociation of methane. Unfortunately, these theoretical criteria are still subject to many difficulties in practical operation, wherefore the modulation of product selectivity is a major challenge in current catalyst design.

Among the numerous studies reported, Ding et al. were able to supplement their exceptional catalytic results in HAS from CO_2 hydrogenation by comprehensive theoretical calculations on the reaction mechanism. The authors prepared Cu@Na-Beta catalysts, which were synthesized by embedding Cu nanoparticles into a Na-Beta zeolite [40]. Accordingly, an ethanol-space time yield (STY) of 8.65 mmol g_{cat}^{-1} h^{-1} and a selectivity to ethanol of 79.0% were achieved, with it being the only organic product. Compared with the Cu/Na-Beta catalyst prepared by conventional impregnation, H_2-temperature-programmed desorption (TPD), X-ray photoelectron spectroscopy (XPS), and Cu LMM Auger spectra results showed that the Cu particles in the Cu@Na-Beta catalysts possessed more intimate interactions with the Na-Beta zeolite framework. According to the infrared (IR) and nuclear magnetic resonance (NMR) spectroscopy results, the desorption potential energy barrier of the surface-adsorbed CH_3COO^* -intermediate is too high for desorption, which ultimately leads to its further hydrogenation to ethanol. TPD-experiments of various reaction intermediates on Cu@Na-Beta showed immediate decomposition of methanol, formic acid, and acetic acid to CO_x upon heating, while ethanol readily desorbed from the catalyst, leading to a higher selectivity. To further explore the mechanism of ethanol formation, DFT calculations were performed on the (211) Cu facet as perfect structure, with Cu vacancy or O-doped at the edge (Fig. 2 (a)). Fig. 2 (b), (c) and (d) shows the comparison of the decomposition of

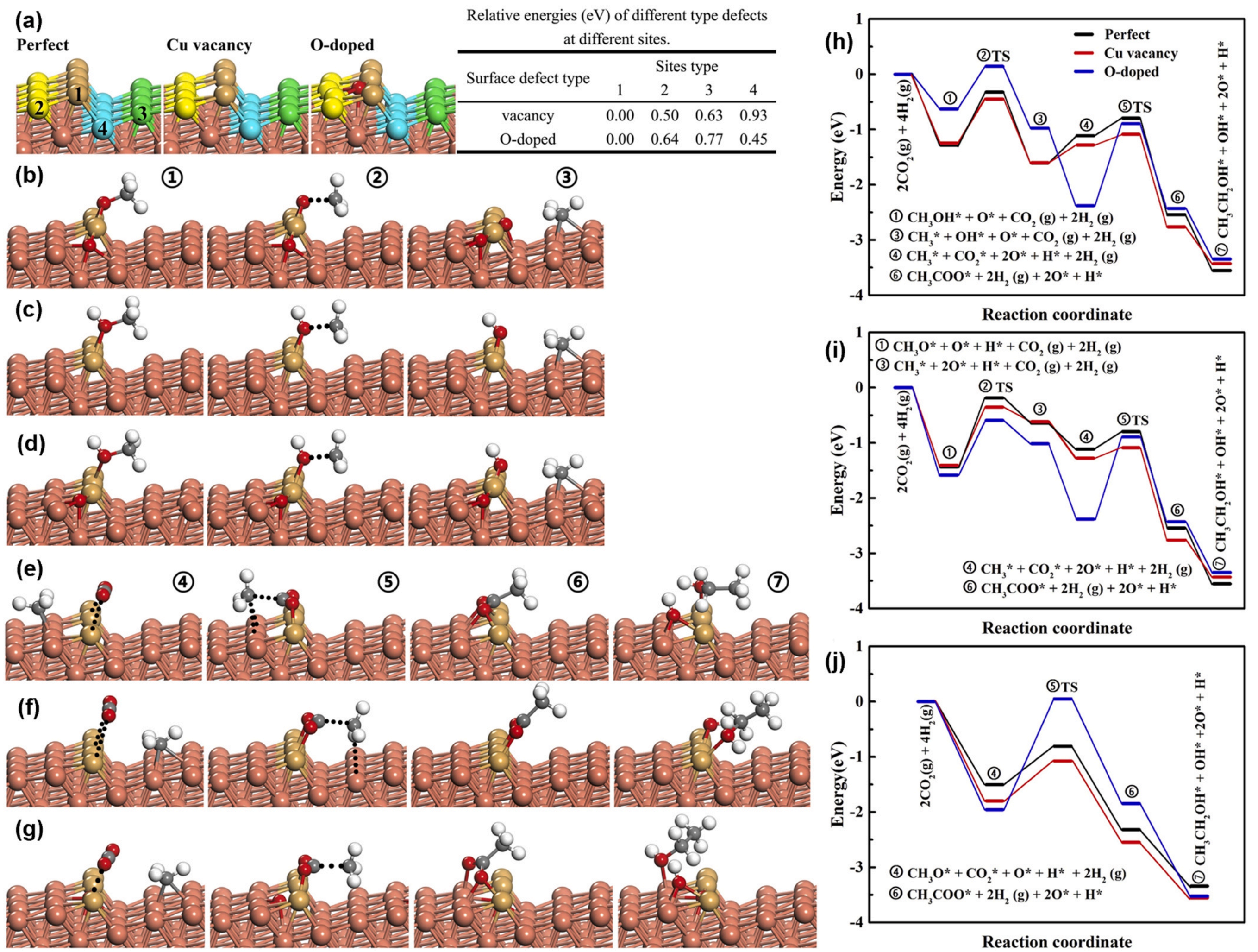

Fig. 2. Reaction Pathway of CO_2 to CH_3CH_2OH and Reaction Energetics Calculated by DFT. (a) Illustrations of perfect, Cu-vacancy, and O-doped surfaces on the edges. The differently colored atoms represent different sites on first layer (yellowish-brown for site type 1, yellow for site type 2, green for site type 3, and blue for site type 4. Dark brown sphere is for Cu at lower layers). (b–d) Illustrations of the initial state, transition state, and final state of methyl formation from CH_3O^* on (b) O-doped Cu(221) and from CH_3OH on (c) Cu vacancy defect surface and (d) O-doped surface. (e–j) Illustrations of the initial state, transition state, and final state of CO_2 +CH_3 reaction paths on (e) Cu vacancy defect surface, (f) perfect surface, (g) O-doped surface and potential energy surfaces for the reaction of (h) CO_2 + CH_3OH → CO_2 + CH_3 → CH_3CH_2OH, (i) CO_2 + CH_3O → CO_2 + CH_3 → CH_3CH_2OH, and (j) CO_2 + CH_3O → CH_3CH_2OH. Dark brown sphere, Cu; red sphere, O; gray sphere, C; white sphere, H; yellowish-brown, Cu on edge.
Reprinted with permission from Ref.[40].

methoxide and methanol, i.e., $CH_3O^* \rightarrow CH_3{}^* + O^*$ and $CH_3OH^* \rightarrow CH_3{}^* + OH^*$. Simulations indicate that the C-O bond breakage of CH_3OH on the oxygen-doped copper (221) surface has a lower energy barrier than the desorption of CH_3OH, wherefore methanol is easily converted to methyl. These results align with the complete absence of methanol from the product fraction. Moreover, Fig. 2(e), (f) and (g) displays the routes of $CO_2{}^* CH_3{}^* + 2H_2 \rightarrow CH_3CH_2OH^*$ and $CO_2{}^* + CH_3O^* + 2H_2 \rightarrow CH_3CH_2OH^* + O^* + OH^*$. Combined with the potential data provided in Fig. 2(h), (i) and (j), it can be deduced that the C-C bond is mainly formed by the reaction of CO_2 with $CH_3{}^*$ rather than methoxide, and the Cu-vacancy containing facet is an effective site for the formation of CH_3COO^* by $CO_2{}^*$ and $CH_3{}^*$, which is ultimately hydrogenated to ethanol.

This example of cooperation between experimental studies and theoretical calculations to support a mechanistic understanding of higher alcohols synthesis exemplifies the complexity of interactions between a multitude of possible intermediates in a dual-functional catalyst. The following chapter will further summarize state-of-the-art research on the direct hydrogenation of CO_2 to alcohols.

3. Direct CO_2 hydrogenation to alcohols

3.1. *Various types of catalysts for CO_2 hydrogenation to higher alcohols*

The direct catalytic hydrogenation of CO_2 to higher alcohols currently represents the predominant approach in CO_2-to-higher alcohols research. It does not rely on various catalyst mixing techniques or multistage bed strategies, but employs one single, possibly multifunctional catalyst for the one-step hydrogenation of CO_2 to higher alcohols. Various types of catalyst materials are investigated for this reaction, which can be broadly classified according to the active components into (1) rhodium-based catalysts, (2) copper-based catalysts, (3) cobalt-based catalysts, (4) molybdenum-based catalysts and (5) other types of catalysts.

3.1.1. *Rh-based catalysts*

Rh-based catalysts originally gained attention for the conversion of syngas to higher alcohols over the last decades.[77,78,97] Rh-catalysts exhibit excellent CO_2 activation capability, namely CO_2 conversion to CO via the RWGS reaction, and subsequent *CO intermediate insertion

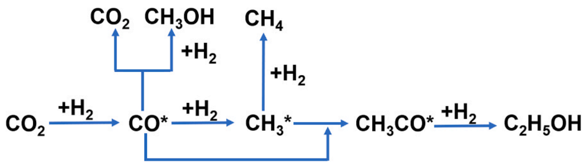

Fig. 3. CO insertion mechanism of CO_2 hydrogenation to ethanol proposed by Kusama et al. [98].

into $^*CH_x$. This CO insertion mechanism (Fig. 3) was proposed by Kusama et al. [98] Izumi et al. investigated the effect of supports and additives on loaded Rh catalysts and found that $Rh_{10}Se/TiO_2$ catalysts possessed the highest selectivity to higher alcohols (83%) [99], significantly higher than Rh/SiO_2 (1.2%) [100]. Over the years, different promoters were employed to prevent excessive *CO dissociation over the highly active Rh-based catalyst systems. Finally, some alkali or transition metals were found to sufficiently inhibit the formation of hydrocarbons.[77] Further studies on promoter effects in SiO_2--supported KFeRh catalysts by Goryachev et al. reported a suppressing effect of K on CO_2 methanation as well as promotion of carbon-chain growth by Fe [101]. Gong's group synthesized TiO_2 nanorods (TiO_2 NR) supported RhFe catalyst (RhFeLi/TiO_2 NR). The TiO_2 NR support contributed to the dispersion of Rh nanoparticles, and the abundant hydroxyl groups on TiO_2 NR played an important role in the synthesis of higher alcohols by CO_2 hydrogenation. Accordingly, CO_2 conversion of 15.7% and a higher alcohol selectivity of 31.3% were achieved at 250 °C, 3 MPa and 6000 mL g_{cat}^{-1} h^{-1}. The in situ diffuse reflectance infrared spectroscopy (DRIFTS) results indicate that the formation of CHO* species is the rate-limiting step in CO_2-to-HA, and that CHO* -dissociation into CH_x* is thermodynamically favored over the formation of CO [102,103]. In addition, the abundant hydroxyl groups on the TiO_2 NR surface favored decomposition of the formyl group into CH_3* , which ultimately promoted the insertion of CO generated from the RWGS reaction to form CH_3CO* , followed by its hydrogenation to ethanol [26]. Furthermore, Wang et al. investigated an efficient VO_x--promoted Rh-based catalyst (Rh-0.3VO_x/MCM-41) which is confined in mesoporous MCM-41 for ethanol production. An ethanol selectivity of 21.2% and CO_2 conversion of 12% could be achieved at 250 °C and 3 MPa. Based on experimental and theoretical results, non-linearly adsorbed CO, formed at the VO_x-Rh interfacial site, can be easily dissociated into the key intermediate $^*CH_x$. Subsequently, $^*CH_x$ can be inserted to CO to form CH_3CO* , which is finally hydrogenated to ethanol [104]. Even though Rh-based catalysts display exceptional activity in CO_2 hydrogenation, their industrial application is hindered by they lack economic viability. Consequently, further research focused on developing non-noble metal-based catalysts.

3.1.2. Cu-based catalysts

Cu-based catalysts are extensively used for methanol synthesis (MS) [71,105–107], and due to the RWGS activity of Cu-based systems [108–110], numerous modified catalysts are used for the synthesis of higher alcohols from syngas [111–114]. Since Cu has the capability of activating CO_2 and is simultaneously good for non-dissociative CO adsorption, modified Cu-based catalysts for CO_2 hydrogenation are a promising class of materials in HAS. However, due to their low affinity to form $^*CH_x$ intermediates from CO, Cu-based catalysts often require transition metal and alkali metal promoters to improve their C-C coupling activity. In general, transition metals (e.g., Fe, Co) improve CO-dissociation to $^*CH_x$ and thus enable CH_x-CH_x coupling, while alkali metals can enhance the selectivity to higher alcohols [77,78]. Li et al. evaluated the catalytic performance of a K/Cu-Zn catalyst for the RWGS reaction and CO_2 hydrogenation to alcohols. The catalyst achieved a high CO selectivity of 84.3% and a mixed alcohol selectivity of 7.6%, respectively. [115] Li et al. discovered a synergistic effect of iron in K/Cu-Zn catalysts improving HA selectivity up to 13.5% [116]. Besides, the Liu group also explored the role of K in Cu-Fe-based catalysts, and found K not only facilitating the RWGS reaction but also modulating the catalyst's ability to dissociate adsorbed and non-dissociated CO, allowing sufficient $^*CH_x$ to couple with *CO to form higher alcohols [117]. An et al. developed unique secondary building units (SBUs) to support bimetallic Cu_2^I sites in a synthesized Z_{12}-MOF for CO_2 hydrogenation to ethanol. Again, different alkali metal promoters were able to fine-tune the local structure of the catalytic sites. [41] Fig. 4(a) shows the enhancement of catalytic activity by different alkali metal promoters and the increase in ethanol selectivity follows the order Li<Na<K<Cs. The best catalytic performance was achieved over the Cs promoted catalyst, exhibiting more than 99% ethanol selectivity at 2 MPa and 100 °C with a turn-over number (TON) of 490. Based on NMR, EXAFS, and XPS characterizations as well as DFT calculations, a more efficient electron donor feature and lower potential barriers for the formation of formyl intermediates could be attributed to the presence of Cs^+ species. The catalytic activity was attributed to a synergistic effect of the close μ_2-Cu···μ_3-Cu bimetallic sites, which cannot only activate H_2 but also facilitate C-C-coupling between methanol and formyl species with the assistance of alkali metal promoters for the efficient formation of ethanol.

Moreover, Wang et al. employed a comprehensive approach, combining experiments with DFT calculations and Kinetic Monte Carlo (KMC) simulations, to investigate the reaction mechanism of ethanol synthesis via CO_2 hydrogenation on Cs/Cu/ZnO(0001‾) catalyst, as illustrated in Fig. 4(b). The introduction of Cs imparts multifunctional sites with a distinctive structure at the Cu-Cs-ZnO interface, facilitating its interaction with CO_2. Notably, the Cu-Cs-ZnO interface plays a pivotal role in modulating the strength of its binding to *CHO. This dual effect not only promotes *CHO-formation by the decomposition of HCOOH, but also facilitates the further hydrogenation of *CHO to methanol. The adept control exerted by Cs/Cu/ZnO(0001‾) over *CHO is instrumental in fostering C-C coupling, culminating in the ultimate formation of ethanol.[118].

3.1.3. Co-based catalysts

Co-based catalysts originate from FTS catalysts [119]. They are well known for their carbon chain growth ability [120] and are widely used in CO hydrogenation as well as syngas conversion reactions [77,121]. However, the inherent ability of metal Co to break C-O bonds leads to easier hydrocarbon synthesis [122,123], which is detrimental to the formation of higher alcohols. Various additives and supports are commonly employed to modify Co-based catalysts and improve the selectivity to higher alcohols. In addition, different types of Co-sites and phases hold a great influence on the performance of the reported catalysts [60]. For example, a Co@Co_3O_4/C-N catalyst synthesized by Lian et al. with metallic Co as the main active component resulted in excessive hydrocarbon formation (80.2%) and very low selectivity to higher alcohols (1.2%).[124] Besides, Ouyang et al. investigated the effect of different Co_3O_4 morphologies as a support on the performance of Pt/Co_3O_4 catalysts. Due to their easier reducibility, Co_3O_4 nanoplates created a synergistic effect with Co and Pt and the oxygen vacancies of Co_3O_4 itself, reaching a STY_{HA} of 0.56 mmol g_{cat}^{-1} h^{-1} and a selectivity to HA of 4.3% at 200 °C and 2 MPa [125].

An et al. developed Ga doped $CoGaAlO_4/SiO_2$ catalyst for CO_2 hydrogenation to ethanol, achieving 20.1% ethanol selectivity and 0.3 mmol g_{cat}^{-1} h^{-1} STY_{EtOH} at 270 ℃, 3 MPa, and 3000 mL g_{cat}^{-1} h^{-1} [126]. The authors attributed the high catalytic activity to the strong interaction between gallium oxide and cobalt, inducing the formation of active Co^0-$Co^{\delta+}$ species. The proposed reaction mechanism is provided in Fig. 5. Initially, CO_2 is adsorbed on the catalyst surface, undergoing the RWGS reaction to form a CO intermediate. Simultaneously, CO and H_2 molecules are activated at the Co^0-$Co^{\delta+}$ site. The strong dissociation capability of Co^0 cleaves the C-O bond, leading to the formation of alkyl intermediates. The spinel structure, along with $Co^{\delta+}$ sites, readily performs non-dissociative adsorption of CO* /HCO* intermediates. Finally,

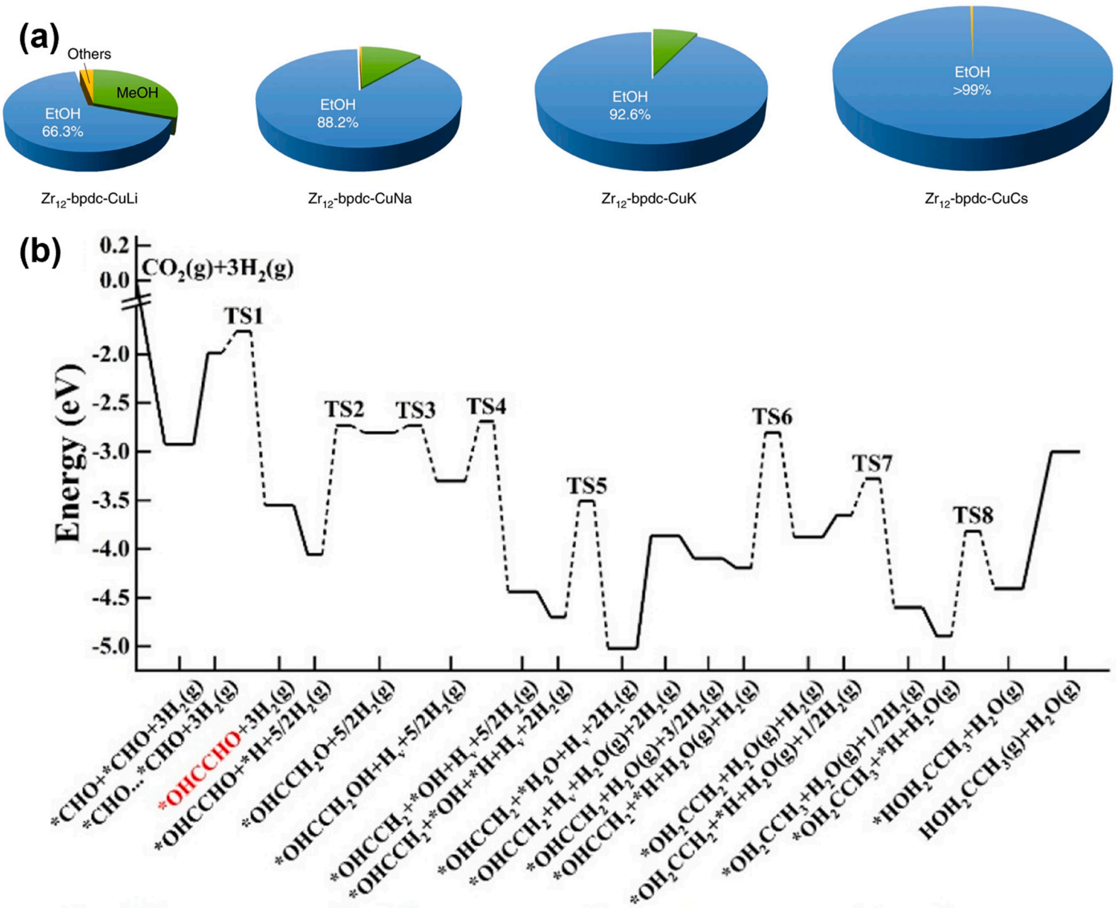

Fig. 4. (a) Selectivity of the catalysts modified with different alkali metals. Reaction conditions: 10 mg of catalysts, $H_2/CO_2 = 3$, $p = 2$ MPa, Temperature = 100 °C, time = 10 h, 10 mL of anhydrous THF. "TS", transition state.
(a) Reprinted with permission from Ref. [41] (b) Potential energy diagram for ethanol synthesis starting from *HCO on the Cu/Cs/ZnO(000$\bar{1}$) surfaces. (b) Reprinted with permission from Ref. [118].

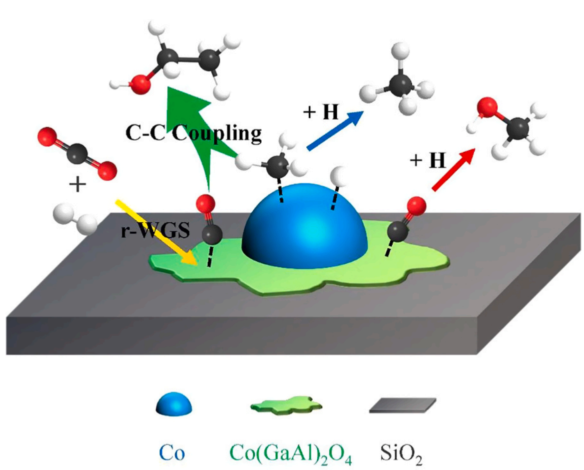

Fig. 5. Plausible mechanism for ethanol synthesis from CO_2 hydrogenation over $CoGaAlO_4/SiO_2$ catalyst.
Reprinted with permission from Ref. [126].

the CH_x * and CO* /HCO* coupling led to ethanol synthesis.

Besides, Wang et al. conducted a study on the selective hydrogenation of CO_2 to ethanol using the non-precious metal catalyst $CoAlO_x$, which exhibited the best performance at a reduction temperature of 600 °C [42]. At a reaction temperature of 140 °C, the catalyst achieves a selectivity of 92.1% and a STY_{EtOH} of 0.444 mmol g_{cat}^{-1} h^{-1}. Through operando FTIR experiments, the authors conducted an in-depth investigation into the reaction intermediates over $CoAlO_x$ catalysts. The results revealed *HCOO as a crucial stable intermediate, impeding the further hydrogenation process and consequently suppressing methanol formation. The synergy between surface Co^0 and CoO on the catalyst promotes the formation of *CH_x intermediates. Subsequently, *CH_x can couple with *HCOO to form acetate, followed by the successive hydrogenation of *CH_3COO to ethanol. To further enhance ethanol yield, Wang et al. introduced Ni as a promoter into $CoAlO_x$, resulting in the synthesis of a $Co_{0.52}Ni_{0.48}AlO_x$ catalyst. The presence of Co-Ni alloy in this catalyst promotes the intermediate *CH_x formation, which ultimately accelerates the C-C coupling to form ethanol. As a result, ethanol selectivity reached 85.7%, and the STY of ethanol improved to 1.32 mmol g_{cat}^{-1} h^{-1} [43].

Additionally, He et al. discovered the synergetic promotion of water and Pt/Co_3O_4 catalysts and thus achieved 57% HA selectivity and a STY_{HA} of 0.29 mmol g_{cat}^{-1} h^{-1} at 200 °C and 8 MPa [29]. The authors observed kinetic influence of water in the hydrogenation of CO_2. D_2 and ^{13}C labeling experiments indicated a crucial role of water in protonating methanol, subsequently dissociating into CH_3* , OH* , and H* species. Finally, CH_3* couples with CO to form CH_3CO* , followed by hydrogenation to produce ethanol.

3.1.4. Mo-based catalysts

Mo-based catalysts are typically applied with MoS_2, Mo_2C, MoO_x or MoP as the active phase and have been widely studied in HAS from

syngas [77]. Transition and alkali metals are common additives to enhance the HAS over Mo-based catalysts. Here, the former enhances the carbon chain growth activity of Mo-based catalysts, while alkali metals can inhibit the formation of hydrocarbons and thus promote the synthesis of alcohols [77]. Nieskens et al. studied the performance of CoMoS catalysts for HAS from CO_2 at 10.4 MPa and 340 °C, with a HA selectivity of 6.0% [36] Liu et al. synthesized a KMoCoS-AC catalyst supported on activated carbon. The authors proposed that online calcination can effectively suppress surface sulfur loss, favoring the formation of Mo^{4+} species, thereby enhancing the catalyst's selectivity towards alcohols. KMoCoS-AC achieved a CO_2 conversion of 8.1% and a selectivity of 4.8% towards higher alcohols at condition of 320 °C, 5 MPa, and 3000 mL g_{cat}^{-1} h^{-1} [35]. Besides, Chen et al. synthesized a series of metal/Mo_2C catalysts for the hydrogenation of CO_2 to alcohols, evaluating their performance in 1,4-dioxane solvent. At 200 °C and 4 MPa, Mo_2C achieved 16% selectivity towards higher alcohols and 53% selectivity towards methanol. Fig. 6 provides the reaction mechanism proposed by the authors. During CO hydrogenation experiments, they observed significantly lower methanol production compared to CO_2 hydrogenation, suggesting that the majority of methanol is derived from the hydrogenation of formate or aldehydes [127,128]. Additionally, independent tests on methanol hydrogenation revealed that methanol itself is not an intermediate for C_{2+}-alcohol and C_{2+}-hydrocarbons. The researchers postulated that carbon chain elongation involves the molecularly adsorbed CO, which is subsequently hydrogenated to methoxy (-CHO) species [33,129].

In summary, the exemplary discussion of Rh-, Cu-, Co-, and Mo-catalysts for the direct hydrogenation of CO_2 to higher alcohols evidenced the possibility of improved CO_2 conversion and HA selectivity over catalysts with tailored properties. However, the improvements often rely on the incorporation of multitude of metals and promoters, which increases the catalysts complexity and leads to a difficulty to draw comprehensive structure-activity relationships. Although at first glance the CO_2 hydrogenation to higher alcohols seems like a relatively straightforward reaction, the design of selective catalysts for higher alcohols synthesis is a highly challenging task for several reasons: (i) catalysts must unite functionalities for both C-C-coupling as well as OH-group formation on one material, (ii) the combination of those functionalities must effectively avoid a wide variety of unwanted side products, such as methanol, carbon monoxide, hydrocarbons, DME and many more, (iii) the developed catalytic systems must exhibit long-term stability in continuous reactions and ideally function without additional solvents to facilitate the route to industrial implementation.

Originally, Rh-based systems suffered from excessive CO-dissociation and thus high hydrocarbon selectivity. However, through significant research efforts, a comprehensive understanding of the role of alkali metal promoters in suppression of hydrocarbon formation was developed [77,101]. Despite these improvements, excessive dissociation and thus high CH_4-selectivity as well as simultaneously high CO-selectivity [26], combined with high material costs, prevent Rh-catalysts from drawing deeper research interest. On the other hand, Cu-based systems often show remarkable CO_2-activation via the RWGS

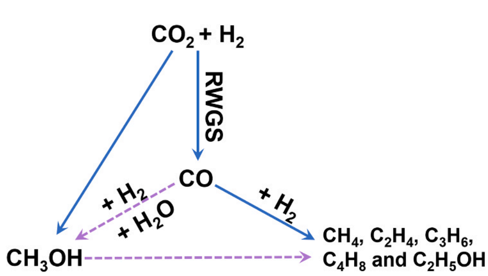

Fig. 6. Reaction pathways to produce alcohols and hydrocarbons by CO_2 hydrogenation over Mo_2C catalyst. The solid arrows denote major pathways and the dashed arrows denote minor pathways [33].

reaction and simultaneously excellent capability of non-dissociative CO-adsorption. However, this strength simultaneously restricts the ability to form $^*CH_x$-species from CO, which represent crucial intermediates for C-C-coupling and thus the generation of higher alcohols. Hence, Cu-based systems often require other transition metals (e.g., Fe or Co) to improve their ability to generate key $^*CH_x$-intermediates [77,78], which in turn significantly increase the share of hydrocarbons, mainly methane, in the product fraction [37,130]. Co-based systems, in turn, display the opposite problem compared to Cu-based catalysts. Known for their strong affinity for carbon chain growth and hydrocarbon formation, Co-catalysts lack OH-group formation functionalities to suppress excessive hydrocarbon selectivity in the direct hydrogenation of CO_2 to higher alcohols. Though some researchers achieved impressive ethanol selectivity over Co-based systems, they required either exotic additives or were obtained under batch conditions [42,126]. Finally, Mo-based catalysts reported so far often suffer from low CO_2 conversion and unsatisfactory HA selectivity. Moreover, current research in Mo-based catalytic systems lacks comprehensive studies on the reaction mechanism.

In summary, catalysts for the direct hydrogenation of CO_2 to higher alcohols still face one major challenge related to having the combination of all necessary functionalities, mainly CO_2 activation, C-C-coupling, and OH-group formation, in a single catalyst. Most of the above-mentioned group of catalysts only achieve outstanding performance due to the presence one or more of these functionalities. Although their catalytic performance was able to be partially enhanced, their shortcoming due to the absence of remaining functionalities often prevents these catalysts from further application. Hence, to tackle the unsatisfactory selectivity for higher alcohols on single catalytic systems, the research focus is quickly shifting towards multifunctional catalysts due to their versatility and flexibility.

3.2. Multifunctional sites for CO_2 hydrogenation

As discussed above, the synthesis of higher alcohols from CO_2 is a complex process involving multiple intermediate reactions. As a result, various proposed mechanisms have been put forward to explain the series of involved steps. Accordingly, the three most common mechanisms for CO_2 hydrogenation are (i) the CO-mediated mechanism, (ii) the formate/methoxy-mediated pathway, and (iii) other C-C coupling mechanisms, respectively. The CO-mediated mechanism was first proposed by Kusama et al [98]. It involves the generation of the key intermediate *CO from CO_2 through the RWGS reaction. Then, *CO partly dissociates into $^*CH_x$, and finally, higher alcohols are formed by inserting the non-dissociated *CO into $^*CH_x$. Therefore, the primary objective of this mechanism is to balance the amount of dissociated *CO ($^*CH_x$) and non-dissociated *CO to maximize the formation of higher alcohols. On the contrary, the formate/methoxy-mediated pathway involves the direct conversion of CO_2 to *HCOO, followed by generating various intermediates such as *CHO, $^*CH_2O$, $^*CH_3O$, $^*CH_3$, and $^*CH_3CO$. Subsequently, C-C coupling between these intermediates leads to the formation of alcohols.

Since higher alcohols are formed step-by-step from intermediates in both CO-mediated and formate/methoxy-mediated mechanisms, a single active site is often not capable of effectively catalyzing the entire catalytic cycle. Therefore, catalysts with multifunctional sites, which enable synergistic effects of CO_2 activation, carbon chain growth, and alcohol generation are crucial for effective alcohol synthesis. For example, the role of different sites on cobalt-based catalysts, such as Co^0, CoO, $Co^{\delta+}$, and Co_2C, and the strategies to tune their structures to affect the performance in CO_2 hydrogenation is discussed in our previous review [60]. The synergistic effect of different sites on the catalyst performance of Co-based catalysts is significant, as it is for other metal-based catalysts. Thus, understanding the mechanisms involved in CO_2 hydrogenation and the design of efficient catalysts with multifunctional sites are crucial for the successful production of higher

Table 2
Representative catalysts with multifunctional sites for the CO_2 hydrogenation to HA.

Catalyst	Reactor[a]	T[b] /°C	p[c] /MPa	X_{CO2}[d] /%	S_{HA}[e] /%	STY_{HA}[f] /mmol g_{cat}^{-1} h^{-1}	Multifunctional sites
Au/aTiO_2[30]	T	200	6	n.a.	> 99	2.83	①Au NCs ②a-TiO_2
RhFeLi/TiO_2[26]	F	250	3	15.7	16	0.36	①Rh NPs ②TiO_2 NRs ③FeO_x ④Li
K-Co-In_2O_3[131]	F	380	4	36.6	11.1	3.73	①In_2O_3 ②Co^0 ③CoO ④K-CoO_2
Na-Co/SiO_2[46]	F	250	5	18.8	8.7	0.16	①Co_2C ②Si-O-Co in SiO_2
$CoAlO_x$[42]	T	140	4	n.a.	92.1	0.444	①Co^0 ②CoO
$Co_{0.52}Ni_{0.48}AlO_x$[43]	T	200	4	n.a.	85.7	1.32	①Co^0 ②CoO ③CoNi alloy
Cs-$C_{0.8}F_{1.0}Z_{1.0}$[37]	F	330	5	36.6	19.8	1.47	①Cu-ZnO ②Cu-Fe_7C_3 ③Cs

[a] T indicates tank reactor, F indicates fixed bed reactor,
[b] temperature,
[c] pressure,
[d] CO_2 conversion,
[e] selectivity to higher alcohols,
[f] space-time yield of higher alcohols.

alcohols by CO_2 hydrogenation.

Table 2 presents a summary of current representative catalysts with multifunctional sites, highlighting their unique features and exceptional performance for CO_2 hydrogenation. Among these, TiO_2-supported Au-nanoclusters (NC) have demonstrated outstanding ethanol selectivity (>99%) and a STY_{EtOH} of 2.83 mmol g_{cat}^{-1} h^{-1}. The authors attributed these results to the synergistic effect of Au NCs and TiO_2 enhancing metal-support interactions due to the abundant oxygen vacancies of the TiO_2-anatase, ultimately enabling effective activation of CO_2 and H_2 [30]. Moreover, Yang et al. reported a RhFeLi/TiO_2 catalyst with 15% CO_2 conversion and 32% ethanol selectivity at 250 °C and 3 MPa. The high catalytic activity was correlated to several factors, including high Rh-dispersion on the TiO_2-nanorods (NRs) support, promotion of the RWGS reaction by FeO_x-species, and increased CO_2 conversion by Li addition. The hydroxyl group introduced on the TiO_2 NRs also facilitates the dissociation of methanol to *CH_x, promoting CO-insertion to form ethanol [26]. The promising STY_{HA} of 3.73 mmol g_{cat}^{-1} h^{-1} on a K-Co-promoted In_2O_3-catalyst by the group of Witoon was attributed to defects on In_2O_3 sites, which effectively catalyzed the RWGS reaction to convert CO_2 to CO, while Co^0 sites simultaneously participate in the dissociative adsorption of C-O and carbon chain growth to form C_xH_y * intermediates. Besides, K was identified to inhibit excessive C_xH_y * hydrogenation to reduce the formation of hydrocarbons and improve the selectivity of higher alcohols [131]. Zhang et al. also conducted a study on the preparation of Na-Co catalysts supported on SiO_2, which exhibited a high selectivity of 62.8% towards ethanol in the alcohol distribution and demonstrated good stability over 300 h time on stream. The observed catalytic activity was attributed to the presence of Co_2C site, while the long-term stability was attributed to the formation of a strong metal-support interaction between Co_2C and SiO_2 on the catalyst surface, resulting in the formation of a Si-O-Co bond. This interaction facilitated the continuous reconstitution of Co_2C even after decomposition [46]. Furthermore, Wang et al. emphasized the importance of the metal Co^0 site on $CoAlO_x$ catalysts for the formation of ethanol. They highlighted that the synergistic effect between suitable proportions of Co^0 and CoO plays a vital role in maximizing ethanol production [42].

In summary, the establishment of multifunctional sites is deemed essential for CO_2 hydrogenation to higher alcohols, because higher alcohol formation requires catalysts with the capacity to activate CO_2, promote carbon chain growth, as well as facilitate alcohol formation at the same time, which cannot be accomplished by a single site alone. Catalysts possessing the various active sites to realize functions for higher alcohols synthesis the core of catalyst design for direct higher alcohols synthesis via CO_2 hydrogenation. Catalysts with modified nanoscale features, such as the introduction of promoters or the construction of specific structures such as MOFs or zeolites, are essential for building synergistic interactions of multiple sites to enhance catalytic activity. However, acquiring functional sites that produce desired synergistic effects remains challenging until now. In general, if the formation of stable key intermediates of the reaction is achieved and each functional site acts sequentially, not only macroscopic tunability of the reaction will be improved, but also the overall catalytic efficiency will be enhanced. Therefore, integrating catalysts with diverse functionalities offers a practical and efficient strategy to achieve multifunctional catalytic reactions.

4. Indirect CO_2 hydrogenation to higher alcohols

In this review, the indirect hydrogenation of CO_2 to higher alcohols is considered as a more general term for processes, that consist of multiple sequential catalytic steps over multiple and clearly distinguishable catalysts. Hence, due to its cooperative process design and the synergy of multiple catalysts within one superordinated process, here the hydrogenation of CO_2 to higher alcohols via this pathway is designated as 'tandem catalysis'. This highly flexible approach can either be performed in one single reactor, e.g. through multiple catalytic beds, or it can also involve sequential reactions in multiple reactors/beds by connecting in series mode. By vastly expanding the number of possible functionalities over the catalytic system, tandem catalysis may unveil novel and flexible approaches to reimagine established catalytic processes.[132] In addition, this approach can help deepen the understanding of the reaction mechanism in HAS. To optimize the activity of such tandem catalysts, the proximity of the multiple functional sites is crucial to consider. Among other things, the integrating mode of the separate catalyst beds has a substantial influence on the proximity of active sites.

4.1. *Tandem catalysis system*

4.1.1. *Physical mixing*

Physical mixing is a commonly employed technique in catalyst synthesis, particularly in HAS by syngas and CO_2 hydrogenation [10, 133–135]. This method allows for the incorporation of multiple functional sites, thereby enhancing catalyst performance. Various mixing modes can be employed, each with its unique effects on the catalyst performance. Fig. 7 illustrates several distinct integration modes for two catalysts A and B. The first mode integrates two reactors in series, enabling two separate reactions under different reaction conditions in tandem, and is characterized by simplicity of regulation. In the second and third modes, dual-bed mixing is employed, wherein catalysts A and B are sequentially stacked within two catalytic beds in one reactor, catalyzing various reactions in series under the same reaction conditions. The fourth mode mixes the granules of catalyst A and B in one catalytic bed, enabling uniform mixing, as well as faster heat and mass exchange between reactions over catalyst A and B. The fifth mode is powder mixing, in which the powders of the two catalysts are mixed to form one granule, further facilitating heat and mass exchange. The sixth mode mixes the catalyst powders by a mortar mixing step before

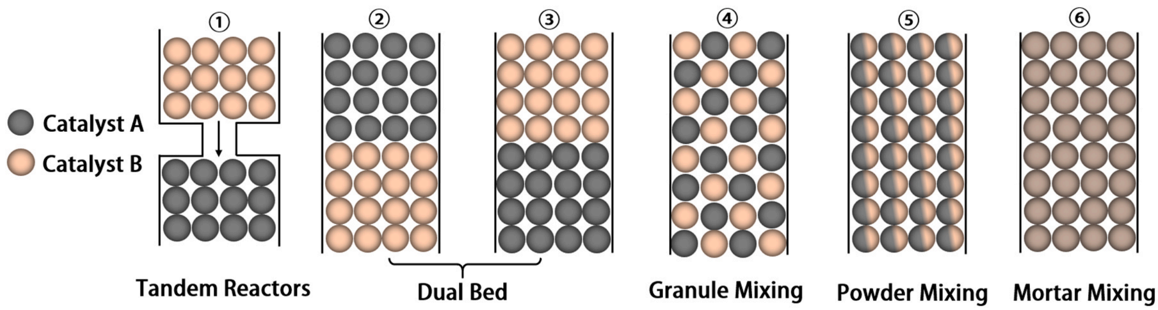

Fig. 7. A variety of different integrating modes of two catalytic functionalities.

granulating, leading to the closest proximity of the catalyst functionalities. However, it is important to note that proximity alone does not guarantee improved catalytic performance. Xu et al. conducted a study on the effect of different reactor filling configurations of CuZnAl/K-CuMgZnFe catalysts on the catalytic performance [63]. Their findings revealed that the catalysts exhibited the highest CO_2 conversion, HA selectivity, and STY when employing the powder mixing mode (⑤). Excessive proximity between the catalysts, as achieved through mortar mixing, led to a decline in catalytic activity. This detrimental effect can be attributed to the promoter K in the K-CuMgZnFe catalyst, which, in excessive proximity, can poison the CuZnAl oxide. Consequently, selecting an appropriate mixing mode is crucial to facilitate the optimal functioning of both catalysts. Thus, the selection of integrating modes needs to consider the difference in the reaction conditions of the planned reactions over catalysts A and B, as well as the necessity to increase proximity of the catalysts, which may enhance the overall reaction by facilitating the heat and mass exchange, as well as the interaction between catalyst A and B. At the same time potential detrimental effects of the catalysts on each other require attention.

The investigation of physically mixed catalysts and their role in the reaction process is of utmost importance to comprehensively understand the factors contributing to enhanced catalytic performance. Santos et al. conducted a study on the reaction mechanism involved in the synthesis of higher alcohols from syngas utilizing K-MoS_2 catalysts [136]. Notably, the incorporation of K into MoS_2 through physical mixing had a profound impact on the catalyst's electronic properties, as well as its ability to facilitate CO-insertion. Huang et al. prepared CCA|ZnO/ZrO_2 catalysts for the synthesis of higher alcohols from syngas, employing a mortar mixing technique to combine CuCoAl and ZnO/ZrO_2. Remarkably, the highest selectivity of higher alcohols was achieved when the ZnO/ZrO_2 ratio was maintained at 4:1. Through rigorous characterization techniques, the researchers determined that an optimal ZnO/ZrO_2 ratio was pivotal in maintaining an optimal equilibrium between the key intermediates CO* and CH_xThis equilibrium enhancement facilitated the probability of CH_x * -CO* coupling, consequently enhancing the HA selectivity [135]. Moreover, the group of Liu devised the CuZnAl/K-CuMgZnFe multifunctional catalyst by physically mixing CuZnAl and K-CuMgZnFe to establish a tandem reaction system for HAS by CO_2 hydrogenation [63]. In this system, CuZnAl was primarily active in the RWGS reaction, leading to the formation of CO* intermediates, while K-CuMgZnFe facilitated the insertion of CO to generate higher alcohols. The synergy between the two catalysts was crucial in achieving comparable reaction rates for both processes. Moreover, the appropriate spacing between CuZnAl and K-CuMgZnFe proved to be instrumental in enhancing the transfer velocity of *CO intermediates between the two catalysts, thereby increasing the yield of higher alcohols.

In summary, the utilization of physical mixing catalysts has demonstrated remarkable performance enhancements in HAS as well as a further understanding of the reaction mechanisms. Consequently, drawing inspiration from these findings and capitalizing on the macroscopic tunability afforded by physical mixing, the idea of employing the physical mixing mode to combine catalysts in well-established tandem reaction systems for the sequential conversion of CO_2 to higher alcohols holds great potential. Mainly, this approach offers considerable potential to integrate catalysts of currently more mature reactions, thus paving the way for the development of a sophisticated tandem reaction system. In the subsequent sections, several pathways for the conversion of CO_2 to higher alcohols will be presented, thereby presenting a novel catalyst design concept.

Generally, when planning new tandem catalytic systems on a research scale, it is crucial to consider basic process parameters, for example, the temperature or pressure profile of the individual reactions, to evaluate the technological feasibility of their combination. Fig. 8 summarizes the overview of the operating temperature ranges of the individual processes that will be discussed in the following chapter. Thus, this in turn helps to identify and evaluate the integration parameters of both promising processes to be coupled in tandem catalysis as well as pairs, which might demand more sophisticated approaches to bridge the temperature gap between individual steps. Besides, such considerations help to identify reasonable integration modes for different catalysts. For example, based on Figs. 7 and 8, it is reasonable to assume that the combined process of CO_2 hydrogenation to methanol + methanol to olefins + olefin hydration to higher alcohols is not suitable for the integration modes ②-⑥ because of the significant differences in reaction temperature of the individual processes. If, however, one aims to couple RWGS with the conversion of synthetic gas to HA, choosing an integration mode within one single reactor might be a good choice.

4.1.2. *Recent advances in tandem-catalyzed CO_2 hydrogenation to HA*

The use of tandem catalysis strategies in the design of catalysts or reaction systems for the hydrogenation of CO_2 to produce higher alcohols dates back over 20 years. In 1998, Inui and Yamamoto employed a method involving physical mixing and packing of catalysts in series to devise distinct tandem catalytic processes for three types of catalysts [137]. These catalysts possess distinct functionalities: the loaded Rh-based catalyst, Rh/silicate, capable of partially reducing CO_2 to CO; the modified FTS catalyst $Fe_{1.0}Cu_{0.03}Al_{2.0}K_{0.7}$, with the ability to form C-C bonds; and the methanol synthesis catalyst with -OH functional groups insertion ability. Through the refinement of reaction conditions, the authors achieved a STY_{HA} of 874 g L^{-1} h^{-1} and a 31.1% CO_2 conversion at 330 °C, 8 MPa, and 50,000 h^{-1} [137,138]. Subsequently, they optimized the Fe-based and Cu-based catalysts using Ga and Pd. Under identical temperature, pressure, and a space velocity of 20000 h^{-1}, they achieved 54.5% CO_2 conversion and a STY_{HA} of 476 g L^{-1} h^{-1} [139].

Currently, the tandem catalysis approach has already proven to be effective in efficiently converting syngas to HA [132,140–145]. However, only some progress has been made in the indirect hydrogenation of CO_2 to higher alcohols using a tandem catalysis method. Catalytic systems designed through various physical mixing methods gain increasing attention [61–63,146,147]. These catalytic systems display effective production and stabilization of key intermediates, such as CH_x * and/or CO* , during the reaction process, thereby converting the intermediates into the final desired product. For example, the Wu group combined an

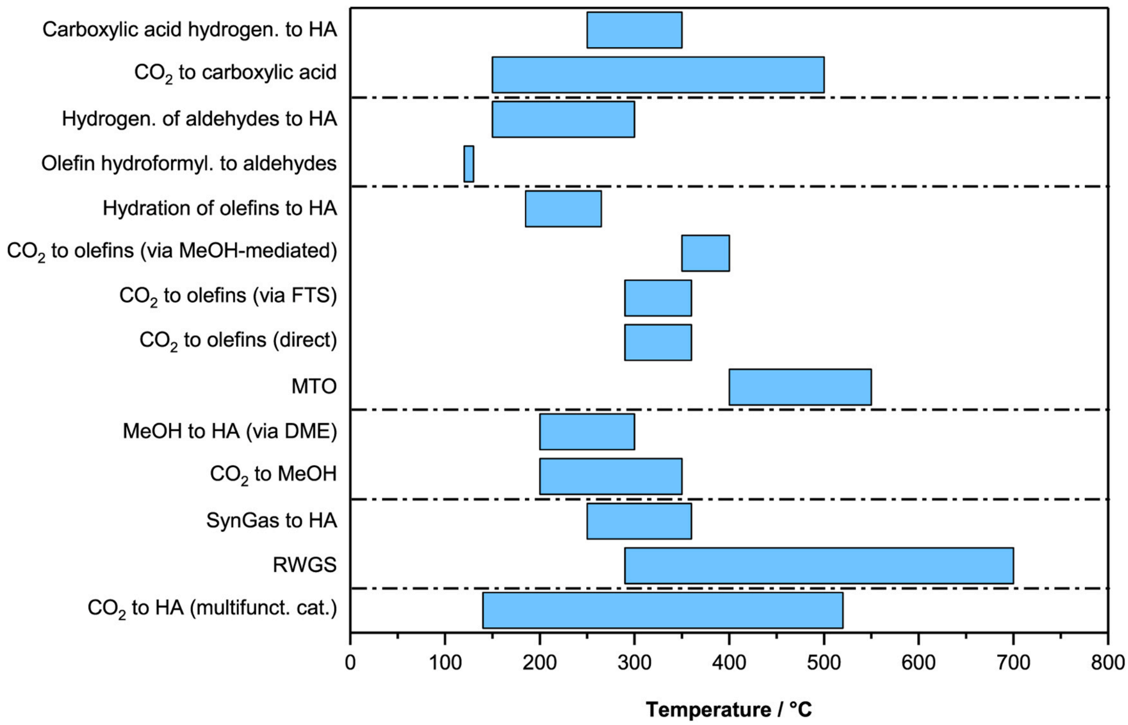

Fig. 8. Temperature ranges of different processes.

ethylene synthesis catalyst (Na-Fe@C) with a methanol synthesis catalyst (CuZnAl). And, the catalytic performance was compared in powder mixing, granule mixing and dual bed modes, and found that granule mixing (mode ④ of Fig. 7) had the best HAS activity. This phenomenon was attributed to the coverage of the active sites of the multifunctional catalyst in the powder mixing mode. Combining two catalysts through granule mixing can increase the spatial distance between different catalytic components, thereby reducing the difficulty of C-C coupling to achieve high ethanol selectivity. However, further increasing the distance between the active sites (dual bed mode), the intermediates produced by the two catalyst beds are difficult to combine directly, resulting in lower selectivity for higher alcohols [147]. In the condition of granule mixing, the resulting catalyst exhibited a CO_2 conversion of 39.2% and ethanol selectivity of 35.0% at 5 MPa and 320 °C. A mechanistic overview of the reaction network over Na-Fe@C/K-CuZnAl catalyst is shown in Fig. 9. The CuZnAl catalyst played a vital role in the RWGS reaction by providing CO* intermediates for subsequent FTS and ethanol synthesis. On the other hand, iron carbide facilitated the dissociation of CO* to form CH_m* intermediates, which underwent C-C coupling to generate key aldehyde-intermediates. Finally, the aldehydes were further hydrogenated to yield ethanol. The closely linked tandem reaction mechanism resulted in a highly active catalyst, enabling efficient diffusion of the reaction intermediates from one catalytic site to another during the multifunctional composite tandem catalytic process, ultimately leading to selective synthesis of the target product.

Zhang et al. also investigated Co_2C||CuZnAl as multifunctional tandem catalyst for CO_2 hydrogenation to higher alcohols in a dual-bed mode and elucidated the specific reaction network. The tandem catalysis design is shown in Fig. 10, and activity test results show that the dual bed mode in which the feed gas first contacts the Co_2C catalyst exhibits the highest HA selectivity, while the other dual bed mode, powder mixing, and catalyst prepared by impregnation method (Co/CuZnAl) can hardly produce higher alcohols. The authors hypothesized that the combination mode can effectively regulate the reaction mechanism, thus affecting the selectivity of the desired product. Based on various in situ characterization techniques, the authors provide the following reaction mechanism for $C_{2+}OH$ formation: first, CO_2 undergoes hydrogenation on Co_2C, resulting in the formation of olefins. Subsequently, these olefins diffuse to CuZnAl sites to dissociate, forming R-CH_2 intermediates. This R-CH_2 species then couples with CHO at the Cu/$ZnAl_2O_4$ interface, leading to the formation of higher alcohols. The incorporation of these multiple active sites in the catalyst design effectively generates R-CH_2 and CHO intermediates, facilitating C-C coupling and enabling a high STY_{HA} of 2.2 mmol g_{cat}^{-1} h^{-1}[62].

Additionally, the Guo group employed Mn, Cu, and K for the modification of iron carbide and combined it with a CuZnAlZr catalyst to design a tandem catalytic system. In situ DRIFTS results indicate a more pronounced formation of ethoxy species (*C_2H_5O) species over the tandem catalytic system compared to a single catalyst, demonstrating that the powder mixing is advantageous for the formation of this crucial intermediate. The authors additionally investigated the impact of different mixing methods on catalytic performance. Accordingly, powder mixing of both catalysts yielded the best results with a CO_2 conversion of 42.1% and a HA selectivity of 15.5% at 300 °C, 3 MPa, and 6000 mL g_{cat}^{-1} h^{-1}. Unsuitable proximity of the different functionalities in dual-bed approaches resulted in considerable decreases in both CO_2 conversion and HA selectivity [61].

To further emphasize the importance of different integration modes on the efficiency of tandem catalytic systems, Fig. 11 illustrates the influence of the adopted integration modes on CO_2 conversion and HA selectivity in five tandem catalytic systems. As depicted in the figure, the dual-bed design is widely utilized in current tandem catalytic CO_2-to-HA systems due to its operational convenience. However, because of the differences in reaction pathways as well as physical and chemical properties of each catalyst, the dual-bed configuration is not necessarily the most effective. On the contrary, the majority of tandem catalytic systems requires closer proximity of their different functionalities for optimal performance. Compared to powder mixing, only the Co_2C||CuZnAl system exhibits higher S_{HA} and X_{CO2} in the dual-bed configuration.

It is worth mentioning that the arrangement sequence of the dual-bed significantly influences the selectivity to higher alcohols. For instance, in the Co_2C-CuZnAl system, Co_2C||CuZnAl dual bed with feed gas flow from Co_2C bed to CuZnAl possesses a HA selectivity of 18%,

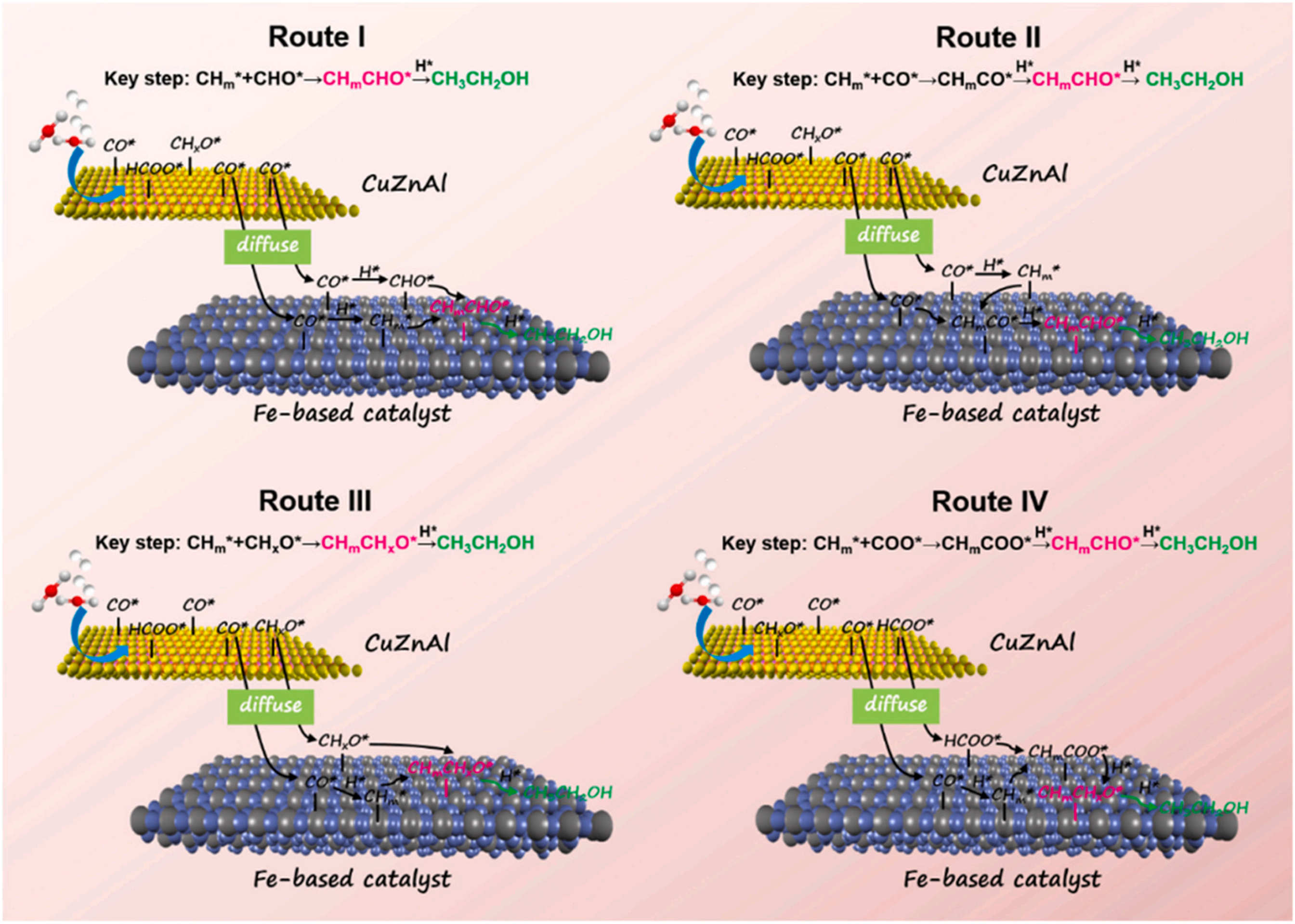

Fig. 9. Reaction network for ethanol synthesis from CO_2 hydrogenation via the Na-Fe@C/K-CuZnAl multifunctional catalyst.
Reprinted with permission from Ref. [147].

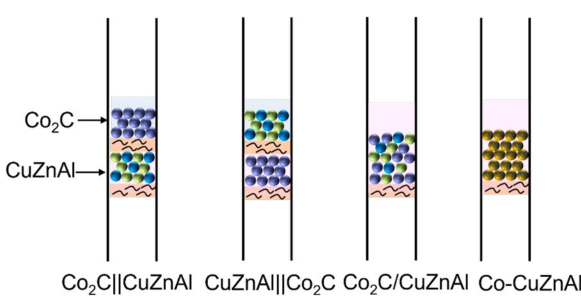

Fig. 10. The multifunctional tandem catalysts combined with Co_2C and CuZnAl.
Reprinted with permission from Ref.[62].

which is much higher than that of 0.2% over CuZnAl||Co_2C dual bed with an inverse packing order. The author hypothesized that the reason for this phenomenon is that the synergistic effect of C-C coupling and elementary reaction in the CuZnAl||Co_2C catalyst no longer exists, so methane is the main product.[62] After thorough studies of literature on tandem catalytic systems for the CO_2 hydrogenation to higher alcohols, most of the reported tandem catalytic processes show a predominant reliance on CuZnAl(Zr)-based methanol synthesis (MS) catalysts for initiating the RWGS reaction for CO generation. Subsequently, CO couples with various intermediates to form higher alcohols. However, there are different catalysts capable of forming alternative stable intermediates, such as light olefins, carboxylic acids, or methanol, that are worth considering. These catalysts could serve as alternative initial components in lieu of CuZnAl(Zr)-based catalysts, initiating a cascade of reactions leading to the production of higher alcohols. Hence, later sections will discuss such alternatives in further detail.

4.2. Reverse water gas shift reaction and conversion of syngas to higher alcohols

4.2.1. Reverse water gas shift reaction

The reverse water gas shift reaction describes the endothermic reaction of CO_2 and H_2 to form CO and H_2O. Here, CO is part of the industrially applied synthesis gas, consisting of CO and H_2. Given the well-established conversion pathways of syngas into valuable chemicals and fuels, the RWGS reaction has gained substantial attention in research. Early-stage research predominantly centered on metal oxide catalysts, including CeO_2, In_2O_3, ZrO_2, ZnO, CuO, Fe_3O_4, and MnO, owing to their abundant oxygen vacancies and resulting favorable CO_2 activation [93,148,149]. Nonetheless, as mono-metal oxides are susceptible to sintering and prone to poisoning, a shift in research focus towards composite oxide catalysts was required. Table 3 shows several state-of-the-art catalysts for RWGS reactions. These catalysts can be broadly categorized into two types: (i) noble metal-based catalysts and (ii) non-noble metal-based catalysts. The extraordinary RWGS activity exhibited by these catalysts stems from their remarkable CO_2 activation and C-O bond breaking capabilities. In recent years, researchers have

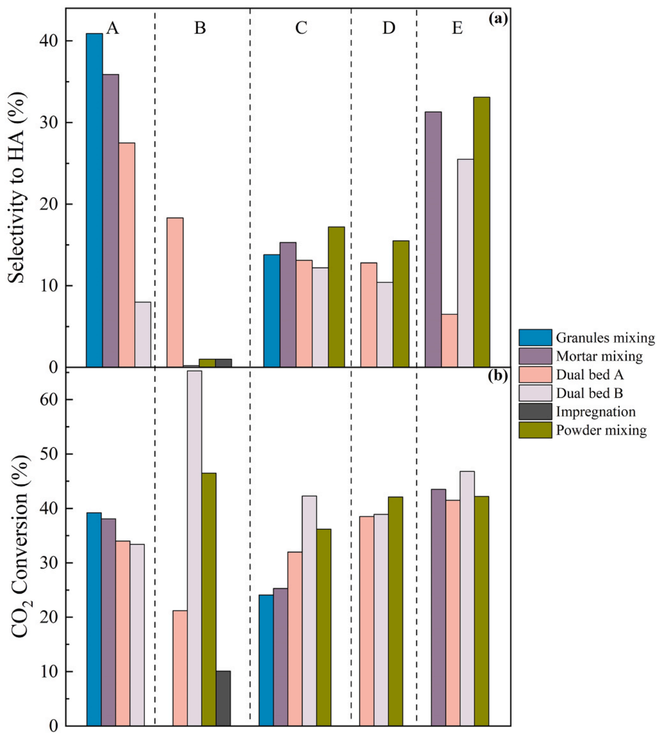

Fig. 11. Effect of different integration modes on catalysts during tandem catalysis: (a) effect on higher alcohol selectivity and (b) effect on CO_2 conversion. Catalysis system **A:** 2%Na-Fe@C & 5%K-CuZnAl, $p = 5$ MPa, $T = 320$ ℃, GHSV $= 4500$ mL g_{cat}^{-1} h^{-1}[147], **B:** Co_2C & CuZnAl, p = 5 MPa, T = 250 ℃, GHSV $= 12000$ mL g_{cat}^{-1} h^{-1}[62], **C:** CuZnAl & K-CuMgZnFe, $p = 5$ MPa, $T = 320$ ℃, GHSV $= 6000$ mL g_{cat}^{-1} h^{-1}[63], **D:** MnCuK-FeC & CuZnAlZr, $p = 3$ MPa, $T = 300$ ℃, GHSV $= 6000$ mL g_{cat}^{-1} h^{-1}[61], **E:** 4.7KCuFeZn & CuZnAlZr, $p = 5$ MPa, $T = 300$ ℃, GHSV $= 3000$ mL g_{cat}^{-1} h^{-1}[146], Bed A and Bed B represent the two sequences in which the feed gas is passed into the reactor bed in a system using a dual bed.

made significant advancements in the development of non-noble metal-based catalysts exhibiting high RWGS activity. Notably, supported Cu-based systems such as Cu/Al_2O_3, Cu/CeO_2, and $Cs\text{-}Cu\text{-}CeO_2$ have emerged as prominent examples. These catalysts have demonstrated the ability to achieve CO_2 conversion and CO selectivity exceeding 50% and 90%, respectively [150–152]. As a consequence of such remarkable catalytic performance, the utilization of highly active non-noble metal-based RWGS catalysts in the initial catalytic step of tandem reactions became a reasonable option. An efficient RWGS reaction effectively leads to a gas mixture consisting, among others, of carbon monoxide and hydrogen, effectively offering a synthesis gas mixture for subsequent reaction steps.

4.2.2. *Synthesis of higher alcohols from syngas*

In the wake of the oil crisis in the 1970 s, the world witnessed an upsurge in research endeavors focused on exploring alternative energy sources, driven by the imperative to reduce reliance on non-renewable oil resources [160]. Among the crucial areas of investigation, the conversion of syngas emerged as a prominent field. Syngas, derived from carbon-containing sources such as coal, natural gas, and biomass, present a versatile feedstock for the production of diverse valuable chemicals and fuels. Within this context, the synthesis of higher alcohols holds particular significance. In general, three primary reactions occur in HAS from syngas: the alcohol-formation reaction (Eq. 1), the hydrocarbon-formation reaction (Eq. 2), and the water-gas-shift reaction (Eq. 3). Notably, these reactions are characterized by their exothermic nature, that requires low-temperature and high-pressure as process conditions [161]. However, an inherent challenge lies in minimizing the formation of by-products, mainly CO_2 and hydrocarbons, to achieve high yields of desired higher alcohols. Hence, an efficient catalyst design is required to suppress the CO_2 as well as hydrocarbons formation and enhance HA selectivity.

$$nCO + 2\,_nH_2 \rightleftharpoons C_nH_{2n+1}OH + (n-1)H_2O \quad (1)$$

$$nCO + (2n+1)\,H_2 \rightleftharpoons C_nH_{2n+2} + nH_2O \quad (2)$$

$$CO + H_2O \rightleftharpoons CO_2 + H_2 \quad (3)$$

Catalysts employed for the syngas conversion to higher alcohols can be divided into four major groups: (i) Rh-based, (ii) Mo-based, (iii) modified Fischer-Tropsch-synthesis and (iv) methanol synthesis catalysts [77,162]. Table 4 displays the catalytic performances under their respective reaction conditions for a selection of such catalysts.

Among the commonly investigated catalytic systems, Rh-based catalysts hold considerable potential for the synthesis of C_{2+}-oxygen-containing compounds through CO hydrogenation, as Rh exhibits a dissociation ability weaker than Co, Fe, and Ru, yet stronger than Pd, Pt, and Ir. For the synthesis of higher alcohols, Rh-based catalysts are considered as ideal systems, and intensive studies are performed on the effect of promoters. Accordingly, transition and alkali metal additives, such as Mn, Fe, and Li, are found to be beneficial to carbon chain growth and suppressing hydrocarbon formation [175,163,176]. Besides, support materials that ensure the high dispersion of Rh nanoparticles (NPs) confer advantages in higher alcohol formation [177]. Notably, ordered mesoporous carbon (OMC)-supported Rh NPs display remarkable catalytic performance due to the highly dispersed and size-controlled

Table 3
Several current state-of-the-art RWGS catalysts.

Catalyst	H_2/CO_2 ratio	T^a /℃	p^b /MPa	WHSV[c] /L·g_{cat}^{-1}·h^{-1}	X^d_{CO2} /%	S^e_{CO} /%
$In_2O_3\text{-}CeO_2$[149]	1:1	500	n.a.	48	20	100
Fe-oxide NPs[153]	1:1	600	n.a.	1.2	38	85
Pt/CeO_2[154]	4:1	290	0.1	600	21.7	100
Au/TiO_2[155]	4:1	400	n.a.	7.5	35	100
Rh@S-1[156]	3:1	500	1.0	3.6	52	80
$Pd\text{-}In/SiO_2$[157]	1:1	600	0.1	60	10	100
NiO/CeO_2[158]	1:1	700	0.1	3	40	100
$Cs\text{-}Cu\text{-}CeO_2$[150]	9:1	500	0.1	30	70	90
Cu/CeO_2-hs[151]	3:1	600	0.1	300	50	100
Cu/Al_2O_3[152]	3:1	600	0.1	n.a.	50	100
$Cs\text{-}Mo_2C$[159]	4:1	500	n.a.	12	42	90

[a] Temperature,
[b] pressure,
[c] weight hourly space velocity,
[d] CO_2 conversion,
[e] CO selectivity.

Table 4
Current typical Syngas-to-HA catalysts.

Catalyst	H_2/CO ratio	T^a /°C	p^b /MPa	WHSV[c] /$L{\cdot}g_{cat}^{-1}{\cdot}h^{-1}$	X^d_{CO} /%	S^e_{HA} /%
Rh-Mn-Li/Fe/SiO_2 [163]	2	300	3	10	28	33
Rh-Mn-Li-Fe/CMK-9 [164]	2	320	3	12	14	55
Rh/$Ce_{0.8}Zr_{0.2}O_2$ [165]	2	275	2.4	2.4	27	40
$Ni_{0.5}Mo_1K_{0.5}$-15%CNTs [166]	1	320	8	4	13.3	32
K-Co-MoS_x-0.13 [167]	1	360	8.7	4.5	18.7	38.5
K-MoP/SiO_2 [168]	1	275	8.2	3.96	8	21
Cu-Co-Red/10%CNTs [169]	2	260	3	3.9	60.8	48.5
Co_1/CeO_2 [170]	2	260	5	9	1.0	14.1
$La_{0.9}K_{0.1}Co_xFe_{1-x}O_3/ZrO_2$ [171]	2	260	4	6	14.3	38.9
Cs_2O-Cu/ZnO/Al_2O_3 [172]	2	310	5.4	3.75	42.6	23.1
K-La-Cu/ZrO_2 [173]	2.5	360	10	3	63	20
P-Cu-Zn-Al [174]	2	250	4.5	n.a.	19	52.9

[a] Temperature,
[b] pressure,
[c] weight hourly space velocity,
[d] CO conversion,
[e] selectivity to higher alcohols.

properties of the aggregated Rh NPs, achieving higher alcohols selectivity of 55% [164]. Furthermore, strong metal-support interactions have also been reported to enhance catalytic activity. For instance, the introduction of Zr^{4+} ions to CeO_2 imparts basicity, resulting in a $Ce_{0.8}Zr_{0.2}O_2$ support simultaneously exhibiting optimized reduction, acidity, and basicity properties. As a result, Rh/$Ce_{0.8}Zr_{0.2}O_2$ exhibits excellent selectivity towards higher alcohols, achieving a selectivity of 40% [165]. Despite the excellent activity demonstrated by Rh-based catalysts for higher alcohol synthesis, their wide-scale application is hindered by their immense cost.

Aiming at cost competitive catalytic systems, extensive research has been conducted on Mo-based catalysts in the context of syngas-to-higher alcohols conversion, owing to their remarkable resistance to sulfur and their favorable selectivity towards alcohols [79]. Most studies on Mo-based catalysts have primarily focused on compounds wherein Mo is combined with ligands such as C, O, S, or P [77]. When single Mo catalysts are employed for CO hydrogenation, they predominantly generate light hydrocarbons and CO_2, with only a limited production of alcohols. Therefore, to improve HA yields, it becomes necessary to employ Mo-based catalysts in conjunction with other elements, particularly alkali and group VIII metals. An exemplary catalyst, $Ni_{0.5}Mo_1K_{0.5}$, demonstrates favorable HA selectivity (32%) through the promotion of K and Ni, while the presence of doped carbon nanotubes facilitates the modulation of surface-active species adsorption and H_2 activation [166]. In a study by Xi et al., the influence of Co-promotion on product selectivity of K-Co-MoS_x catalysts was investigated. It was observed that K-Co-MoS_x-0.13, containing the highest quantity of Co-Mo-S and Co_9S_8 phase, exhibited the highest selectivity towards higher alcohols (38.5%) and an unprecedented selectivity of 28.7% towards C_{3+} alcohols. The exceptional results were attributed to the intimate contact between the K-modified Co_9S_8 phase and the Co-promoted Mo-S phase [167]. Furthermore, Mo-based catalysts with active centers such as MoP, MoO_x and Mo_2C have also demonstrated commendable performance in HAS [168,178–180]. Consequently, Mo-based catalysts are considered as promising alternatives to noble-metal based catalysts. However, it should be noted that Mo-based catalysts require harsh reaction conditions, often requiring temperatures of approximately 300 °C and pressures of 10 MPa, which currently leads to difficulties in its industrial application.

Moreover, considerable research efforts have been dedicated to the development of modified Fischer-Tropsch-Synthesis-based catalysts for the synthesis of higher alcohols [180–182]. Among the metal catalysts, Co has shown enhanced HAS activity owing to its superior carbon chain growth capability [120] and relatively low water-gas shift reaction activity [183]. However, Co also exhibits a strong tendency to dissociate CO, requiring exploration of different Co sites and the addition of suitable additives to suppress excessive hydrogenation. For this purpose, Gao et al. synthesized CuCo-layered double hydroxides (LDHs) on the surface of carbon nanotubes. The resulting Cu-Co alloy exhibited excellent dispersion, facilitated by the robust interaction between CuCo-LDHs and CNTs. The high thermal conductivity of the catalyst effectively inhibited the formation of hydrocarbons and CO_2, thus imparting favorable selectivity towards higher alcohols [169]. In addition to different promoters, the presence of diverse Co sites on catalysts has proven beneficial for HAS [60]. The Co_1/CeO_2 catalyst, for instance, provides enhanced opportunities for the synthesis of higher alcohols through the synergistic effects of two types of Co sites: dissociative adsorption CO sites (Co^0) and non-dissociative adsorption CO sites ($Co^{\delta+}$) [170]. Furthermore, the incorporation of Co_2C sites has been demonstrated to effectively increase HA selectivity. The $La_{0.9}K_{0.1}Co_xFe_{1-x}O_3/ZrO_2$ catalyst, derived from perovskite precursors, exhibits abundant oxygen vacancy sites due to the incorporation of Fe. The synergistic interplay among three distinct sites, namely Co^0, Co_2C, and oxygen vacancy sites, confers exceptional catalytic activity to the system [171]. Generally, FTS-based catalysts hold tremendous potential for the conversion of syngas into higher alcohols owing to their cost-effectiveness, mild reaction conditions, and favorable catalytic activity.

Cu-based catalysts, particularly Cu/ZnO/Al_2O_3, have emerged as prominent catalysts for methanol synthesis, gaining extensive research attention over the past century [114,184–186]. These modified Cu-based catalysts possess remarkable potential for HAS owing to the exceptional non-dissociative CO-adsorption properties of Cu. Similarly, to Cu-based systems in CO_2 hydrogenation to HA, alkali promoters have proven beneficial to increase HA selectivity from syngas. Sun et al. investigated the influence of Cs on the performance of Cu/ZnO/Al_2O_3 catalysts. The presence of Cs facilitated the coupling of pivotal intermediates such as *HCO and *H_2CO, thereby leading to improved selectivity towards higher alcohols [172]. Besides, phosphorus-promoted Cu-Zn-Al catalysts, devoid of alkali or FTS metals, exhibited commendable performance. The phosphorus addition increased the quantity of weak acid sites on the catalyst, facilitated the reduction of Cu^+ species, and promoted the synergistic effects between Cu and Al [174]. In brief, modified Cu-based catalysts for methanol synthesis also bare potential in HA synthesis. Overall, in recent years, catalysts for the conversion of syngas to higher alcohols have made considerable progress, wherefore a significant increase in market share of HAS from syngas is to be expected.

4.2.3. Combined RWGS reaction with syngas-to-HA

It is apparent from the chapters above, that considerable progress has been made in catalyst research for both RWGS and syngas conversion

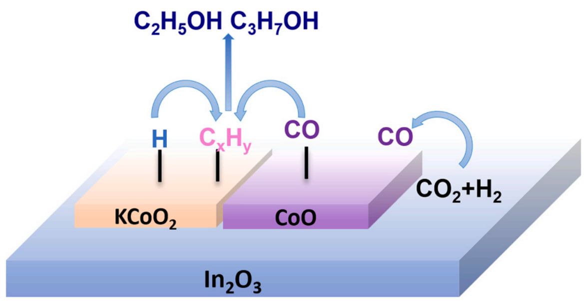

Fig. 12. Proposed mechanism for the formation of hydrocarbon and oxygenated products over K-Co-In_2O_3 catalyst.
Reprinted with permission from Ref.[131].

reactions, and that the combination of these two state-of-the-art reactions may enable a more efficient conversion of CO_2 to higher alcohols. In fact, Kusama et al. proposed a widely accepted mechanism for the generation of CO by RWGS followed by further reactions to produce higher alcohols during CO_2 hydrogenation [98]. As shown in Fig. 3, CO_2 initially reacts via the RWGS reaction to form CO* intermediates, which are subsequently dissociated to CH_3* and then further hydrogenated to form hydrocarbons. However, undissociated CO* can also be inserted into CH_3* to form ethanol. As previously mentioned, this CO-mediated mechanism [25] is a widely accepted mechanism for a significant fraction of CO_2-to-HA catalysts [37,44,187–189]. In recent years, multiple research groups effectively employed in situ DRIFTS as a powerful technique to investigate the formation of various reaction intermediates under reaction conditions. Amongst, CO species, generated by RWGS reaction, were identified as a crucial reaction intermediate on a variety of different catalysts, ranging from K-CuMgZnFe over Na-Co/SiO_2 to K-Co-In_2O_3 [46,117,131]. Moreover, the suggested reaction mechanism presented by Witoon et al. within their investigation of K-Co-In_2O_3 catalysts underscores its alignment with the CO-mediated pathway, as depicted in Fig. 12. They proposed that the existence of oxygen defects on the In_2O_3 surface promotes the transformation of CO_2 into CO, with $KCoO_2$ and CoO species assuming crucial responsibilities in the dissociation of CO and the subsequent insertion of CO into the C_xH_y intermediates that arise from CO dissociation. This complex series of stages ultimately leads to the synthesis of higher alcohols [131].

Drawing support from the CO-mediated mechanism, it is reasonable to consider a physically mixed catalysts approach to harness the CO generated from the RWGS reaction for subsequent syngas conversion to synthesize higher alcohols. For example, the two-stage bed reaction system by Guo et al. (illustrated in Fig. 13a) combined the low-temperature RWGS catalyst $CuZnK_{0.15}$ with the high-temperature modified FTS $Cu_{25}Fe_{22}Co_3K_3$ catalyst to obtain a CO_2 conversion of 32.4% and a mixed alcohol yield of 131 mg mL^{-1} h^{-1} at 350 °C and 6 MPa [39]. The authors identified a combination of a thermal coupling and product coupling effect between the two-stages to be responsible for the catalytic performance. The effect of catalyst proximity on CuZnAl/K-CuMgZnFe catalysts on the catalytic performance was studied by Xu et al. and is visualized in Fig. 13(b) [63]. The HA selectivity initially increases with increasing proximity but ultimately decreases as the two catalysts become less distant from each other. This again highlights the sensitivity of catalyst proximity in tandem catalytic systems. Furthermore, it is crucial to address certain issues and consider the following specific recommendations to attain an optimized catalyst design:

(1) The reaction conditions are the key factor to consider first, due to the different thermodynamic limitations of the RWGS reaction (Table 1 entry 2) and the formation of higher alcohols (Table 1 entries 4–6). Hence, the successful implementation of a tandem reaction system requires combining components that exhibit robust RWGS reaction activity at low temperatures and showcase HAS activity at elevated temperatures.

(2) Although Cu-Zn-Al catalyst systems stand as exemplary RWGS active components, it is worth noting that a series of metal or metal oxide catalysts such as Fe, In, Ce, Zr, also demonstrate commendable RWGS activity. These catalysts present intriguing prospects and merit comprehensive exploration to assess their viability as potential alternatives to the Cu-Zn-Al system.

(3) It is crucial to recognize that different catalysts correspond to distinct reaction mechanisms, which result in performance variations. Consequently, the performance of catalysts in different mixing modes is not necessarily transferable. It is therefore worthwhile to explore different mixing modes of multiple catalysts to make HAS more

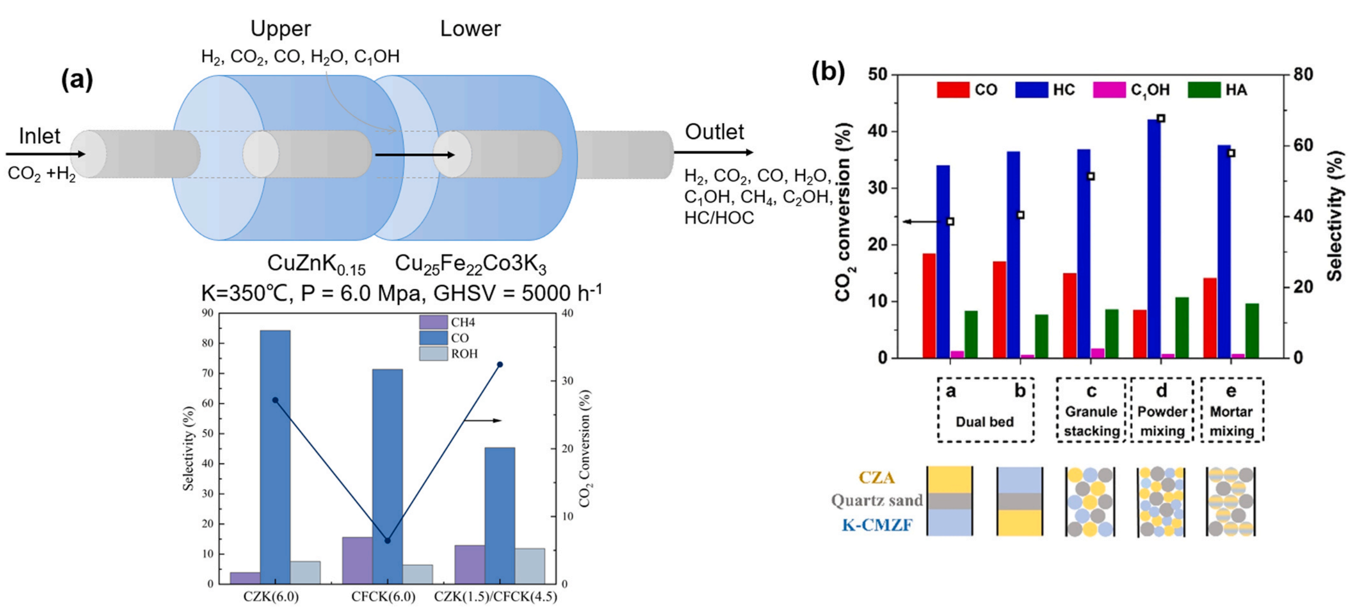

Fig. 13. (a) A two-stage bed reaction system designed by Guo et al. for the synthesis of higher alcohols by CO_2 hydrogenation. (b) CO_2 conversion and products selectivity. Reaction conditions: 5 MPa, $CO_2/H_2 = 1/3$, 6 L g_{cat}^{-1} h^{-1}, and 320 °C. CZA: CuZnAl and CMZF: CuMgZnFe.
(a) Reprinted with permission from Ref.[39] Results of CO_2 hydrogenation over the catalysts packed in different manners. (b) Reprinted with permission from Ref. [63].

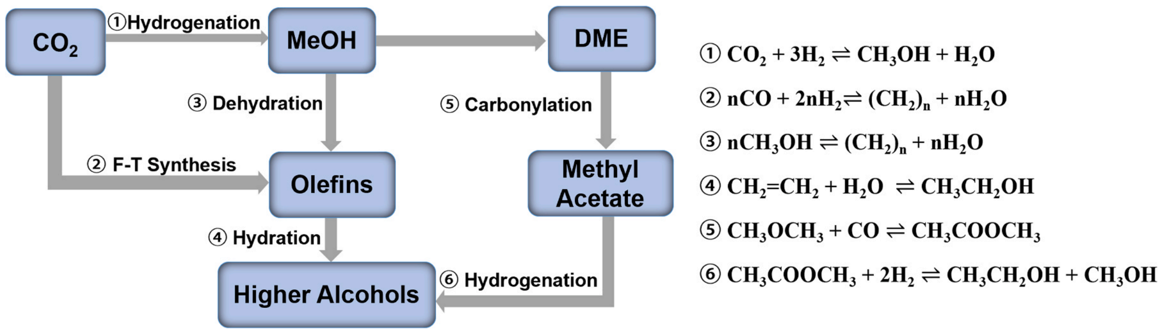

Fig. 14. Multiple synthesis routes of CO_2-to-HA based on olefins as key intermediates.

desirable.

4.3. Combined CO_2 to olefins and olefins to alcohols

The hydration of olefins to higher alcohols is already a well-established process. Its combination with an efficient CO_2 conversion to olefins would therefore enable a novel tandem pathway for the synthesis of higher alcohols. In general, the conversion of CO_2 to olefins can be categorized into two primary pathways (Fig. 14): (i) the direct hydrogenation of CO_2 to olefins, and (ii) the indirect conversion, predominantly through the hydrogenation of CO_2 to methanol followed by its subsequent conversion to olefins. Within the latter pathway, the Methanol-to-Olefins (MTO) process also consists of two key routes. The first involves the direct dehydration of methanol to yield olefins, while the second entails the dehydration of methanol to Dimethyl Ether (DME), followed by the conversion of DME to olefins. Notably, the DME to olefins route represents a promising emerging process due to lower energy requirements and reduced equipment costs compared to traditional MTO.[190] However, it must be noted that HAS via the DME pathway results in at least four distinctive reaction steps and thus growing complexity. As a result, this discussion will primarily focus on the following two processes: (1) the direct hydrogenation of CO_2 to olefins and (2) the hydrogenation of CO_2 to methanol, subsequently followed by its conversion to olefins. Fig. 14 gives an overview of different synthesis routes for CO_2 hydrogenation to higher alcohols via olefins intermediates.

4.3.1. Hydrogenation of CO_2 to olefins via FTS route

Currently, light olefins are mainly produced by thermal cracking of crude oil-based naphtha, a process that not only requires large amounts of energy but also emits large quantities of CO_2 [191]. The direct conversion of CO_2 to light olefins is therefore not only attractive because of potential cost savings but also mitigates the greenhouse effect of CO_2. As mentioned above, the direct hydrogenation of CO_2 to olefins consists of consecutive RWGS reaction (Table 1 entry 2) and FTS reaction (Eq. 4) [192]. The latter reaction is mainly catalyzed by Fe-based, Co-based and Ni-based systems, while the direct CO_2 hydrogenation to olefins is predominantly catalyzed by Fe-based catalysts due to their lower methanation activity at high reaction temperatures [122],[193]. In recent years, various promoted Fe-based catalysts have been investigated in the FTS-to-olefins process with a special focus on possible promoters. As a result, a regulation of electronic properties was attributed to alkali metal promoters, such as K, Na, Rb, and Cs, while transition metal promoters, including Zn, Co, Cu, V, and Mn, have been utilized to modulate the catalyst's structure [194–199]. In addition, multiple studies highlighted the optimization potential of supported Fe-based catalysts owing to

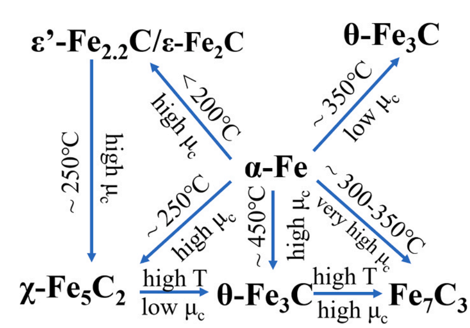

Fig. 16. Conditions of iron carbide phases transformation. Reprinted with permission from Ref.[207].

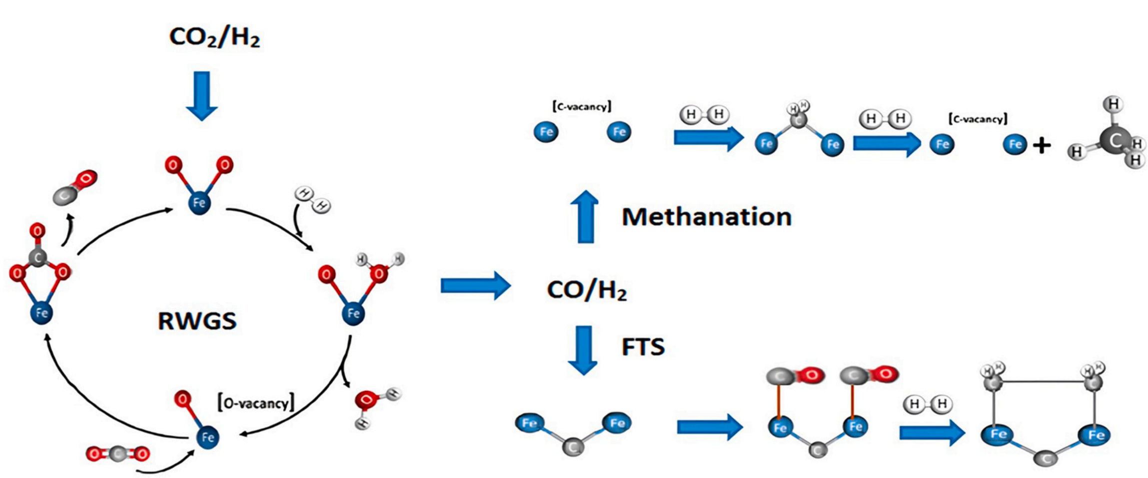

Fig. 15. Schematic diagram of RWGS, FTS and methanation reactions for CO_2 hydrogenation on Fe-based catalysts. Reprinted with permission from Ref.[203].

Table 5
Recent catalysts for CO_2 hydrogenation to olefins via FTS route.

Catalyst	H_2/CO ratio	T[a] /°C	p[b] /MPa	WHSV[c] /L·g_{cat}^{-1}·h^{-1}	X^{d}_{CO2} /%	$S^{e}_{olefins}$ /%	S^{f}_{CH4} /%
10Mn-Fe_3O_4[198]	3	350	2	4	44.7	46.2(C_2-C_4)	22
5%Na-Fe-oxide[208]	3	290	1.5	10	34.7	62(C_2-C_7)	26
Na-Zn-Fe[194]	3	340	2.5	15	38	42(C_2-C_4)	13
C-2Fe-1Zn/K[209]	3	320	2	1	54.8	54.1(C_2-C_4)	21.7
Co_1Fe_2[210]	3	320	2	8	40.9	42.5(C_2-C_4)	22.9
$ZnCo_{0.5}Fe_{1.5}O_4$[197]	3	320	2.5	4.8	49.6	36.1(C_2-C_4)	18.9
NaSrFe[211]	3	320	3	8	40.5	24.9(C_2-C_3)	8.9
FeNa/ZrO_2[212]	3	320	2	9	32.7	65.2(C_2-C_7)	26.7
15Fe-K/m-ZrO_2[213]	3	320	1.5	10	38.8	42.8(C_2-C_4)	30.1
Fe-Co/K-CL-Al_2O_3[214]	3	360	2	5.4	41.6	41.2(C_2-C_4)	32.2
0.58%Zn-FeCo/K-Al_2O_3[215]	3	340	2	9	46.5	40.4(C_2-C_4)	n.a.
0.8Fe-0.1 K@N-OMC[216]	3	320	3	4.8	54.5	60.4(C_2-C_4)	12.8

[a] Temperature,
[b] pressure,
[c] weight hourly space velocity,
[d] CO_2 conversion,
[e] selectivity to light olefins (CO-free),
[f] selectivity to methane.

different metal-support interactions [200–202].

$$nCO + 2nH_2 \rightleftharpoons (CH_2)_n + nH_2O \quad \Delta H_{298}^{\circ} = -152 \text{ kJ/mol} \tag{4}$$

The specific pathways for both olefin and methane formation over Fe-based catalysts were summarized by Landau et al. (Fig. 15) [203]. Throughout the reaction, Fe exists in various forms and undergoes continuous evolution, wherein different types of Fe play distinct roles [204]. Notably, Fe_3O_4 displays high activity in the RWGS reaction, while Fe^0 and Fe-carbides exhibit the capacity to adsorb and activate CO, leading to the formation of hydrocarbons [205]. These distinctive reactivities can be attributed to the different structures of the iron carbides formed during Fe carburization. Recent advancements in in situ characterization techniques enabled researchers to identify several critical phases of Fe during carburization, including χ-Fe_5C_2, θ-Fe_3C, ε'-$Fe_{2.2}C$, ε-Fe_2C, and Fe_7C_3 [206]. The phase transition conditions of various iron carbides are summarized in Fig. 16 [207]. Despite recent progress in identifying active species, the dynamic and complex nature of the carbide phases poses significant barriers in elucidating comprehensive structure-activity relationships.

Table 5 provides an overview of recently published catalysts for the CO_2 hydrogenation to olefins. The group of Jiang identified a Mn-modification of Fe_3O_4-microsphere catalysts to facilitate the reduction of Fe_3O_4, ultimately preventing excessive hydrogenation of intermediates and leading to excellent light olefins selectivity [198]. It is noteworthy to mention the promotional effect of Na on iron oxide catalysts as Wei et al. achieved remarkable selectivity towards C_2-C_7 olefins over such catalysts [208]. In situ XRD and in situ Raman spectroscopy investigations confirm that the interaction between Na and the catalyst inhibits the hydrogenation of surface Fe_5C_2 and graphitic carbon species, thereby suppressing alkane formation.

Besides, bimetallic Fe-based catalysts display impressive activity in olefin synthesis, with the Co_1Fe_2 bimetallic catalyst derived from $CoFe_2O_4$ spinel exhibiting an activity of 1810.8 mg g_{cat}^{-1} h^{-1}, surpassing that of conventional Fe-based catalysts. In situ XRD, Mössbauer effect spectroscopy (MES), Temperature-programmed hydrogenation (TPH), and XPS analyses reveal a structural evolution of Co_1Fe_2 over $CoFe_2O_4 \rightarrow (Co_xFe_{1-x})O \rightarrow Co_xFe_y \rightarrow χ\text{-}(Co_xFe_{1-x})_5C_2$, which promotes olefin synthesis [210]. Similar trends were observed over another spinel-based $ZnCo_{0.5}Fe_{1.5}O_4$ catalyst. Its excellent performance can be attributed to several factors: (1) the addition of Co reduces the χ-Fe_5C_2 phase responsible for C-C coupling, thus weakening its coupling ability; (2) the CoFe alloy promotes the formation of Co_2C species, effectively inhibiting methanation; (3) formation of the θ-Fe_3C phase weakens the catalysts hydrogenation ability and prevents secondary hydrogenation of alkanes [197].

Additionally, the choice of catalyst supports in Fe-based catalysts significantly influences the catalyst's structure and performance evolution [217]. Liu et al. investigated the impact of various supports (SiO_2, Al_2O_3, CNT, and ZrO_2) on the synthesis of olefins by CO_2 hydrogenation. The results indicate that the supports regulate the Fe_3O_4/Fe_xC_y ratio as well as the composition of Fe_xC_y. Notably, ZrO_2 with a carbon-rich surface possesses a stronger modulating ability and weaker H_2 adsorption ability, resulting in lower methane selectivity [212]. Moreover, different crystalline forms of the same support and varying pore sizes also naturally contribute to performance disparities [213,215].

In conclusion, it can be stated that the influence of both promoters as well as supports in Fe-based catalysts on the product distribution in the CO_2 hydrogenation to olefins through the FTS route has been extensively researched. Current catalysts display notable differences in CO_2 conversion, ranging from 32.7% to 54.8%. This signifies the excellent ability of these catalysts to activate CO_2. Moreover, the selectivity towards light olefins falls within a desirable range of 36.1% to 60.4% (C_2-C_4). However, although most catalysts achieve remarkably low CH_4 selectivity, few Fe-based systems still struggle with undesirably high methanation activity. Based on the aforementioned literature analysis, it is evident that additives and supports contribute to the formation of specific active phases, which in turn fulfill distinct functionalities in their respective catalytic cycles. Consequently, the key to design a selective catalyst for CO_2 hydrogenation to olefins lies in the adjustment of the various active phases present during the reaction. By reasonably regulating the ratio of each phase, catalysts can be tailored to maximize olefin production, thereby establishing a foundation for subsequent olefin hydration to higher alcohols.

4.3.2. CO_2 to olefins via methanol synthesis route

The second pathway to synthesize olefins from CO_2 hydrogenation, besides the FTS route, involves methanol synthesis followed by methanol-to-olefins (MTO) reactions. It can be categorized into two subtypes: (i) The hydrogenation of CO_2 forms methanol as a reaction product, which is converted in a separate MTO reaction. (ii) The methanol-mediated route involves methanol only as a crucial intermediate in the reaction, which is subsequently converted to light olefins. Regardless of the chosen pathway, the approach involving methanol as an intermediate always encompasses the CO_2-to-methanol reaction and the subsequent MTO reaction (refer to Table 1, entry 3 and Eq. 5).

$$nCH_3OH \rightleftharpoons (CH_2)_n + nH_2O \tag{5}$$

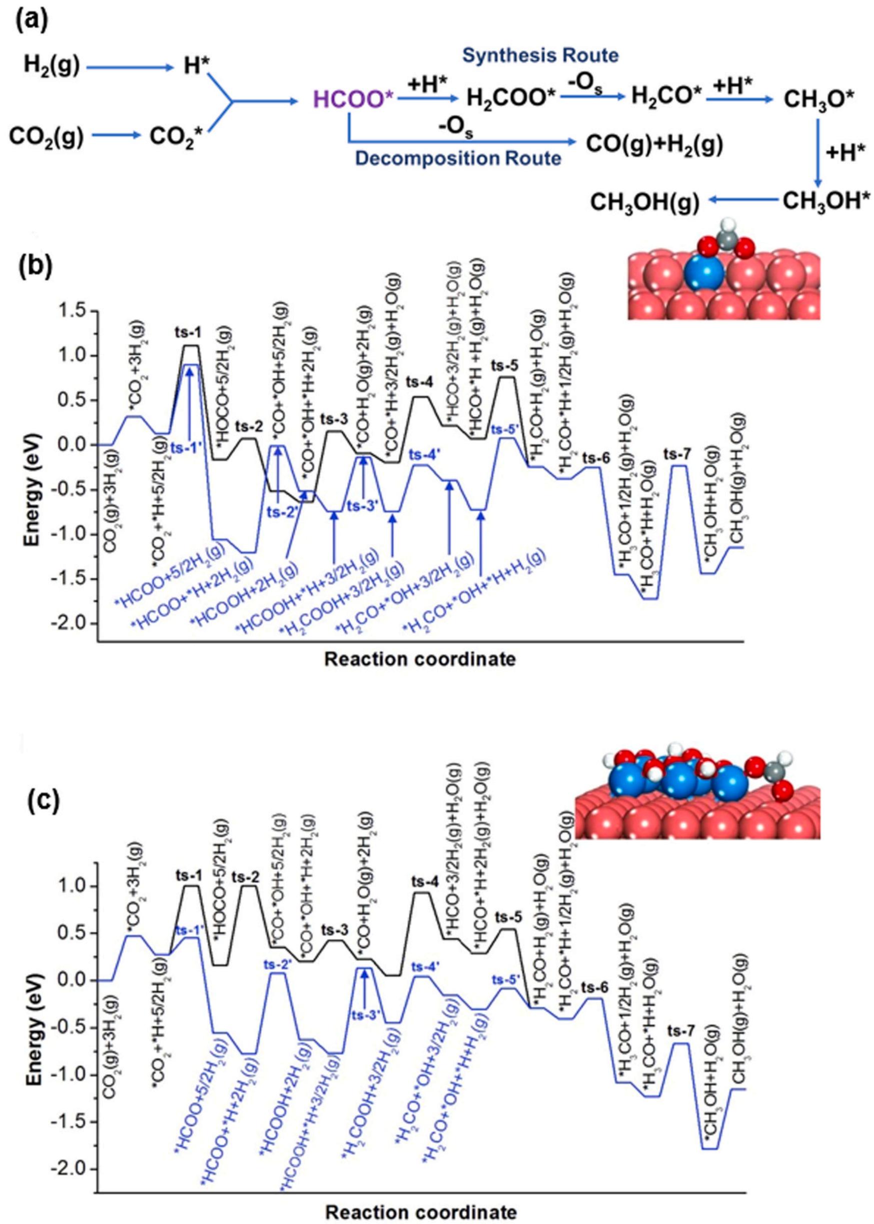

Fig. 17. (a) The methanol synthesis mechanism for the reaction on ZnO. ts, transition state. (Inset) Structures of *HCOO on ZnCu(211) (b) and ZnO/Cu(111) (c). Cu, brown; Zn, blue; O, red; H, white; C, gray.
(a) Reprinted with permission from Ref.[220] Potential energy diagram for the hydrogenation of $CO_{2(g)}$ to $CH_3OH_{(g)}$ on (b) ZnCu(211) and (c) ZnO/Cu(111) via the formate and RWGS + CO-hydro pathways. (b) Reprinted with permission from Ref.[221].

4.3.2.1. CO_2 hydrogenation to methanol. The synthesis of methanol from CO_2 hydrogenation (Table 1 entry 3) has been extensively studied since the beginning of the last century [218]. Among a multitude of different catalysts, Cu/Zn/Al_2O_3, invented by ICI, has emerged as one of the most active catalysts for methanol synthesis from CO_2 hydrogenation [219]. In 1983, Bowker proposed a first reaction mechanism via a crucial formate intermediate as depicted in Fig. 17 (a). Here, hydrogen initially dissociates and subsequently reacts with adsorbed CO_2 to form a formate intermediate, which is then further hydrogenated to produce methanol [220].

In a significant contribution to the understanding of Cu/ZnO catalysts, Kattel et al. have provided a comprehensive elucidation of the active site involved in these catalytic systems. The authors employed DFT calculations to investigate the mechanism of CO_2 hydrogenation to methanol over ZnCu(211) (Fig. 17b) and ZnO/Cu(111) (Fig. 17c) model catalysts, considering two primary reaction pathways: (i) the RWGS reaction producing CO intermediates, which are then hydrogenated to methanol (RWGS + CO-hydro pathway), and (ii) CO_2 hydrogenation to *HCOO intermediates, followed by hydrogenation and dissociation to methanol (formate pathway). The authors concluded that the formate pathway is favored on both ZnCu(211) and ZnO/Cu(111) sites due to hindered *CO and *CHO hydrogenation in the RWGS + CO-hydro pathway. Experimental and computational results indicate that CO_2 activation over ZnO/Cu(111) and ZnCu(211) follows similar patterns after ZnCu undergoes surface oxidation under reaction conditions, transforming Zn into ZnO, ultimately enabling comparable activity to ZnO/Cu sites [221]. Due to their excellent performance and toxicity resistance, Cu/ZnO-based catalysts remain promising candidates for achieving short-term CO_2 emission reductions via methanol synthesis [222]. Research based on non-traditional Cu/ZnO catalysts proved challenging in several aspects, mostly due to thermodynamic limitations, low selectivity, and low stability. Hence, only by overcoming these

difficulties $Cu/ZnO/Al_2O_3$ catalysts can eventually be replaced by the next generation of catalysts.

In recent years, a series of In_2O_3-based catalysts for CO_2 hydrogenation to methanol have entered the limelight. Various synthesis methods and pretreatments have been employed to prepare In_2O_3 catalysts with abundant oxygen vacancy sites for efficient CO_2 activation [223]. Notably, Shi et al. successfully prepared In_2O_3 with controlled mixed phases (i.e., comprising cubic and hexagonal phases) using a solvothermal method. Their investigation presented a pronounced mixed-crystal effect, leading to a significant enhancement in oxygen vacancy formation and medium-strength CO_2 adsorption. The mixed-phase catalyst achieved nearly 70% methanol selectivity and a STY of 3.2 $mmol_{MeOH}\ g_{cat}^{-1}\ h^{-1}$ at 300 °C, 3 MPa and 7500 mL $g_{cat}^{-1}\ h^{-1}$, which nearly doubled the activity of its single-phase counterpart.[224] Interestingly, promoting In_2O_3 with ZrO_2 can modify its electronic structure, thereby increasing the number of oxygen vacancies in In_2O_3 and facilitating the synthesis of methanol [56]. Yang et al. discovered strong electronic interactions between In_2O_3 and monoclinic ZrO_2 (m-ZrO_2) in the In_2O_3/m-ZrO_2 catalyst. This interaction resulted in a methanol selectivity of up to 84.6% and a CO_2 conversion of 12.1%. Investigations by in situ Raman spectroscopy revealed the presence of highly dispersed In-O-In structures on m-ZrO_2. XPS studies and DFT calculations further validated that the electron transfer between m-ZrO_2 and In_2O_3 increased the electron density of In_2O_3, promoting the formation of formate intermediates and thus enhancing methanol yield [225].

Moreover, supported Ni/In_2O_3 catalysts demonstrated exceptional catalytic performance, again as a result of enhanced oxygen vacancy formation and highly dispersed Ni species that facilitated strong metal-support interactions. Remarkably, this catalyst exhibited exclusive methanol selectivity below 225 °C, while at 275 °C and 5 MPa, it still achieved a methanol selectivity of 64% with a CO_2 conversion of 18.5%, resulting in a methanol yield of 17.6 $mmol_{MeOH}\ g_{cat}^{-1}\ h^{-1}$ [226]. Another notable example is the Co_3O_4 @In_2O_3 composite oxide catalyst prepared by a MOF-mediated method, which achieved a remarkable maximum methanol STY of 20.8 $mmol_{MeOH}\ g_{cat}^{-1}\ h^{-1}$. Impressively, this catalyst maintained a high methanol selectivity of 87% even after 100 h of continuous operation under industrial conditions. The exceptional performance of this catalyst is attributed to the structural tunability of MOF-derived catalysts, enabling the optimized distribution of In dopants within the metal-organic matrix, thereby enhancing In utilization for outstanding catalytic performance.[227].

In addition to In_2O_3-based catalysts, another noteworthy catalytic system is the ZnO-ZrO_2 catalyst [228–234]. Wang et al. reported a binary metal oxide ZnO-ZrO_2 solid solution catalyst, which exhibits excellent methanol synthesis activity and extraordinary stability for 500 h [228]. At 5 MPa and 315 to 320 °C, methanol selectivity reaches as high as 86% to 91%, respectively. Both experimental results and theoretical calculations indicate that the excellent catalytic activity can be attributed to the synergistic effect between the Zn and Zr sites. Moreover, the ZnO-ZrO_2 catalysts also possess sintering resistance at high temperatures and show anti-sulfur poisoning properties, advantages not available in the $Cu/ZnO/Al_2O_3$-based catalysts. Wang et al. explored the interactions among these three components by introducing a Cu component into ZnO-ZrO_2 [229]. The resulting Cu-ZnO-ZrO_2 catalyst exhibits high activity for methanol production with 18.2% CO_2 conversion and 80.2% methanol selectivity at 220 °C and 3 MPa. Furthermore, Han et al. synthesized a ZnO-ZrO_2 solid solution through an evaporation-induced self-assembly (EISA) process, leading to an ordered mesoporous structure [231]. The catalyst exhibits a high methanol STY of 22.1 $mmol_{MeOH}\ g_{cat}^{-1}\ h^{-1}$ at 320 °C and 5.5 MPa. Various characterization results indicate that the excellent activity is related to the larger specific surface area and an increased number of H_2 and CO_2 activation sites of the catalyst.

In summary, the current generation of $Cu/ZnO/Al_2O_3$-based catalysts has demonstrated the capability for industrial application in methanol synthesis (MS). In_2O_3-based and ZnO-ZrO_2-based catalysts prepared through various methods possess significant potential to replace the traditional $Cu/ZnO/Al_2O_3$ catalysts. Consequently, utilizing methanol synthesis catalysts for efficient methanol production, followed by the indirect production of olefins, is a highly reliable approach.

4.3.2.2. Methanol-to-olefin. In 1977, researchers at Mobil Oil Corporation initially discovered that, under a sub-atmospheric pressure condition, methanol can be selectively transformed into a mixture of light olefins using zeolite catalysts like HZSM-5, triggering extensive attention [235]. Subsequently, Chang et al. optimized the reaction parameters for methanol-to-olefins (Eq.5) over ZSM-5 catalysts in a fixed-bed reactor. They found that combining high temperature (e.g., 500 °C) and low catalyst acidity (e.g., $SiO_2/Al_2O_3 = 1670$) favor the synthesis of light olefins. The authors achieved a methanol conversion of 98.2% under 0.1 MPa pressure and LSHV of 10 h^{-1} [236]. However, the susceptibility of ZSM-5 to form coke on its external surface, accompanied by poisoning of active sites or pore blockage, results in catalyst deactivation [237]. Therefore, research attention shifted towards SAPO-34 zeolite catalysts, which possess unique pore sizes and geometric shapes. In comparison to ZSM-5, SAPO-34 has a reduced pore size of 3.5 Å, restricting the diffusion of heavy hydrocarbons and branched alkanes, thereby enhancing the selectivity towards light olefins [238,239]. Additionally, SAPO-34 exhibits milder acidity than ZSM-5, reducing the extent of hydrogen transfer reactions and suppressing the formation of paraffinic products [240]. Marchi and Froment investigated the catalytic activity of SAPO-34 catalysts in the MTO reaction and identified pores with diameters smaller than 0.45 nm as well as Brønsted acid sites from aluminum hydroxyl groups to play a crucial role in synthesizing light olefins. At 480 °C and 0.1 MPa, the authors achieved nearly 100% methanol conversion and high selectivity towards C_{2-4} olefins (i.e., 90% to 95% in the hydrocarbon product fraction).[241].

This high catalytic efficiency translates to a high industrial applicability of MTO processes. Currently, there are mainly four industrial MTO technologies, namely: (i) D-MTO by Dalian Institute of Chemical Physics (DICP), (ii) S-MTO by Sinopec, (iii) MTO by UOP/Norsk Hydro, and (iv) MTP by Lurgi.[240] Table 6 summarizes the technical parameters of the industrial installations of MTO technologies. It becomes apparent that SAPO-34 zeolites are the most commonly employed catalysts, and the reaction generally occurs at 400–550 °C and 1–5 atm.

However, despite its already established industrial success, future research on MTO-catalysts may focus on enhancing SAPO-34's resistance to coke deposition, further optimizing SAPO-34 performance, and exploring new zeolite components to achieve higher yields. In summary, the MTO process to convert methanol into olefins is a mature process and consequently holds great promise as part in an integrated CO_2-to-olefin process.

4.3.2.3. Synthesis of light olefins via methanol-mediated route. Although the FTS route from CO_2 to olefins has made significant progress, it is imperative to acknowledge the inherent limitations associated with this approach. One notable challenge lies in the intricate manipulation of the C-C bond on the surface of FTS catalysts [192.] Furthermore, conventional FTS catalysts encounter difficulties in surpassing the Anderson-Schulz-Flory (ASF) product distribution, which naturally imposes constraints on the C_2-C_4 selectivity. In contrast, implementing methanol synthesis (MS) catalysts offers a promising alternative to address these limitations and achieve higher olefin selectivity. Typical composite catalysts often consist of metal oxides like CuO, ZnO, In_2O_3 in combination with zeolites. Table 7 provides some MS-based zeolite--modified catalysts for the CO_2-to-Olefins process.

Tan et al. evaluated the performance of a mixed catalyst consisting of In_2O_3/ZrO_2 metal oxide and SAPO-34 zeolite for CO_2 to olefins conversion. Remarkably, this synergistic combination yielded an exceptional light olefins selectivity of 77.6% [242]. Fig. 18 depicts the

Table 6
Industrial installations of the methanol-to-olefins technology (pilot/demonstration-scale or commercial-scale, post-2000) [240].

No.	MTO technology	Licensor/operator	Scale	Catalyst	Process conditions (*T*, *p*, WHSV)	Catalyst performance (*C*, *S*, *Y*)
1	UOP/Hydro advanced MTO (with olefin cracking)	UOP (Feluy, Belgium)	0.2 MM MTPA	SAPO-34 (attrition-resistant formulation)	400–550 °C, 1–4 atm	~100%, 80%+ C-selectivity to C_2, C_3, olefins
2	D-MTO (Dalian Institute of Chemical Physics)	Shenhua China Energy (Mongolia, China)	0.6 TPA	SAPO-34	400–550 °C, 4–5 atm	N/A
3	S-MTO (Sinopec MTO)	Sinopec	0.2 MM TPA	SAPO-34	400–550 °C, 1–5 atm	N/A
4	MTP (Lurgi)	Shenhua Group with Ningxia Provincial Govt. (Ningxia, China)	0.5 MM TPA	SAPO-34	N/A	N/A
5	MTP (Lurgi)	Datang Int'l Power with China Datang (Mongolia, China)	0.5 MM TPA	SAPO-34	N/A	N/A
6	Honeywell UOP	Jiangsu Sailboat Petrochemical company (Jiangsu Province, China)	0.8 MM TPA	SAPO-34	400–550 °C, 1–5 atm	~100%, ~85% to C_2 +C_3
7	Honeywell UOP	Wison China Energy (Ningxia Province, China)	0.3 MM TPA	SAPO-34	400–550 °C, 1–5 atm	~100%, ~85% to C_2 +C_3

Table 7
Recent catalysts for CO_2 hydrogenation to olefins via the methanol-mediated route.

Catalyst	H_2/CO ratio	T^a /°C	p^b /MPa	WHSV[c] /$L \cdot g_{cat}^{-1} \cdot h^{-1}$	$X^d{}_{CO2}$ /%	$S^{e=}_{C2\text{-}C4}$ /%	$S^f{}_{CH4}$ /%
In_2O_3/ZrO_2-SAPO-34[242]	2.65	400	2	2.16	20.17	77.59	5.35
NiCu/CeO_2-SAPO-34[243]	3	375	2	12	17	78	2.1
(CuO-ZnO)-kaolin-SAPO-34[244]	3	400	3	1.8	57.6	63.8	11.4
$ZnAl_2O_4$/SAPO-34[245]	3	370	3	5.4	15	87	0.7
6.7%ZnO-Y_2O_3/SAPO-34[246]	4	390	4	1.8	27.6	83.9	1.8
In_2O_3-$ZnZrO_x$-SAPO-34-S-a[247]	3.04	380	3	9	17	85	1.6
$Zn_{0.5}Ce_{0.2}Zr_{1.8}O_4$/H-RUB-13[248]	6	350	3.5	4.8	30.1	72.7	6.4
$ZnZrO_x$-Bio-ZSM-5[249]	3	380	3	2	10	64.4	< 5
Fe/K-6Ca/ZSM-5[250]	3	375	3	5	47	38	15
$InCeZrO_x$/H-SAPO-34[251]	3	300	3	4	6.6	85.6	3.8
In_2O_3-ZrO_2/SAPO-5 (0.3Si)[252]	3	300	3	4	6.7	83	2

[a] Temperature,
[b] pressure,
[c] weight hourly space velocity,
[d] CO_2 conversion,
[e] selectivity to C_2-$C_4^=$ (CO-free),
[f] selectivity to methane.

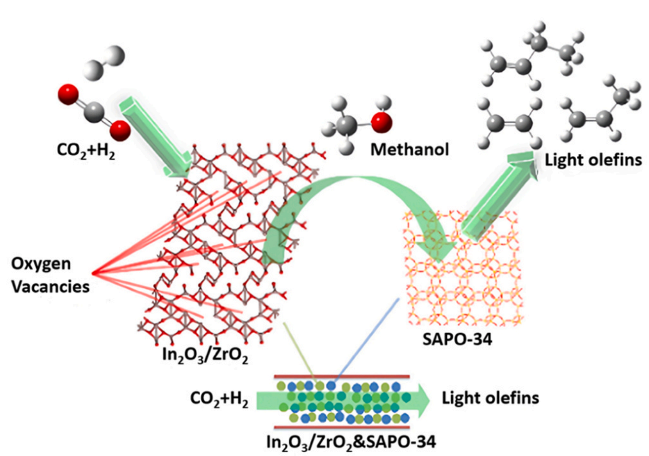

Fig. 18. Process of CO_2 hydrogenation to olefins over In_2O_3/ZrO_2-SAPO34 catalyst proposed by Tan et al.
Reprinted with permission from Ref.[242].

proposed reaction pathway, wherein CO_2 and H_2 initially form methanol on the oxygen vacancy surface of In_2O_3/ZrO_2. Subsequently, methanol traverses the intricate network of SAPO-34 zeolite channels, facilitating its transformation into light olefins. Similarly, Wang et al. designed (CuO-ZnO)-kaolin/SAPO-34 catalysts by leveraging kaolinite as a precursor, facilitating an even dispersion of CuO-ZnO particles on its surface and leading to maximized exposure of active sites for CO_2 conversion. Furthermore, the (CuO-ZnO)-kaolin/SAPO-34 catalysts exhibited a domain-limiting effect, effectively impeding methanol dissipation and thus enhancing MTO efficiency.[244].

Another noteworthy composite catalyst was developed by combining $Zn_{0.5}Ce_{0.2}Zr_{1.8}O_4$ with H-RUB-13 zeolite. This composite catalyst displayed notable activity for propylene and butene production. In-depth characterization by in situ DRIFTS, XPS, as well as DFT calculations elucidated the pivotal role of the rapid generation of methanol on $Zn_{0.5}Ce_{0.2}Zr_{1.8}O_4$, which subsequently facilitated its conversion to olefins over the H-RUB-13 zeolite. Furthermore, an increased Si/Al ratio in the zeolite framework alleviated the excessive hydrogenation of olefins and promoted the diffusion of propylene and butene from the zeolite structure [248]. Finally, the group of Li designed a layered porous bio-ZSM-5 derived from natural rice husk as a template and mixed it with $ZnZrO_x$ nanoparticles to prepare a multifunctional catalyst for CO_2 hydrogenation to light olefins. Bio-ZSM-5 showed better catalytic activity and stability compared with commercial ZSM-5. The in situ DRIFTS results shed light on the crucial role of $*CH_xO$ as the key intermediate formed over $ZnZrO_x$, which subsequently migrated to the acid sites on bio-ZSM-5, leading to the formation of olefins [249].

As shown in Table 7, SAPO-34 and ZSM-5 zeolites are the most commonly employed zeolite materials to catalyze the synthesis of olefins via the methanol-mediated route at 300–400 °C and 2–4 MPa. This exceptional research interest may be attributed to the hierarchical pore structure and moderate amount of Brønsted acid sites of SAPO-34 [247], which enable effective inhibition of methanation and high selectivity for light olefins. ZSM-5, on the other hand, has demonstrated a tendency for

synthesizing aromatics [253–255], while displaying comparably lower selectivity for light olefins. Based on the currently rather narrow choices of applied zeolites, there is still great potential to explore more suitable porous structures to accomplish a more efficient conversion of methanol to light olefins.

4.3.3. Hydration of olefins to higher alcohols

Hydration of olefins to alcohols is a widely applied industrial process and is currently one of the main sources for alcohol synthesis [256] It bears the potential to replace grain fermentation methods and thus alleviate the issue of grain shortage. The most representative example of olefin hydration is the production of ethanol through the hydration of ethylene (Eq. 6). The two main pathways for olefin hydration are (i) the sulfuric acid hydration method, which has been to this day largely replaced due to the severe corrosiveness of sulfuric acid by (ii) the direct hydration. In the latter process, proposed by Shell in 1947, ethylene reacts with water vapor to produce ethanol [257].

Acid catalysts, such as phosphoric acid or heteropoly acids, supported on carriers like silica or clay, have practical applications in the vapor-phase hydration of olefins like ethylene or propylene. This process leads to the formation of their respective alcohols (Eqs. 6, 7), [258] For instance, the production of ethanol from ethylene and water employs a silica-supported phosphoric acid catalyst, operating within the temperature range of 235–265 °C and a reaction pressure of 3–10 MPa [259]. These conditions enable STY_{EtOH} between 98 and 143 g L^{-1} h^{-1}, while achieving ethylene conversions of 7.8% to 10.4%. The synthesis of iso-propanol, on the other hand, was performed at 185–200 °C and 3.9 MPa over silica-supported phosphoric acid, achieving STY_{iPrOH} between 208 and 238 g L^{-1} h^{-1} [259]. However, supported acid catalysts are known to induce reactor corrosion, making it unsuitable for long-term applications [260]. However, various solid acid catalysts, such as metal oxides [261,262], zeolites [256,263], and metal phosphates [260,264], have been discovered and tested in the hydration of olefins, demonstrating excellent activity [258].

$$CH_2{=}CH_2\ (g) + H_2O\ (g) \rightleftharpoons CH_3CH_2OH\ (g)\ \Delta H_{298}{}^{\circ} = -42\ \text{kJ/mol} \quad (6)$$

$$CH_2{=}CH - CH_3\ (g) + H_2O\ (g) \rightleftharpoons CH_3CH_2CH_2OH\ (g)\ \Delta H_{298}{}^{\circ} = -57{\cdot}2\ \text{kJ/mol} \quad (7)$$

Both the CO_2 to olefins and hydration of olefins to alcohols processes have been intensively studied and thus hold tremendous potential to effectively synthesize higher alcohols through their combination in tandem catalysis. Among the many alternatives, three potential combinations are discussed below.

(1) Combined direct CO_2 hydrogenation to olefins with olefins to alcohols.

Direct CO_2 hydrogenation to olefins generally occurs at 290–360 °C and 1.5–3 MPa, while olefins hydration occurs at lower temperatures (235–265 °C for ethylene and 185–200 °C for propylene) and higher pressures (3–10 MPa) [259]. Integrating both reactions via two separate reactors (Fig. 7, mode ①) lacks efficient heat and mass exchange between them. Although catalyst modification is necessary to match the rather different reaction conditions of both processes, mode ②-⑥ (Fig. 7) in one reactor can be employed to further increase the proximity between the two catalysts. Moreover, catalyst functionalities must be carefully chosen to prevent catalyst internal reactions and ultimately deactivation. For example, the catalysts for direct CO_2 hydrogenation to olefins may contain alkaline metals, which may react with acid functionalities used for olefins hydration. It therefore becomes apparent that rational catalyst design as well as proper selection of the integrating mode is of great importance for an efficient implementation of both reactions.

(2) Combined CO_2-methanol-olefins synthesis with olefins to alcohols.

As CO_2 hydrogenation to methanol, methanol to olefins, and olefins hydration to alcohols have been intensively studied separately, it is also possible to combine these reactions to synthesize higher alcohols. However, the reaction conditions for these reactions differ. CO_2 hydrogenation to methanol occurs at 200–350 °C and 3–5 MPa, while MTO is conducted at 400–550 °C and 0.1–0.5 MPa [240]. Since this proposed route needs to integrate three reactions, and the reaction temperatures of MTO (> 400 °C) and olefins hydration (< 265 °C) differ significantly as well, the integration into one continuous process poses significant challenges [259].

(3) Combined methanol mediated CO_2 to olefins with olefins hydration.

CO_2 hydrogenation to olefins via the methanol-mediated route in some cases can be performed at relatively low temperatures. For instance, In_2O_3-ZrO_2/SAPO-5 and $InCeZrO_x$/H-SAPO-34 catalyze CO_2 to olefins at 300 °C and 3 MPa. These conditions are relatively close to those of olefins hydration (for ethanol synthesis: 235–265 °C; 3–10 MPa [259]), making it possible to integrate the two reactions in one reactor (Fig. 7, mode ②-⑥) and tailoring the proximity between the two catalysts to optimize the heat and mass exchange.

4.3.4. Olefins hydroformylation

Olefins can also undergo metal-catalyzed olefin hydroformylation reactions (Eq. 8), where they react with synthesis gas to form aldehydes. This reaction was first proposed by Otto Roelen in 1938 and has since attracted extensive research in both academia and industry [265]. The produced aldehydes from olefin hydroformylation are important intermediates in large-scale chemical synthesis and can be further converted into widely used alcohols and carboxylic acids. Typical catalysts are homogeneous complexes based on $[HM(CO)_xL_y]$, where L can be either CO or an organic ligand. The activity order of transition metals in hydroformylation follows the order Rh > > Co>Ir, Ru > Os > Pt > Pd > > Fe > Ni. To date, the only industrially applied catalysts are Rh- and Co-based [266]. Rh-based catalysts exhibit the highest hydroformylation activity but suffer from high costs. Co-based catalysts not only have the economic advantage but also display good resistance to toxic components in the feedstock. Franke et al. provided a detailed summary of the practical applications of hydroformylation [267]. It is worth mentioning that tandem catalytic system based on

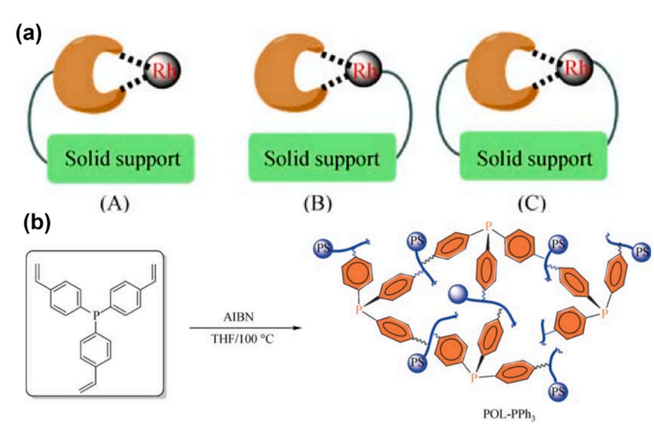

Fig. 19. (a) Strategies to immobilize Rh complex catalysts on solid supports: (A) ligand-immobilized catalysts, (B) Rh-immobilized catalysts, and (C) Rh and ligand simultaneously immobilized catalysts. (b) Synthesis of POL-PPh_3 via solvothermal polymerization of 3 V-PPh_3 ligands.
Reprinted with permission from Ref.[275].

Fischer-Tropsch synthesis and reductive hydroformylation have been developed for the synthesis of higher alcohols from syngas. Jeske et al. integrated solid Co-based FTS catalysts and molecular hydroformylation catalysts in tandem in a one-pot slurry phase, and this hybrid system of multiphase and homogeneous catalysis achieved ultra-high CO conversion (>70%) and higher alcohol selectivity (>50 wt%) at 200 ℃ and 12 MPa. The excellent catalytic activity is attributed to the rapid capture of the FT primary *1*-olefin by the molecular hydroformylation catalyst [268].

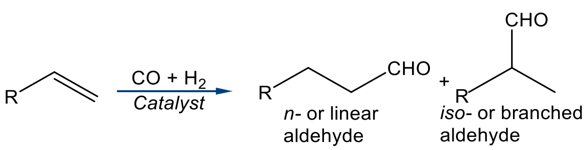

(8)

Recently, there has been a surge of interest in the study of heterogeneous catalysts for hydroformylation [269,270]. Two main strategies are currently explored to achieve the heterogeneous catalytic hydroformylation: solid support immobilized catalysts (Fig. 19 (a)) and porous organic ligand (POL)-supported catalysts (Fig. 19 (b)), both of which have shown promising results [271–274]. The former approach has been extensively investigated over the years, involving Rh immobilization (Fig. 19 (a) (A)), ligands (Fig. 19 (a) (B)), or a combination of both (Fig. 19 (a) (C)) on solid supports to achieve the heterogenization of homogeneous Rh-based catalysts. Unfortunately, these immobilized Rh-based catalysts have shown limitations in terms of their activity and selectivity compared to their homogeneous counterparts.[275] This is mainly attributed to the relatively low utilization of Rh metal and nanoparticles, as well as the low concentration of organic ligands near the metal species in the heterogeneous system.

In contrast, novel porous organic ligand (POL)-supported catalysts offer significant advantages due to their high concentration of crucial phosphine ligands within the catalytic framework. This characteristic facilitates the dispersion of Rh species and promotes the formation of Rh-P multiple bonds,[275] which play an important role in enhancing catalytic activity and stability. Consequently, these catalysts demonstrate great promise for industrial applications. Jiang et al. conducted tests using a series of 3 V-PPh_3 polymer supported single-site Rh catalysts in a fixed-bed reactor for the hydroformylation of olefins. The catalytic performance is summarized in Table 8, with reaction conditions set at 120 °C and 1 MPa. Remarkably, the obtained catalysts not only exhibit excellent catalytic activity and selectivity, achieving 96.2% ethylene conversion and 96.1% aldehyde selectivity, but also demonstrate great stability. Advanced characterization techniques, such as high-angle annular dark-field scanning transmission electron microscopy (HAADF-STEM) and Extended X-Ray Absorption Fine Structure (EXAFS), revealed that Rh atoms exist as single-site species, forming strong coordination bonds with exposed phosphorus atoms over the POL-PPh_3 support. Further analysis through ^{31}P MAS NMR and in situ IR experiments confirmed that the outstanding catalytic activity could be attributed to the similarity in catalytic functionality between Rh/POL-PPh_3 and the homogeneous $HRh(CO)(PPh_3)_3$ complex [276]. While the high cost of Rh still impedes industrial application, the exceptional hydroformylation activity exhibited by the POL-supported Rh-based catalysts makes them a compelling option to explore and further develop.

The subsequent hydrogenation of aldehydes to alcohols represents a significant industrial method with roots dating back to the mid-twentieth century [277]. Metal catalysts, including Cu, Ni, Co, as well as noble metals such as Pt, Pd, and Ru, are typically employed as the active components in these catalytic processes. Among these, Cu- and Ni-based catalysts are predominantly applied in industrial processes. The reaction temperatures, pressures and space velocities for the hydrogenation of aldehydes range from 150 to 300 °C, 1.5 to 4 MPa, and 3000 to 20000 h^{-1}, respectively [278]. However, industrial processes face a major challenge in suppressing various side reactions, particularly the condensation between aldehydes and alcohols, which results in significant downstream processing difficulties [279].

Generally, this route to synthesize higher alcohols involves the conversion of CO_2 to olefins, followed by olefins hydroformylation, and finally the hydrogenation of aldehydes to alcohols. As direct CO_2 hydrogenation to olefins as well as aldehyde hydrogenation generally occur at significantly higher temperatures (90–360 °C and 150 to 300 °C, respectively)[259],[278], the lower reaction temperature of olefins hydroformylation (i.e., ~120 °C) makes this tandem process unsuitable for modes ②-⑥ (Fig. 7), but would require a multi-reactor setup (Fig. 7, mode ①) to bridge the temperature differences.

4.4. Combined CO_2 to carboxylic acid and carboxylic acid hydrogenation to alcohols

Carboxylic acids, such as formic and acetic acid, evoke a wide range of applications in various industries [280,281]. Research on CO_2 conversion to carboxylic acids has also been extensively performed. The industrial synthesis of acetic acid typically involves methanol carbonylation based on the Monsanto process ($CH_3OH + CO \rightarrow CH_3COOH$) [281]. Currently, various emerging technologies for converting CO_2 into carboxylic acids have been developed [282–289]. For instance, Wang et al. achieved a 9.5% yield of acetic acid at 300 °C and 5 MPa by direct reduction of CO_2 over a specific hexagonal close-packed cobalt (HCP-Co) catalyst obtained by hydrothermal synthesis [290]. The experimental results showed that the CoO/Co^0 interface formed in situ played a key role in completing the CO_2 activation and realizing the subsequent C-C coupling. Moreover, the unique nature of the hydrothermal reaction can regulate the metal oxides/metals ratio on the catalyst surface, resulting in the formation of a stable CoO/Co interface. Through DFT calculations, the authors proposed a reaction pathway involving *CH_2 and HCOO as intermediates, which then combine to form CH_3COO^- through a carbene reaction.

Besides the hydrogenation process, acetic acid can be efficiently synthesized via the reaction of CO_2 with other readily available feedstocks (e.g., methane, methanol). Here, the direct conversion of CO_2 and CH_4 to acetic acid (Eq. 9) is a 100% atom-efficient process. Tu et al. have provided profound insights into this process, suggesting that the C-H bond breaking in CH_4, and the subsequent formation of C-C bonds are crucial for the reaction. Currently, conventional catalysts for this process consist of metals, metal oxides, and metal-modified zeolites [291]. However, the disparity in reaction conditions between different reaction systems is significant, with reaction temperatures ranging from 150 to

Table 8
Results of ethylene hydroformylation over various Rh catalysts.[a].

Catalyst	GHSV (h^{-1})	Rh loading (wt%)	Conversion (%)	Selectivity (%)	TOF (h^{-1})
Rh/POL–PPh_3	2000	0.125	96.2	96.1	4530
Rh/POL–PPh_3	2000	0.063	65.3	96.4	6166
$Rh(CO)_2(acac)/SiO_2$	2000	0.125	0.6	99.9	30
$HRh(CO)(PPh_3)_3/SiO_2$	2000	0.125	22.4	99.5	1091
Rh/POL–PPh_3	5000	0.125	88.8	95.4	10373
Rh/POL–PPh_3	5000	0.063	45.5	94.6	10534

[a] Reaction conditions: fixed-bed reactor, 120 ℃, 1.0 MPa, $C_2H_4:CO:H_2 = 1:1:1$, GHSV of $C_2H_4/CO/H_2 = 2000\ h^{-1}$.

500 °C and reaction pressures from atmospheric pressure to 2 MPa [292–295]. Rabie et al. achieved the synthesis of acetic acid in a continuous flow microreactor system by simultaneously feeding methane and CO_2 over Cu-loaded M+ -ZSM-5 catalysts (M=Li^+, Na^+, K^+ and Ca^{2+}). The catalytic activity increased in the order K>Na>Ca>Li. Furthermore, the results showed that over Cu^0-H-ZSM-5 catalysts, M^+ contributes to the enrichment of surface-active CO_2 in the form of carbonate and subsequently reacts with homolytically activated C-H. At 500 °C and $CH_4/CO_2 = 1$, the highest acetic acid yield of 395 μmol g_{cat}^{-1} h^{-1} was obtained [295]. Moreover, Shavi et al. synthesized montmorillonite (MMT) supported dual active site ZnO-CeO_2/MMT catalyst for the co-conversion of CO_2 and CH_4 to acetic acid. The dual active sites resolved the competitive surface adsorption of the reactant gases and maximized the yield of acetic acid. Accordingly, $STY_{acetid\ acid}$ of 625 μmol g_{cat}^{-1} h^{-1} was achieved at 300 °C and 0.2 MPa. The authors identified the atomic size of the active site as well as the presence of Lewis acid ZnO sites as crucial parameters in the carbonylation reaction of CH_4 [296].

Besides, the reduction of CO_2 by indirect hydrogen has also attracted research interest [297,298]. For example, Sagar et al. synthesized novel Mn-based ZrO_2 catalysts for the hydrogenation of pure CO_2 to formic acid and acetic acid via hydrazine monohydrate as the indirect hydrogen source. The presence of Mn in a lower oxidation state facilitated the decomposition of hydrazine to hydrogen, thus promoting the formation of carboxylic acid. An acetic acid yield of 906 μmol g_{cat}^{-1} h^{-1} was achieved at 225 °C and 1 MPa CO_2 [283].

$$CH_4 + CO_2 \rightleftharpoons CH_3COOH \tag{9}$$

The direct hydrogenation of carboxylic acids to higher alcohols, for example, the hydrogenation of acetic acid to ethanol (Eq.10), promises enormous potential due to a comparably accessible conversion. Commonly used catalysts include noble metal catalysts such as Pd, Pt, and Rh, as well as non-noble metal catalysts such as Cu, Ni, Zn, Cr [299]. Rakshit et al. prepared a series of Pt-Sn catalysts supported on SiO_2-Al_2O_3 for the hydrogenation of acetic acid to ethanol in a fixed-bed reactor. By adjusting the appropriate Pt/Sn ratio, optimal catalytic activity was achieved with 81% acetic acid conversion and 95% ethanol selectivity at 270 ℃ and 2 MPa [300]. Similarly, Pt-Sn/SiO_2 catalysts prepared by sol-gel method also exhibited excellent activity in a fixed-bed reactor, with 100% acetic acid conversion and 93% ethanol selectivity at 270 ℃ and 2.6 MPa. The outstanding catalytic performance was attributed to the sol-gel method promoting the synergistic interaction between Pt and Sn, resulting in a balanced effect between the exposed Pt surface and Lewis acid sites [301]. Although noble metal catalysts possess superior catalytic performance for this process, their high-cost limits large-scale applications. Hence, as potential catalytic systems, Cu-based catalysts are investigated and have shown excellent performance in the hydrogenation of acetic acid. Dong et al. investigated the performance of Cu_2In/SBA-15 catalysts for the hydrogenation of acetic acid and found a promotional effect of the Cu_2In alloy for the decomposition of acetic acid, while simultaneously inhibiting the formation of ethyl acetate. The catalyst achieved a 99.1% acetic acid conversion and a 90.9% ethanol selectivity at 350 °C and 2.5 MPa [85]. Further optimizing the catalyst led to Cu-MnO/SBA-15 with enhanced stability for up to 72 h time on stream [302].

In summary, combining CO_2 to carboxylic acid and carboxylic acid hydrogenation to alcohols is currently considered as a double-edged sword. At first sight, the reaction conditions between direct CO_2 hydrogenation to acetic acid and acetic acid hydrogenation to ethanol are reasonably similar as both may occur at temperatures between 250–350 °C, which would allow integrating both reactions in one reactor using integrating mode ②-⑥ (Fig. 7) to enhance heat and mass exchange. However, most direct CO_2 hydrogenation to carboxylic acid experiments are performed in liquid-phase using batch experimental systems under the addition of crucial additives, while others are either electrochemically or phototactically catalyzed [282–289]. This impedes a straightforward coupling with the continuously performed carboxylic acid reduction to alcohols. In addition, the processes are at significantly different stages in process maturity. While the latter part of the possible tandem process already reaches outstanding conversion and selectivity over comparably inexpensive catalysts, the conversion of CO_2 to carboxylic acids is clearly the bottleneck of this process. Consequently, further research is necessary to improve current catalyst generations towards higher carboxylic acid yields thus increasing the overall efficiency of the tandem system.

$$CH_3COOH_{(g)} + 2\,H_2 \rightleftharpoons C_2H_5OH_{(g)} + H_2O_{(g)}\ \Delta H_{298\ K} = -44.17\ kJ/mol \tag{10}$$

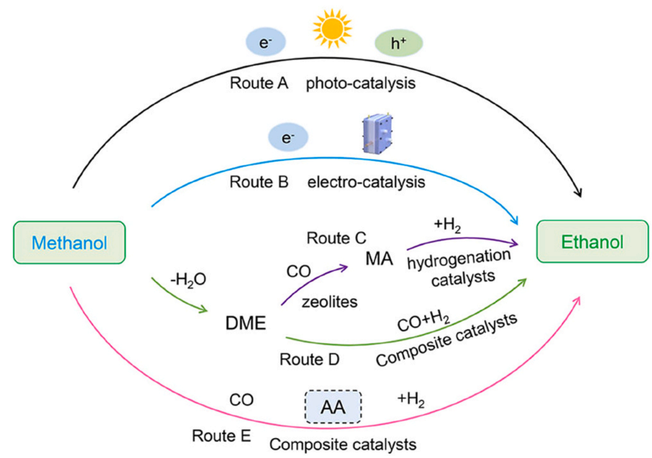

Fig. 20. Typical reaction processes to generate ethanol from methanol. Route A: Photocatalysis; Route B: Electrocatalysis; Routes C–E: thermal-catalysis. Reprinted with permission from Ref.[141].

4.5. *Methanol to higher alcohols*

The industrial-scale synthesis of methanol from CO_2 and H_2 has been achieved through thermal catalysis. Naturally, the conversion of methanol to higher alcohols through a non-olefin synthesis pathway is auspicious. Zhang et al. provided a comprehensive overview of several feasible routes for the conversion of methanol to ethanol (Fig. 20) [141]. Routes A and B in Fig. 20 involve photocatalysis and electrocatalysis, respectively, while routes C-E (Fig. 20) are based on thermal catalysis [303,304]. However, due to a low ethanol yield in photo-electrocatalytic CO_2 reduction, which is currently limited to only laboratory-scale research, thermal catalysis appears to have more sophisticated industrial application prospects. Route C (Fig. 20) involves dimethyl ether and methyl acetate as key intermediates [305]. In this process, methanol is first dehydrated to produce DME, which is then carbonylated to form methyl acetate. Finally, ethanol is produced by hydrogenation of methyl acetate. This pathway typically employs acid zeolite catalysts. It is noteworthy that a DME to HA process using coal derived syngas as feedstocks, based on key intermediates of methyl acetate, has been developed by the Dalian Institute of Chemical Physics and put into production in Shaanxi, China, in 2017, which can achieve an annual production of 100,000 tons of ethanol [306]. However, due to the excessive number of synthesis steps and high energy consumption, route C has been optimized to process D. In route D, DME reacts directly with synthesis gas to generate ethanol. However, current state-of-the-art catalysts generally achieve ethanol selectivity of less than 49% [307–309]. In route E (Fig. 20), methanol also directly reacts with synthesis gas to produce ethanol, but acetic acid is involved as a crucial intermediate.

It is noteworthy that Liu et al. recently achieved a successful cascade

conversion of methanol to higher alcohols at reaction temperatures ranging from 350 to 425 °C, all without the presence of metal catalysts and hydrogen. The process initiates by the reaction of methanol with CaC_2, leading to the formation of methyl vinyl ether (MVE). Subsequently, MVE undergoes hydrocracking into ethanol through the cleavage of the ether bond on the methyl side. Finally, the interaction between ethanol and methanol gives rise to n-propanol and iso-butanol. Under optimized conditions, HA yield of 54.6% was reached. The authors propose that a solid derivative of CaC_2, calcium methoxide ($Ca(OCH_3)_2$), may play a catalytic role in the dehydrogenation reaction [310]. Besides, Zhang et al. designed a tandem catalytic system using H-MOR-DA@C and Pt-Sn/CNT catalysts for methanol-to-ethanol conversion. This catalyst exhibited strong resistance to ethanol dehydration and achieved a methanol conversion rate of 98% with ethanol selectivity as high as 60% [141]. In summary, the direct synthesis of ethanol from methanol complements the multitude of various processes presented in this review, that are capable of efficiently synthesizing higher alcohols via indirect CO_2 hydrogenation. The high maturity of methanol synthesis from CO_2 hydrogenation coupled with a rather high-efficiency ethanol synthesis from methanol make this tandem catalysis system a promising candidate for higher alcohols synthesis.

5. Conclusion and future perspective

The synthesis of higher alcohols from the conversion of CO_2 is an extremely versatile and future-oriented process. It not only effectively mitigates greenhouse gas emissions, but also converts CO_2 into valuable chemicals and fuels to alleviate the energy crisis. Currently, the direct hydrogenation of CO_2 to higher alcohols faces challenges such as low CO_2 conversion rates, insufficient selectivity towards higher alcohols, and intense competition from side reactions. To address these persistent obstacles, we propose the construction of suitable tandem catalysis systems, which involve two modes: physically mixed, multifunctional catalysts and cascade reactors. The core of the tandem catalytic system lies in utilizing industrially mature or well-developed reaction processes to convert CO_2 and intermediate products, thereby achieving the multi-step synthesis of higher alcohols.

In the previous sections, we introduced the following conversion processes: (a) the "RWGS + syngas conversion" based on CO as a key intermediate; (b) the "olefin synthesis + olefin hydration" based on olefins as key intermediates; (c) the "olefin synthesis + olefin hydroformylation + aldehyde hydrogenation" based on aldehydes as intermediates; as well as (d) other processes based on carboxylic acids, methanol, and other intermediates. CO_2 undergoing these steps to form higher alcohols offers the following advantages: (i) the stability of indirect synthesis intermediates ensures the smooth progression of the tandem reactions compared to one-step synthesis processes; (ii) significant progress has already been made in the aforementioned multi-step processes, thereby enhancing the activation of CO_2 and increasing its conversion compared to the direct hydrogenation; (iii) since the multi-step tandem process changes the overall reaction mechanism, the competing reactions of the reaction system are well avoided, which enhances selectivity toward higher alcohols; (iv) in designing catalysts for the tandem system, only the rational mixing of various catalysts, selection of reactors, and control of reaction conditions need to be considered, providing a relatively convenient and macroscopic control approach. This eliminates the need for designing catalysts from the nanoscale through extensive characterization, ultimately saving cost and time. Table 9 provides an overview over the advantages/disadvantages of the various pathways.

Although a detailed life cycle analysis, as well as technological readiness level evaluation, are required, in this review, we attempted to evaluate a wide variety of individual chemical processes and their respective potential to synthesize higher alcohols from CO_2 in an integrated tandem catalysis system. However, for tandem catalysis systems to be competitive to the direct hydrogenation of CO_2 to higher alcohols, one must consider a multitude of influential parameters, for example, the technological readiness of the distinctive catalytic steps as well as their potential for efficient coupling process application. Therefore, as shown in Fig. 21, the application potential for the most important tandem catalysis systems for synthesizing higher alcohols from CO_2 is presented. More precisely, to enable a direct comparison, technological compatibility and maturity of the individual reactions are considered as key parameters. For technological compatibility, process parameters, thermodynamic aspects as well as a process-engineering perspective of the individual reactions comprising a tandem catalysis system are compared. This includes, among others, the respective process temperatures and pressures, endo- and exothermicity of reactions, and compatibility of established catalysts. Technological maturity, here, describes the development stage of a catalyst-reaction-combination. It is mainly influenced by catalytic efficiency (i.e. higher alcohols selectivity, substrate conversion), but also by catalyst costs and operational mode (batch/continuous; the use of additives). Based on these findings, each tandem process was rated on a scale of 1–10 in terms of their technological compatibility and maturity, respectively. As the technological compatibility of a tandem process is strongly dependent on the number of process steps, it was normalized to the number of process steps involved. As depicted in Fig. 21, among the various integration alternatives discussed in this review and the evaluation criteria employed, the tandem catalysis systems based on RWGS reaction + Syngas to higher alcohols as well as CO_2 to olefins + olefin hydroformylation + hydrogenation to higher alcohols display the best technological compatibility and process maturity.

However, there are still several challenges to be addressed to achieve satisfactory yields of higher alcohols through indirect conversion of CO_2 via tandem reactions:

Table 9
The advantages/disadvantages of the various pathways.

Reaction combination	Intermediate (s)	Advantages	Disadvantages/challenges
• RWGS • Syngas conversion	CO	• High CO_2 conversion • Stable formation of the intermediate CO	• Reaction conditions are difficult to modulate
• CO_2 hydrogenation to olefins via FTS route • Olefins hydration/hydroformylation	Olefins	• Excellent CO_2 activation capability • Easy to regulate reaction conditions	• High methanation activity • Conventional FTS struggles to overcome ASF distribution
• CO_2 to olefins via MS route • Olefins hydration	Methanol Olefins	• High light olefins selectivity • Excellent inhibition of methanation	• Low CO_2 conversion • High RWGS activity
• CO_2 hydrogenation to methanol • Methanol to olefins • Olefins hydration	Methanol Olefins	• The former two reaction processes have progressed significantly	• Multiple reaction steps and difficulties with tandem connections • Difficulties in reactor design
• Other routes	Olefins Carboxylic acid Methanol	• Scheme has potential to be further explored	• Lack of number of studies, feasibility needs to be further verified

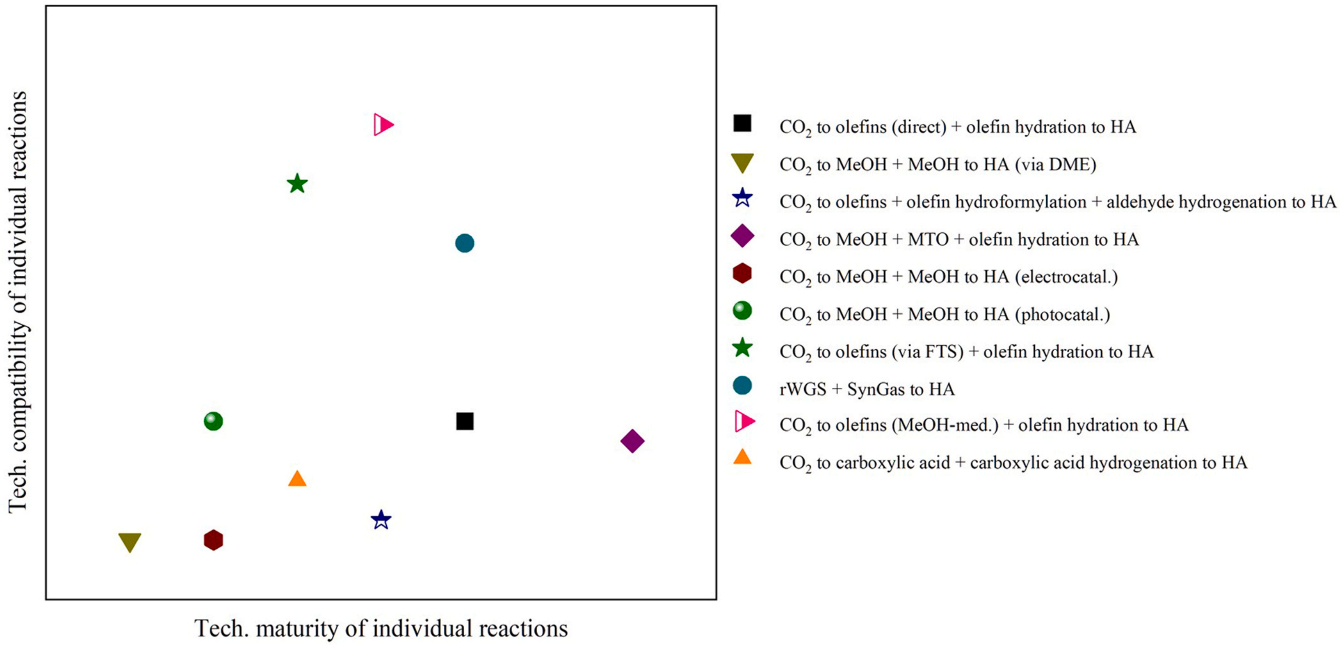

Fig. 21. Technological maturity vs. compatibility of individual reactions for potential tandem catalysis processes.

(a) Reasonable tandem configurations must be considered. Since the reaction networks of catalysts based on different active components vary, it is crucial to carefully analyze the specific circumstances and determine whether to employ physically mixed catalysts or cascade reactors. If the reaction conditions of the two catalysts are similar, and the interaction between different active components doesn't deteriorate their catalytic activity, a simple and effective approach is to use physical mixing. Here, the performance of different mixing modes needs to be evaluated to identify the optimal blending scheme. However, if the reaction conditions of the two catalysts differ significantly, using physical mixing may result in suboptimal activity. In such cases, employing multistage beds or cascade reactors is more appropriate.

(b) Catalyst poisoning challenges. In multi-step reactions, numerous byproducts, such as CO or H_2O, are formed in addition to the intermediate required for the subsequent reaction. These byproducts may not affect the catalyst in the first step but can poison the subsequent catalyst in the following steps. Therefore, when designing catalysts, it is essential to consider the tolerance of different catalysts to the potential intermediates that may lead to catalyst poisoning. Separating toxins from the reaction process using membranes or distillation is a feasible strategy. Moreover, the interaction between different active components may also lead to deactivation. Thus, the effects due to the increasing proximity of various catalytical active species should be further investigated.

(c) Catalyst design challenges. Although many of the mentioned multi-step processes in the previous sections are relatively mature, and other reactions, such as RWGS, synthesis gas conversion, and olefin synthesis, some catalysts still fall short in practical applications due to issues like demanding reaction conditions or low activity. Therefore, further in-depth research on these systems is necessary to enhance the conversion of CO_2 and the synthesis of higher alcohols to a higher level.

(d) Reactor design issues. Based on the descriptions in the previous chapters, the differences in reaction mechanisms and characteristics have led to variations in reaction conditions and reactor setups for each step of the reaction. Different reactors, such as fixed-bed, fluidized-bed, and batch reactors, along with significant temperature and pressure variations, pose challenges in constructing tandem reaction systems. Establishing a temperature gradient reaction system is a promising approach, for instance, in the case of RWGS reaction + syngas conversion reactions, which require a temperature reduction in the course of the process. Initially, one reactor stage can carry out the RWGS reaction at 400 to 600 °C, followed by a subsequent reactor stage at 200 to 300 °C for syngas conversion. This design offers the advantage of simultaneously meeting the conditions of both reactions while potentially saving energy consumption.

In summary, the tandem catalytic system concept presented in this review provides a new approach to the synthesis of higher alcohols based on CO_2. Although the conversion of CO_2 to higher alcohols through tandem reactions is still in the experimental research stage, its advantages are expected to outweigh the challenges it faces. We believe that further research on synthesis steps and exploration of catalyst design will mitigate the negative impacts of tandem reactions.

CRediT authorship contribution statement

He Yiming: Conceptualization, Formal analysis, Writing – original draft. **Müller Fabian H.:** Conceptualization, Formal analysis, Writing – original draft. **Palkovits Regina:** Conceptualization, Funding acquisition, Supervision, Writing – review & editing. **Zeng Feng:** Conceptualization, Funding acquisition, Supervision, Validation, Writing – review & editing. **Mebrahtu Chalachew:** Conceptualization, Supervision, Validation, Writing – review & editing.

Declaration of Competing Interest

The authors declare that they have no known competing financial interests or personal relationships that could have appeared to influence the work reported in this paper.

Data Availability

No data was used for the research described in the article.

Acknowledgment

This work was supported by DFG (PA 1689/22-1, Project ID: 512546329) and the Cluster of Excellence Fuel Science Center (EXC 2186, ID: 390919832), which is funded by the Excellence Initiative by the German federal and state governments to promote science and research at German universities. Besides, we are also grateful for the financial support provided by National Natural Science Foundation of China (ID: 22208143 and U22B20148). Feng Zeng also acknowledges financial support from China National Petroleum Corporation.

References

[1] J.G. Olivier, K. Schure, J. Peters, Trends Glob. CO_2 Total Greenh. Gas. Emiss., PBL Neth. Environ. Assess. Agency 5 (2017) 1–11. ⟨https://policycommons.net/artifacts/2187308/trends-in-global-co-2-and-total-greenhouse-gas-emissions/2943285/⟩.

[2] M. Kniirilä, Industrial development for the 21st century: sustainable development perspectives, Ind. Dev. Econ. Growth.: Implic. Poverty Reduct. Income Inequal. (2007) 295–332. ⟨https://sdgs.un.org/publications/industrial-development-21st-century-sustainable-development-perspectives-16993⟩.

[3] G. Clark, Industrial Revolution. Economic Growth, Springer,, London, 2010, pp. 148–160, https://doi.org/10.1057/9780230280823_22.

[4] S.C. Doney, V.J. Fabry, R.A. Feely, J.A. Kleypas, Ocean acidification: the other CO_2 problem, Annu. Rev. Mar. Sci. 1 (2009) 169–192, https://doi.org/10.1146/annurev.marine.010908.163834.

[5] TCFM (The Chinese Foreign Ministry), statement by H.E. Xi Jinping president of the People's Republic of China at the general debate of the 75th session of The United Nations general assembly, 2020. ⟨https://www.fmprc.gov.cn/mfa_eng/wjdt_665385/zyjh_665391/202009/t20200922_678904.html⟩.

[6] S. Chen, J. Liu, Q. Zhang, F. Teng, B.C. McLellan, A critical review on deployment planning and risk analysis of carbon capture, utilization, and storage (CCUS) toward carbon neutrality, Renew. Sustain. Energy Rev. 167 (2022) 112537, https://doi.org/10.1016/j.rser.2022.112537.

[7] X. Ma, G. Huang, J. Cao, The significant roles of anthropogenic aerosols on surface temperature under carbon neutrality, Sci. Bull. 67 (2022) 470–473, https://doi.org/10.1016/j.scib.2021.10.022.

[8] N. Mac Dowell, P.S. Fennell, N. Shah, G.C. Maitland, The role of CO_2 capture and utilization in mitigating climate change, Nat. Clim. Change 7 (2017) 243–249, https://doi.org/10.1038/nclimate3231.

[9] W.K. Fan, M. Tahir, Recent trends in developments of active metals and heterogenous materials for catalytic CO_2 hydrogenation to renewable methane: A review, J. Environ. Chem. Eng. 9 (2021) 105460, https://doi.org/10.1016/j.jece.2021.105460.

[10] A. Álvarez, A. Bansode, A. Urakawa, A.V. Bavykina, T.A. Wezendonk, M. Makkee, J. Gascon, F. Kapteijn, Challenges in the greener production of formates/formic acid, methanol, and DME by heterogeneously catalyzed CO_2 hydrogenation processes, Chem. Rev. 117 (2017) 9804–9838, https://doi.org/10.1021/acs.chemrev.6b00816.

[11] G.H. Gunasekar, K. Park, K.-D. Jung, S. Yoon, Recent developments in the catalytic hydrogenation of CO_2 to formic acid/formate using heterogeneous catalysts, Inorg. Chem. Front. 3 (2016) 882–895, https://doi.org/10.1039/C5QI00231A.

[12] X. Jiang, X. Nie, X. Guo, C. Song, J.G. Chen, Recent advances in carbon dioxide hydrogenation to methanol via heterogeneous catalysis, Chem. Rev. 120 (2020) 7984–8034, https://doi.org/10.1021/acs.chemrev.9b00723.

[13] G.A. Mills, Status and future opportunities for conversion of synthesis gas to liquid fuels, Fuel 73 (1994) 1243–1279, https://doi.org/10.1016/0016-2361(94)90301-8.

[14] E. Christensen, J. Yanowitz, M. Ratcliff, R.L. McCormick, Renewable oxygenate blending effects on gasoline properties, Energy Fuels 25 (2011) 4723–4733, https://doi.org/10.1021/ef2010089.

[15] V.R. Surisetty, A.K. Dalai, J. Kozinski, Alcohols as alternative fuels: An overview, Appl. Catal. A: Gen. 404 (2011) 1–11, https://doi.org/10.1016/j.apcata.2011.07.021.

[16] C.J. Kenneally, Alcohols, higher aliphatic, survey and natural alcohols manufacture, Kirk-Othmer Encyclopedia of Chemical Technology. ⟨https://doi.org/10.1002/0471238961.1921182216052005.a01.pub2⟩.

[17] C. Jia, J. Gao, Y. Dai, J. Zhang, Y. Yang, The thermodynamics analysis and experimental validation for complicated systems in CO_2 hydrogenation process, J. Energy Chem. 25 (2016) 1027–1037, https://doi.org/10.1016/j.jechem.2016.10.003.

[18] M. Devarapalli, H. Atiyeh, A review of conversion processes for bioethanol production with a focus on syngas fermentation, Biofuel Res J. 7 (2015) 268–280, https://doi.org/10.18331/BRJ2015.2.3.5.

[19] F.R. Bengelsdorf, M. Straub, P. Dürre, Bacterial synthesis gas (syngas) fermentation, Environ. Technol. 34 (2013) 1639–1651, https://doi.org/10.1080/09593330.2013.827747.

[20] Y. Nakagawa, N. Tajima, K. Hirao, A theoretical study of catalytic hydration reactions of ethylene, J. Comput. Chem. 21 (2000) 1292–1304, https://doi.org/10.1002/1096-987X(20001115)21:14<1292::AID-JCC8>3.0.CO;2-5.

[21] H. Younesi, G. Najafpour, A.R. Mohamed, Ethanol and acetate production from synthesis gas via fermentation processes using anaerobic bacterium, Clostridium ljungdahlii, Biochem. Eng. J. 27 (2005) 110–119, https://doi.org/10.1016/j.bej.2005.08.015.

[22] V.J. Johnston, A. Orosco, L. Sarager, M.O. Scates, R.D. Shaver, J.H. Zink, Producing ethanol using two different streams from acetic acid carbonylation process, Google Patents, 2014.

[23] T. Horton, R. Jevtic, V.J. Johnston, T. Pan, R.J. Warner, H. Weiner, N. Bower, J.T. Chapman, G. Grusendorf, Processes for maximizing ethanol formation in the hydrogenation of acetic acid, Google Patents, 2013.

[24] F. Zeng, C. Mebrahtu, X. Xi, L. Liao, J. Ren, J. Xie, H.J. Heeres, R. Palkovits, Catalysts design for higher alcohols synthesis by CO_2 hydrogenation: Trends and future perspectives, Appl. Catal. B: Environ. 291 (2021), https://doi.org/10.1016/j.apcatb.2021.120073.

[25] D. Xu, Y. Wang, M. Ding, X. Hong, G. Liu, S.C.E. Tsang, Advances in higher alcohol synthesis from CO_2 hydrogenation, Chem 7 (2021) 849–881, https://doi.org/10.1016/j.chempr.2020.10.019.

[26] C. Yang, R. Mu, G. Wang, J. Song, H. Tian, Z.-J. Zhao, J. Gong, Hydroxyl-mediated ethanol selectivity of CO_2 hydrogenation, Chem. Sci. 10 (2019) 3161–3167, https://doi.org/10.1039/C8SC05608K.

[27] S. Bai, Q. Shao, P. Wang, Q. Dai, X. Wang, X. Huang, Highly active and selective hydrogenation of CO_2 to ethanol by ordered Pd–Cu nanoparticles, J. Am. Chem. Soc. 139 (2017) 6827–6830, https://doi.org/10.1021/jacs.7b03101.

[28] Y. Lou, F. jiang, W. Zhu, L. Wang, T. Yao, S. Wang, B. Yang, B. Yang, Y. Zhu, X. Liu, CeO_2 supported Pd dimers boosting CO_2 hydrogenation to ethanol, Appl. Catal. B: Environ. 291 (2021) 120122, https://doi.org/10.1016/j.apcatb.2021.120122.

[29] Z. He, Q. Qian, J. Ma, Q. Meng, H. Zhou, J. Song, Z. Liu, B. Han, Water-enhanced synthesis of higher alcohols from CO_2 hydrogenation over a Pt/Co_3O_4 catalyst under milder conditions, Angew. Chem. Int. Ed. 55 (2016) 737–741, https://doi.org/10.1002/anie.201507585.

[30] D. Wang, Q. Bi, G. Yin, W. Zhao, F. Huang, X. Xie, M. Jiang, Direct synthesis of ethanol via CO_2 hydrogenation using supported gold catalysts, Chem. Commun. 52 (2016) 14226–14229, https://doi.org/10.1039/C6CC08161D.

[31] F. Zhang, W. Zhou, X. Xiong, Y. Wang, K. Cheng, J. Kang, Q. Zhang, Y. Wang, Selective hydrogenation of CO_2 to ethanol over sodium-modified Rhodium nanoparticles embedded in zeolite silicalite-1, J. Phys. Chem. C. 125 (2021) 24429–24439, https://doi.org/10.1021/acs.jpcc.1c07862.

[32] X. Ye, C. Yang, X. Pan, J. Ma, Y. Zhang, Y. Ren, X. Liu, L. Li, Y. Huang, Highly selective hydrogenation of CO_2 to ethanol via designed bifunctional Ir_1–In_2O_3 single-atom catalyst, J. Am. Chem. Soc. 142 (2020) 19001–19005, https://doi.org/10.1021/jacs.0c08607.

[33] Y. Chen, S. Choi, L.T. Thompson, Low temperature CO_2 hydrogenation to alcohols and hydrocarbons over Mo_2C supported metal catalysts, J. Catal. 343 (2016) 147–156, https://doi.org/10.1016/j.jcat.2016.01.016.

[34] S. Liu, H. Zhou, Q. Song, Z. Ma, Synthesis of higher alcohols from CO_2 hydrogenation over Mo–Co–K sulfide-based catalysts, J. Taiwan Inst. Chem. Eng. 76 (2017) 18–26, https://doi.org/10.1016/j.jtice.2017.04.007.

[35] S. Liu, H. Zhou, L. Zhang, Z. Ma, Y. Wang, Activated carbon-supported Mo-Co-K sulfide catalysts for synthesizing higher alcohols from CO_2, Chem. Eng. Technol. 42 (2019) 962–970, https://doi.org/10.1002/ceat.201800401.

[36] D.L.S. Nieskens, D. Ferrari, Y. Liu, R. Kolonko, The conversion of carbon dioxide and hydrogen into methanol and higher alcohols, Catal. Commun. 14 (2011) 111–113, https://doi.org/10.1016/j.catcom.2011.07.020.

[37] D. Xu, M. Ding, X. Hong, G. Liu, S.C.E. Tsang, Selective C_{2+} alcohol synthesis from direct CO_2 hydrogenation over a Cs-promoted Cu-Fe-Zn catalyst, ACS Catal. 10 (2020) 5250–5260, https://doi.org/10.1021/acscatal.0c01184.

[38] W. Guo, W.G. Gao, H. Wang, J.J. Tian, Higher alcohols synthesis from CO_2 hydrogenation over K_2O-modified $CuZnFeZrO_2$ catalysts, Adv. Mater. Res. 827 (2014) 20–24, https://doi.org/10.4028/www.scientific.net/AMR.827.20.

[39] H. Guo, S. Li, F. Peng, H. Zhang, L. Xiong, C. Huang, C. Wang, X. Chen, Roles Investigation of Promoters in K/Cu–Zn Catalyst and Higher Alcohols Synthesis from CO_2 Hydrogenation over a Novel Two-Stage Bed Catalyst Combination System, Catal. Lett. 145 (2015) 620–630, https://doi.org/10.1007/s10562-014-1446-7.

[40] L. Ding, T. Shi, J. Gu, Y. Cui, Z. Zhang, C. Yang, T. Chen, M. Lin, P. Wang, N. Xue, L. Peng, X. Guo, Y. Zhu, Z. Chen, W. Ding, CO_2 hydrogenation to ethanol over Cu@Na-Beta, Chem 6 (2020) 2673–2689, https://doi.org/10.1016/j.chempr.2020.07.001.

[41] B. An, Z. Li, Y. Song, J. Zhang, L. Zeng, C. Wang, W. Lin, Cooperative copper centres in a metal–organic framework for selective conversion of CO_2 to ethanol, Nat. Catal. 2 (2019) 709–717, https://doi.org/10.1038/s41929-019-0308-5.

[42] L.X. Wang, L. Wang, J. Zhang, X.L. Liu, H. Wang, W. Zhang, Q. Yang, J.Y. Ma, X. Dong, S.J. Yoo, J.G. Kim, X.J. Meng, F.S. Xiao, Selective hydrogenation of CO_2 to ethanol over cobalt catalysts, Angew. Chem. -Int. Ed. 57 (2018) 6104–6108, https://doi.org/10.1002/anie.201800729.

[43] L. Wang, S. He, L. Wang, Y. Lei, X. Meng, F.-S. Xiao, Cobalt–Nickel catalysts for selective hydrogenation of carbon dioxide into ethanol, ACS Catal. 9 (2019) 11335–11340, https://doi.org/10.1021/acscatal.9b04187.

[44] B. Liu, B. Ouyang, Y. Zhang, K. Lv, Q. Li, Y. Ding, J. Li, Effects of mesoporous structure and Pt promoter on the activity of Co-based catalysts in low-temperature CO_2 hydrogenation for higher alcohol synthesis, J. Catal. 366 (2018) 91–97, https://doi.org/10.1016/j.jcat.2018.07.019.

[45] C. Yang, S. Liu, Y. Wang, J. Song, G. Wang, S. Wang, Z.J. Zhao, R. Mu, J. Gong, The interplay between structure and product selectivity of CO_2 hydrogenation,

Angew. Chem. Int. Ed. 58 (2019) 11242–11247, https://doi.org/10.1002/anie.201904649.

[46] S. Zhang, X. Liu, Z. Shao, H. Wang, Y. Sun, Direct CO_2 hydrogenation to ethanol over supported Co_2C catalysts: Studies on support effects and mechanism, J. Catal. 382 (2020) 86–96, https://doi.org/10.1016/j.jcat.2019.11.038.

[47] Synergy of Co0-Co2+ in cobalt-based catalysts for CO2 hydrogenation: Quantifying via reduced and exposed atoms fraction, Applied Catalysis A: General, Volume 670, 2024, 119549, https://doi.org/10.1016/j.apcata.2023.119549.

[48] H. Xin, L. Lin, R. Li, D. Li, T. Song, R. Mu, Q. Fu, X. Bao, Overturning CO_2 hydrogenation selectivity with high activity via reaction-induced strong metal–support interactions, J. Am. Chem. Soc. 144 (2022) 4874–4882, https://doi.org/10.1021/jacs.1c12603.

[49] J.C. Matsubu, S. Zhang, L. DeRita, N.S. Marinkovic, J.G. Chen, G.W. Graham, X. Pan, P. Christopher, Adsorbate-mediated strong metal–support interactions in oxide-supported Rh catalysts, Nat. Chem. 9 (2017) 120–127, https://doi.org/10.1038/nchem.2607.

[50] S. Li, Y. Xu, Y. Chen, W. Li, L. Lin, M. Li, Y. Deng, X. Wang, B. Ge, C. Yang, S. Yao, J. Xie, Y. Li, X. Liu, D. Ma, Tuning the selectivity of catalytic carbon dioxide hydrogenation over Iridium/Cerium oxide catalysts with a strong metal–support interaction, Angew. Chem. Int. Ed. 56 (2017) 10761–10765, https://doi.org/10.1002/anie.201705002.

[51] X. Lu, Y. Liu, Y. He, A.N. Kuhn, P.-C. Shih, C.-J. Sun, X. Wen, C. Shi, H. Yang, Cobalt-based nonprecious metal catalysts derived from Metal–Organic Frameworks for high-rate hydrogenation of carbon dioxide, ACS Appl. Mater. Interfaces 11 (2019) 27717–27726, https://doi.org/10.1021/acsami.9b05645.

[52] A. Modak, A. Ghosh, A. Bhaumik, B. Chowdhury, CO_2 hydrogenation over functional nanoporous polymers and metal-organic frameworks, Adv. Colloid Interface Sci. 290 (2021) 102349, https://doi.org/10.1016/j.cis.2020.102349.

[53] B. An, J. Zhang, K. Cheng, P. Ji, C. Wang, W. Lin, Confinement of ultrasmall Cu/ZnOx nanoparticles in Metal–Organic Frameworks for selective methanol synthesis from catalytic hydrogenation of CO_2, J. Am. Chem. Soc. 139 (2017) 3834–3840, https://doi.org/10.1021/jacs.7b00058.

[54] J.D. Jimenez, C. Wen, J. Lauterbach, Design of highly active cobalt catalysts for CO_2 hydrogenation via the tailoring of surface orientation of nanostructures, Catal. Sci. Technol. 9 (2019) 1970–1978, https://doi.org/10.1039/C9CY00402E.

[55] B. Ouyang, W. Tan, B. Liu, Morphology effect of nanostructure ceria on the Cu/CeO2 catalysts for synthesis of methanol from CO_2 hydrogenation, Catal. Commun. 95 (2017) 36–39, https://doi.org/10.1016/j.catcom.2017.03.005.

[56] O. Martin, A.J. Martín, C. Mondelli, S. Mitchell, T.F. Segawa, R. Hauert, C. Drouilly, D. Curulla-Ferré, J. Pérez-Ramírez, Indium oxide as a superior catalyst for methanol synthesis by CO_2 hydrogenation, Angew. Chem. Int. Ed. 55 (2016) 6261–6265, https://doi.org/10.1002/anie.201600943.

[57] J. Ye, C. Liu, D. Mei, Q. Ge, Active oxygen vacancy site for methanol synthesis from CO_2 hydrogenation on $In_2O_3(110)$: A DFT study, ACS Catal. 3 (2013) 1296–1306, https://doi.org/10.1021/cs400132a.

[58] S. Zhang, Z. Wu, X. Liu, K. Hua, Z. Shao, B. Wei, C. Huang, H. Wang, Y. Sun, A Short review of recent advances in direct CO_2 hydrogenation to alcohols, Top. Catal. 64 (2021) 371–394, https://doi.org/10.1007/s11244-020-01405-w.

[59] S.S. Ali, S.S. Ali, N. Tabassum, A review on CO_2 hydrogenation to ethanol: Reaction mechanism and experimental studies, J. Environ. Chem. Eng. 10 (2022) 106962, https://doi.org/10.1016/j.jece.2021.106962.

[60] S. Liu, Y. He, W. Fu, J. Chen, J. Ren, L. Liao, R. Sun, Z. Tang, C. Mebrahtu, F. Zeng, Hetero-site cobalt catalysts for higher alcohols synthesis by CO_2 hydrogenation: A review, J. CO_2 Util. 67 (2023) 102322, https://doi.org/10.1016/j.jcou.2022.102322.

[61] J. Huang, G. Zhang, M. Wang, J. Zhu, F. Ding, C. Song, X. Guo, The synthesis of higher alcohols from CO_2 hydrogenation over Mn-Cu-K modified Fe5C2 and CuZnAlZr tandem catalysts, Front. Energy Res. 10 (2023), https://doi.org/10.3389/fenrg.2022.995800.

[62] S. Zhang, C. Huang, Z. Shao, H. Zhou, J. Chen, L. Li, J. Lu, X. Liu, H. Luo, L. Xia, H. Wang, Y. Sun, Revealing and regulating the complex reaction mechanism of CO_2 hydrogenation to higher alcohols on multifunctional tandem catalysts, ACS Catal. 13 (2023) 3055–3065, https://doi.org/10.1021/acscatal.2c06245.

[63] D. Xu, H. Yang, X. Hong, G. Liu, S.C. Edman Tsang, Tandem catalysis of direct CO_2 hydrogenation to higher alcohols, ACS Catal. 11 (2021) 8978–8984, https://doi.org/10.1021/acscatal.1c01610.

[64] Y.A. Daza, J.N. Kuhn, CO_2 conversion by reverse water gas shift catalysis: comparison of catalysts, mechanisms and their consequences for CO_2 conversion to liquid fuels, RSC Adv. 6 (2016) 49675–49691, https://doi.org/10.1039/C6RA05414E.

[65] X. Chen, Y. Chen, C. Song, P. Ji, N. Wang, W. Wang, L. Cui, Recent advances in supported metal catalysts and oxide catalysts for the reverse water-gas shift reaction, Front. Chem. 8 (2020), https://doi.org/10.3389/fchem.2020.00709.

[66] P. Ebrahimi, A. Kumar, M. Khraisheh, A review of CeO_2 supported catalysts for CO_2 reduction to CO through the reverse water gas shift reaction, Catalysts 12 (2022) 1101, https://doi.org/10.3390/catal12101101.

[67] G. Centi, G. Iaquaniello, S. Perathoner, Can we aford to waste carbon dioxide? carbon dioxide as a valuable source of carbon for the production of light olefins, ChemSusChem 4 (2011) 1265–1273, https://doi.org/10.1002/cssc.201100313.

[68] S. Yang, L. Zhang, Z. Wang, Advances in the preparation of light alkene from carbon dioxide by hydrogenation, Fuel 324 (2022) 124503, https://doi.org/10.1016/j.fuel.2022.124503.

[69] O.A. Ojelade, S.F. Zaman, A review on CO_2 hydrogenation to lower olefins: Understanding the structure-property relationships in heterogeneous catalytic systems, J. CO_2 Util. 47 (2021) 101506, https://doi.org/10.1016/j.jcou.2021.101506.

[70] H.M. Torres Galvis, J.H. Bitter, C.B. Khare, M. Ruitenbeek, A.I. Dugulan, K.P. de Jong, Supported Iron nanoparticles as catalysts for sustainable production of lower olefins, Science 335 (2012) 835–838, https://doi.org/10.1126/science.1215614.

[71] J. Zhong, X. Yang, Z. Wu, B. Liang, Y. Huang, T. Zhang, State of the art and perspectives in heterogeneous catalysis of CO_2 hydrogenation to methanol, Chem. Soc. Rev. 49 (2020) 1385–1413, https://doi.org/10.1039/C9CS00614A.

[72] R. Guil-López, N. Mota, J. Llorente, E. Millán, B. Pawelec, J.L.G. Fierro, R. M. Navarro, Methanol synthesis from CO_2: A review of the latest developments in heterogeneous catalysis, Materials 12 (2019) 3902. ⟨https://www.mdpi.com/1996-1944/12/23/3902⟩.

[73] S. Dang, H. Yang, P. Gao, H. Wang, X. Li, W. Wei, Y. Sun, A review of research progress on heterogeneous catalysts for methanol synthesis from carbon dioxide hydrogenation, Catal. Today 330 (2019) 61–75, https://doi.org/10.1016/j.cattod.2018.04.021.

[74] J.-F. Wu, S.-M. Yu, W.D. Wang, Y.-X. Fan, S. Bai, C.-W. Zhang, Q. Gao, J. Huang, W. Wang, Mechanistic insight into the formation of acetic acid from the direct conversion of methane and carbon dioxide on zinc-modified H–ZSM-5 zeolite, J. Am. Chem. Soc. 135 (2013) 13567–13573, https://doi.org/10.1021/ja406978q.

[75] M. Cui, Q. Qian, J. Zhang, C. Chen, B. Han, Efficient synthesis of acetic acid via Rh catalyzed methanol hydrocarboxylation with CO_2 and H_2 under milder conditions, Green. Chem. 19 (2017) 3558–3565, https://doi.org/10.1039/C7GC01391D.

[76] Q. Qian, J. Zhang, M. Cui, B. Han, Synthesis of acetic acid via methanol hydrocarboxylation with CO_2 and H_2, Nat. Commun. 7 (2016) 11481, https://doi.org/10.1038/ncomms11481.

[77] H.T. Luk, C. Mondelli, D.C. Ferré, J.A. Stewart, J. Pérez-Ramírez, Status and prospects in higher alcohols synthesis from syngas, Chem. Soc. Rev. 46 (2017) 1358–1426, https://doi.org/10.1039/C6CS00324A.

[78] J.J. Spivey, A. Egbebi, Heterogeneous catalytic synthesis of ethanol from biomass-derived syngas, Chem. Soc. Rev. 36 (2007) 1514–1528, https://doi.org/10.1039/B414039G.

[79] S. Zaman, K.J. Smith, A review of molybdenum catalysts for synthesis gas conversion to alcohols: catalysts, mechanisms and kinetics, Catal. Rev. 54 (2012) 41–132, https://doi.org/10.1080/01614940.2012.627224.

[80] N.S. Hidzir, A. Som, Z. Abdullah, Ethanol production via direct hydration of ethylene: A review, Int. Conf. Glob. Sustain. Chem. Eng. (ICGSE) (2014).

[81] Y. Maki, K. Sato, A. Isobe, N. Iwasa, S. Fujita, M. Shimokawabe, N. Takezawa, Structures of H_3PO_4/SiO_2 catalysts and catalytic performance in the hydration of ethene, Appl. Catal. A: Gen. 170 (1998) 269–275, https://doi.org/10.1016/S0926-860X(98)00054-4.

[82] B. Ayaou, A. Bodson, L. Dehottay, R. Farai, A. Farcy, D. Hendrickx, Ethanol production by catalytic hydration of ethylene. Liege, Liège Université Library Press, Belgium, 2020.

[83] T. Hanaoka, H. Arakawa, T. Matsuzaki, Y. Sugi, K. Kanno, Y. Abe, Ethylene hydroformylation and carbon monoxide hydrogenation over modified and unmodified silica supported rhodium catalysts, Catal. Today 58 (2000) 271–280, https://doi.org/10.1016/S0920-5861(00)00261-3.

[84] K. Tomishige, I. Furikado, T. Yamagishi, S.-i Ito, K. Kunimori, Promoting effect of Mo on alcohol formation in hydroformylation of propylene and ethylene on Mo-Rh/SiO_2, Catal. Lett. 103 (2005) 15–21, https://doi.org/10.1007/s10562-005-6497-3.

[85] X. Dong, J. Lei, Y. Chen, H. Jiang, M. Zhang, Selective hydrogenation of acetic acid to ethanol on Cu-In catalyst supported by SBA-15, Appl. Catal. B: Environ. 244 (2019) 448–458, https://doi.org/10.1016/j.apcatb.2018.11.062.

[86] H. Olcay, L. Xu, Y. Xu, G.W. Huber, Aqueous-phase hydrogenation of acetic acid over transition metal catalysts, ChemCatChem 2 (2010) 1420–1424, https://doi.org/10.1002/cctc.201000134.

[87] M. Zhou, H. Zhang, H. Ma, W. Ying, The catalytic properties of K modified PtSn/Al_2O_3 catalyst for acetic acid hydrogenation to ethanol, Fuel Process. Technol. 144 (2016) 115–123, https://doi.org/10.1016/j.fuproc.2015.12.022.

[88] Y. He, S. Liu, W. Fu, C. Wang, C. Mebrahtu, R. Sun, F. Zeng, Thermodynamic analysis of CO_2 hydrogenation to higher alcohols ($C_{2-4}OH$): Effects of isomers and methane, ACS Omega (2022), https://doi.org/10.1021/acsomega.2c00502.

[89] Y. He, S. Liu, W. Fu, J. Chen, Y. Zhai, X. Bi, J. Ren, R. Sun, Z. Tang, C. Mebrahtu, F. Zeng, Assessing the efficiency of CO_2 hydrogenation for emission reduction: Simulating ethanol synthesis process as a case study, Chem. Eng. Res. Des. 195 (2023) 106–115, https://doi.org/10.1016/j.cherd.2023.05.043.

[90] W. Fu, Z. Tang, S. Liu, Y. He, R. Sun, C. Mebrahtu, F. Zeng, Thermodynamic analysis of CO_2 hydrogenation to ethanol: solvent effects, ChemistrySelect 8 (2023) e202203385, https://doi.org/10.1002/slct.202203385.

[91] Y. He, W. Fu, Z. Tang, S. Liu, J. Chen, Q. Zhong, X. Tan, R. Sun, C. Mebrahtu, F. Zeng, Thermodynamic analysis of ethanol synthesis by CO_2 hydrogenation using Aspen Plus: effects of tail gas recycling and CO co-feeding, Chem. Eng. Commun. (2023) 1–11, https://doi.org/10.1080/00986445.2023.2240709.

[92] M. Konsolakis, The role of Copper–Ceria interactions in catalysis science: recent theoretical and experimental advances, Appl. Catal. B: Environ. 198 (2016) 49–66, https://doi.org/10.1016/j.apcatb.2016.05.037.

[93] A.M. Bahmanpour, M. Signorile, O. Kröcher, Recent progress in syngas production via catalytic CO_2 hydrogenation reaction, Appl. Catal. B: Environ. 295 (2021) 120319, https://doi.org/10.1016/j.apcatb.2021.120319.

[94] M.K. Gnanamani, G. Jacobs, R.A. Keogh, W.D. Shafer, D.E. Sparks, S.D. Hopps, G. A. Thomas, B.H. Davis, Fischer-Tropsch synthesis: effect of pretreatment

conditions of cobalt on activity and selectivity for hydrogenation of carbon dioxide, Appl. Catal. A: Gen. 499 (2015) 39–46, https://doi.org/10.1016/j.apcata.2015.03.046.
[95] C. Vogt, E. Groeneveld, G. Kamsma, M. Nachtegaal, L. Lu, C.J. Kiely, P.H. Berben, F. Meirer, B.M. Weckhuysen, Unravelling structure sensitivity in CO_2 hydrogenation over nickel, Nat. Catal. 1 (2018) 127–134, https://doi.org/10.1038/s41929-017-0016-y.
[96] L.-X. Wang, L. Wang, F.-S. Xiao, Tuning product selectivity in CO_2 hydrogenation over metal-based catalysts, Chem. Sci. 12 (2021) 14660–14673, https://doi.org/10.1039/D1SC03109K.
[97] V. Subramani, S.K. Gangwal, A review of recent literature to search for an efficient catalytic process for the conversion of syngas to ethanol, Energy Fuels 22 (2008) 814–839, https://doi.org/10.1021/ef700411x.
[98] H. Kusama, K. Okabe, K. Sayama, H. Arakawa, CO_2 hydrogenation to ethanol over promoted Rh/SiO_2 catalysts, Catal. Today 28 (1996) 261–266, https://doi.org/10.1016/0920-5861(95)00246-4.
[99] Y. Izumi, H. Kurakata, K.-i Aika, Ethanol synthesis from carbon dioxide on $[Rh_{10}Se]/TiO_2$ catalyst characterized by X-ray absorption fine structure spectroscopy, J. Catal. 175 (1998) 236–244, https://doi.org/10.1006/jcat.1998.1998.
[100] H. Kusama, K. Okabe, K. Sayama, H. Arakawa, The effect of rhodium precursor on ethanol synthesis by catalytic hydrogenation of carbon dioxide over silica supported rhodium catalysts, in: T. Inui, M. Anpo, K. Izui, S. Yanagida, T. Yamaguchi (Eds.), Studies in Surface Science and Catalysis, Elsevier, 1998, pp. 431–434, https://doi.org/10.1016/S0167-2991(98)80788-X.
[101] A. Goryachev, A. Pustovarenko, G. Shterk, N.S. Alhajri, A. Jamal, M. Albuali, L. van Koppen, I.S. Khan, A. Russkikh, A. Ramirez, T. Shoinkhorova, E.J. M. Hensen, J. Gascon, A multi-parametric catalyst screening for CO_2 hydrogenation to ethanol, ChemCatChem 13 (2021) 3324–3332, https://doi.org/10.1002/cctc.202100302.
[102] R. Zhang, B. Wang, H. Liu, L. Ling, Effect of surface hydroxyls on CO_2 hydrogenation over Cu/γ-Al_2O_3 catalyst: a theoretical study, J. Phys. Chem. C. 115 (2011) 19811–19818, https://doi.org/10.1021/jp206065y.
[103] J. Xu, X. Su, H. Duan, B. Hou, Q. Lin, X. Liu, X. Pan, G. Pei, H. Geng, Y. Huang, T. Zhang, Influence of pretreatment temperature on catalytic performance of rutile TiO_2-supported ruthenium catalyst in CO_2 methanation, J. Catal. 333 (2016) 227–237, https://doi.org/10.1016/j.jcat.2015.10.025.
[104] G. Wang, R. Luo, C. Yang, J. Song, C. Xiong, H. Tian, Z.-J. Zhao, R. Mu, J. Gong, Active sites in CO_2 hydrogenation over confined VO_x-Rh catalysts, Sci. China Chem. 62 (2019) 1710–1719, https://doi.org/10.1007/s11426-019-9590-6.
[105] F. Liao, Y. Huang, J. Ge, W. Zheng, K. Tedsree, P. Collier, X. Hong, S.C. Tsang, Morphology-dependent interactions of ZnO with Cu nanoparticles at the materials' interface in selective hydrogenation of CO_2 to CH_3OH, Angew. Chem. Int. Ed. 50 (2011) 2162–2165, https://doi.org/10.1002/anie.201007108.
[106] J. Toyir, P. de la Piscina, J. Fierro, N. Homs, Highly effective conversion of CO_2 to methanol over supported and promoted copper-based catalysts: influence of support and promoter, Appl. Catal. B: Environ. 29 (2001) 207–215, https://doi.org/10.1016/S0926-3373(00)00205-8.
[107] J. Niu, H. Liu, Y. Jin, B. Fan, W. Qi, J. Ran, Comprehensive review of Cu-based CO_2 hydrogenation to CH_3OH: Insights from experimental work and theoretical analysis, Int. J. Hydrog. Energy 47 (2022) 9183–9200, https://doi.org/10.1016/j.ijhydene.2022.01.021.
[108] M.J.L. Ginés, A.J. Marchi, C.R. Apesteguía, Kinetic study of the reverse water-gas shift reaction over CuO/ZnO/Al_2O_3 catalysts, Appl. Catal. A: Gen. 154 (1997) 155–171, https://doi.org/10.1016/S0926-860X(96)00369-9.
[109] T. Mathew, S. Saju, S.N. Raveendran, Survey of heterogeneous catalysts for the CO_2 reduction to CO via reverse water gas shift, Eng. Solut. CO_2 Convers. (2021) 281–316, https://doi.org/10.1002/9783527346523.ch12.
[110] C.-S. Chen, W.-H. Cheng, S.-S. Lin, Study of reverse water gas shift reaction by TPD, TPR and CO_2 hydrogenation over potassium-promoted Cu/SiO_2 catalyst, Appl. Catal. A: Gen. 238 (2003) 55–67, https://doi.org/10.1016/S0926-860X(02)00221-1.
[111] Research progress on Cu-based catalysts for alcohol synthesis, Acta Petrolei Sinica (Petroleum Processing Section), 31 (2015) 821–830, {⟨http://www.syxbsyjg.com/EN/10.3969/j.issn.1001–8719.2015.03.030⟩}.
[112] J. Anton, J. Nebel, H. Song, C. Froese, P. Weide, H. Ruland, M. Muhler, S. Kaluza, Structure–activity relationships of Co-modified Cu/ZnO/Al_2O_3 catalysts applied in the synthesis of higher alcohols from synthesis gas, Appl. Catal. A: Gen. 505 (2015) 326–333, https://doi.org/10.1016/j.apcata.2015.07.002.
[113] G. Wang, R. Zhang, B. Wang, Insight into the preference mechanism for CC chain formation of C_2 oxygenates and the effect of promoters in syngas conversion over Cu-based catalysts, Appl. Catal. A: Gen. 466 (2013) 77–89, https://doi.org/10.1016/j.apcata.2013.06.042.
[114] M. Gupta, M.L. Smith, J.J. Spivey, Heterogeneous catalytic conversion of dry syngas to ethanol and higher alcohols on Cu-based catalysts, ACS Catal. 1 (2011) 641–656, https://doi.org/10.1021/cs2001048.
[115] S.G. Li, H.J. Guo, H.R. Zhang, J. Luo, L. Xiong, C.R. Luo, X.D. Chen, The reverse water-gas shift reaction and the synthesis of mixed alcohols over K/Cu-Zn catalyst from CO_2 hydrogenation. Advanced Materials Research, Trans Tech Publ,, 2013, pp. 275–280, https://doi.org/10.4028/www.scientific.net/AMR.772.275.
[116] S. Li, H. Guo, C. Luo, H. Zhang, L. Xiong, X. Chen, L. Ma, Effect of Iron promoter on structure and performance of K/Cu–Zn catalyst for higher alcohols synthesis from CO_2 hydrogenation, Catal. Lett. 143 (2013) 345–355, https://doi.org/10.1007/s10562-013-0977-7.
[117] D. Xu, M. Ding, X. Hong, G. Liu, Mechanistic aspects of the role of K promotion on Cu–Fe-based catalysts for higher alcohol synthesis from CO_2 hydrogenation, ACS Catal. 10 (2020) 14516–14526, https://doi.org/10.1021/acscatal.0c03575.
[118] X. Wang, P.J. Ramírez, W. Liao, J.A. Rodriguez, P. Liu, Cesium-induced active sites for C–C coupling and ethanol synthesis from CO_2 hydrogenation on Cu/ZnO $(000\bar{1})$ surfaces, J. Am. Chem. Soc. 143 (2021) 13103–13112, https://doi.org/10.1021/jacs.1c03940.
[119] Z. Gholami, Z. Tišler, V. Rubáš, Recent advances in Fischer-Tropsch synthesis using cobalt-based catalysts: a review on supports, promoters, and reactors, Catal. Rev. 63 (2021) 512–595, https://doi.org/10.1080/01614940.2020.1762367.
[120] A.Y. Khodakov, W. Chu, P. Fongarland, Advances in the development of novel cobalt Fischer−Tropsch catalysts for synthesis of long-chain hydrocarbons and clean fuels, Chem. Rev. 107 (2007) 1692–1744, https://doi.org/10.1021/cr050972v.
[121] P. Wang, S. Chen, Y. Bai, X. Gao, X. Li, K. Sun, H. Xie, G. Yang, Y. Han, Y. Tan, Effect of the promoter and support on cobalt-based catalysts for higher alcohols synthesis through CO hydrogenation, Fuel 195 (2017) 69–81, https://doi.org/10.1016/j.fuel.2017.01.050.
[122] M.K. Gnanamani, G. Jacobs, H.H. Hamdeh, W.D. Shafer, F. Liu, S.D. Hopps, G. A. Thomas, B.H. Davis, Hydrogenation of carbon dioxide over Co–Fe bimetallic catalysts, ACS Catal. 6 (2016) 913–927, https://doi.org/10.1021/acscatal.5b01346.
[123] S. Liu, C. Yang, S. Zha, D. Sharapa, F. Studt, Z.-J. Zhao, J. Gong, Moderate surface segregation promotes selective ethanol production in CO_2 hydrogenation reaction over CoCu catalysts, Angew. Chem. Int. Ed. 61 (2022) e202109027, https://doi.org/10.1002/anie.202109027.
[124] Y. Lian, T. Fang, Y. Zhang, B. Liu, J. Li, Hydrogenation of CO_2 to alcohol species over Co@Co_3O_4/C-N catalysts, J. Catal. 379 (2019) 46–51, https://doi.org/10.1016/j.jcat.2019.09.018.
[125] B. Ouyang, S. Xiong, Y. Zhang, B. Liu, J. Li, The study of morphology effect of Pt/Co_3O_4 catalysts for higher alcohol synthesis from CO_2 hydrogenation, Appl. Catal. A: Gen. 543 (2017) 189–195, https://doi.org/10.1016/j.apcata.2017.06.031.
[126] K. An, S. Zhang, H. Wang, N. Li, Z. Zhang, Y. Liu, $Co^0 - Co^{\delta+}$ active pairs tailored by Ga-Al-O spinel for CO_2-to-ethanol synthesis, Chem. Eng. J. 433 (2022) 134606, https://doi.org/10.1016/j.cej.2022.134606.
[127] J. Ye, C.-J. Liu, D. Mei, Q. Ge, Methanol synthesis from CO_2 hydrogenation over a Pd_4/In_2O_3 model catalyst: A combined DFT and kinetic study, J. Catal. 317 (2014) 44–53, https://doi.org/10.1016/j.jcat.2014.06.002.
[128] L.C. Grabow, M. Mavrikakis, Mechanism of methanol synthesis on Cu through CO_2 and CO hydrogenation, ACS Catal. 1 (2011) 365–384, https://doi.org/10.1021/cs200055d.
[129] J.A. Schaidle, L.T. Thompson, Fischer–Tropsch synthesis over early transition metal carbides and nitrides: CO activation and chain growth, J. Catal. 329 (2015) 325–334, https://doi.org/10.1016/j.jcat.2015.05.020.
[130] Y. Ge, T. Zou, A.J. Martín, J. Pérez-Ramírez, ZrO_2-promoted Cu-Co, Cu-Fe and Co-Fe catalysts for higher alcohol synthesis, ACS Catal. 13 (2023) 9946–9959, https://doi.org/10.1021/acscatal.3c02534.
[131] T. Witoon, T. Numpilai, S. Nijpanich, N. Chanlek, P. Kidkhunthod, C.K. Cheng, K. H. Ng, D.-V.N. Vo, S. Ittisanronnachai, C. Wattanakit, M. Chareonpanich, J. Limtrakul, Enhanced CO_2 hydrogenation to higher alcohols over K-Co promoted In_2O_3 catalysts, Chem. Eng. J. 431 (2022) 133211, https://doi.org/10.1016/j.cej.2021.133211.
[132] J. Kang, S. He, W. Zhou, Z. Shen, Y. Li, M. Chen, Q. Zhang, Y. Wang, Single-pass transformation of syngas into ethanol with high selectivity by triple tandem catalysis, Nat. Commun. 11 (2020) 827, https://doi.org/10.1038/s41467-020-14672-8.
[133] G. Bonura, M. Cordaro, C. Cannilla, A. Mezzapica, L. Spadaro, F. Arena, F. Frusteri, Catalytic behaviour of a bifunctional system for the one step synthesis of DME by CO_2 hydrogenation, Catal. Today 228 (2014) 51–57, https://doi.org/10.1016/j.cattod.2013.11.017.
[134] C. Huang, C. Zhu, M. Zhang, Y. Lu, Q. Wang, H. Qian, J. Chen, K. Fang, Direct conversion of syngas to higher alcohols over a CuCoAl|t-ZrO_2 multifunctional catalyst, ChemCatChem 13 (2021) 3184–3197, https://doi.org/10.1002/cctc.202100293.
[135] C. Huang, C. Zhu, M. Zhang, J. Chen, K. Fang, Design of efficient ZnO/ZrO_2 modified CuCoAl catalysts for boosting higher alcohol synthesis in syngas conversion, Appl. Catal. B: Environ. 300 (2022) 120739, https://doi.org/10.1016/j.apcatb.2021.120739.
[136] V.P. Santos, B. van der Linden, A. Chojecki, G. Budroni, S. Corthals, H. Shibata, G. R. Meima, F. Kapteijn, M. Makkee, J. Gascon, Mechanistic insight into the synthesis of higher alcohols from syngas: the Role of K promotion on MoS_2 catalysts, ACS Catal. 3 (2013) 1634–1637, https://doi.org/10.1021/cs4003518.
[137] T. Inui, T. Yamamoto, Effective synthesis of ethanol from CO_2 on polyfunctional composite catalysts, Catal. Today 45 (1998) 209–214, https://doi.org/10.1016/S0920-5861(98)00217-X.
[138] T. Inui, T. Yamamoto, M. Inoue, H. Hara, T. Takeguchi, J.-B. Kim, Highly effective synthesis of ethanol by CO_2-hydrogenation on well balanced multi-functional FT-type composite catalysts, Appl. Catal. A: Gen. 186 (1999) 395–406, https://doi.org/10.1016/S0926-860X(99)00157-X.
[139] T. Yamamoto, T. Inui, Highly effective synthesis of ethanol from CO_2 on Fe, Cu-based novel catalysts, in: T. Inui, M. Anpo, K. Izui, S. Yanagida, T. Yamaguchi (Eds.), Studies in Surface Science and Catalysis, Elsevier, 1998, pp. 513–516, https://doi.org/10.1016/S0167-2991(98)80809-4.
[140] S. Han, D. Fan, N. Chen, W. Cui, L. He, P. Tian, Z. Liu, Efficient conversion of syngas into ethanol by tandem catalysis, ACS Catal. 13 (2023) 10651–10660, https://doi.org/10.1021/acscatal.3c01577.

[141] F. Zhang, K. Chen, Q. Jiang, S. He, Q. Chen, Z. Liu, J. Kang, Q. Zhang, Y. Wang, Selective transformation of methanol to ethanol in the presence of syngas over composite catalysts, ACS Catal. 12 (2022) 8451–8461, https://doi.org/10.1021/acscatal.2c01725.

[142] Y. Li, Z. Zhao, W. Lu, M. Jiang, C. Li, M. Zhao, L. Gong, S. Wang, L. Guo, Y. Lyu, L. Yan, H. Zhu, Y. Ding, Highly selective conversion of syngas to higher oxygenates over tandem catalysts, ACS Catal. 11 (2021) 14791–14802, https://doi.org/10.1021/acscatal.1c04442.

[143] Y. Feng, J. Wang, L. Ling, B. Hou, R. Zhang, D. Li, B. Wang, Direct conversion of syngas to ethanol over Rh-based and Cu-based tandem catalyst: Effect of Cu crystal plane, Fuel 313 (2022) 122981, https://doi.org/10.1016/j.fuel.2021.122981.

[144] Z. Cao, T. Hu, J. Guo, J. Xie, N. Zhang, J. Zheng, L. Che, B.H. Chen, Stable and facile ethanol synthesis from syngas in one reactor by tandem combination CuZnAl-HZSM-5, modified-H-Mordenite with CuZnAl catalyst, Fuel 254 (2019) 115542, https://doi.org/10.1016/j.fuel.2019.05.125.

[145] Y. Zhang, C. Ding, J. Wang, Y. Jia, Y. Xue, Z. Gao, B. Yu, B. Gao, K. Zhang, P. Liu, Intermediate product regulation over tandem catalysts for one-pass conversion of syngas to ethanol, Catal. Sci. Technol. 9 (2019) 1581–1594, https://doi.org/10.1039/C8CY02593B.

[146] Y. Wang, D. Xu, X. Zhang, X. Hong, G. Liu, Selective C_{2+} alcohol synthesis by CO_2 hydrogenation via a reaction-coupling strategy, Catal. Sci. Technol. 12 (2022) 1539–1550, https://doi.org/10.1039/D1CY02196F.

[147] Y. Wang, K. Wang, B. Zhang, X. Peng, X. Gao, G. Yang, H. Hu, M. Wu, N. Tsubaki, Direct conversion of CO_2 to ethanol boosted by iIntimacy-sensitive multifunctional catalysts, ACS Catal. 11 (2021) 11742–11753, https://doi.org/10.1021/acscatal.1c01504.

[148] X. Su, X. Yang, B. Zhao, Y. Huang, Designing of highly selective and high-temperature endurable RWGS heterogeneous catalysts: recent advances and the future directions, J. Energy Chem. 26 (2017) 854–867, https://doi.org/10.1016/j.jechem.2017.07.006.

[149] W. Wang, Y. Zhang, Z. Wang, J.-m Yan, Q. Ge, C.-j Liu, Reverse water gas shift over In_2O_3–CeO_2 catalysts, Catal. Today 259 (2016) 402–408, https://doi.org/10.1016/j.cattod.2015.04.032.

[150] G. Varvoutis, M. Lykaki, E. Papista, S.A.C. Carabineiro, A.C. Psarras, G. E. Marnellos, M. Konsolakis, Effect of alkali (Cs) doping on the surface chemistry and CO_2 hydrogenation performance of CuO/CeO_2 catalysts, J. CO_2 Util. 44 (2021) 101408, https://doi.org/10.1016/j.jcou.2020.101408.

[151] Y. Zhang, L. Liang, Z. Chen, J. Wen, W. Zhong, S. Zou, M. Fu, L. Chen, D. Ye, Highly efficient Cu/CeO_2-hollow nanospheres catalyst for the reverse water-gas shift reaction: Investigation on the role of oxygen vacancies through in situ UV-Raman and DRIFTS, Appl. Surf. Sci. 516 (2020) 146035, https://doi.org/10.1016/j.apsusc.2020.146035.

[152] S. Choi, B.-I. Sang, J. Hong, K.J. Yoon, J.-W. Son, J.-H. Lee, B.-K. Kim, H. Kim, Catalytic behavior of metal catalysts in high-temperature RWGS reaction: In-situ FT-IR experiments and first-principles calculations, Sci. Rep. 7 (2017) 41207, https://doi.org/10.1038/srep41207.

[153] D.H. Kim, S.W. Han, H.S. Yoon, Y.D. Kim, Reverse water gas shift reaction catalyzed by Fe nanoparticles with high catalytic activity and stability, J. Ind. Eng. Chem. 23 (2015) 67–71, https://doi.org/10.1016/j.jiec.2014.07.043.

[154] A. Goguet, F. Meunier, J.P. Breen, R. Burch, M.I. Petch, A. Faur Ghenciu, Study of the origin of the deactivation of a Pt/CeO_2 catalyst during reverse water gas shift (RWGS) reaction, J. Catal. 226 (2004) 382–392, https://doi.org/10.1016/j.jcat.2004.06.011.

[155] L.F. Bobadilla, J.L. Santos, S. Ivanova, J.A. Odriozola, A. Urakawa, Unravelling the role of oxygen vacancies in the mechanism of the reverse water–gas shift reaction by *operando* DRIFTS and ultraviolet–visible spectroscopy, ACS Catal. 8 (2018) 7455–7467, https://doi.org/10.1021/acscatal.8b02121.

[156] C. Wang, E. Guan, L. Wang, X. Chu, Z. Wu, J. Zhang, Z. Yang, Y. Jiang, L. Zhang, X. Meng, B.C. Gates, F.-S. Xiao, Product selectivity controlled by nanoporous environments in zeolite crystals enveloping Rhodium nanoparticle catalysts for CO_2 hydrogenation, J. Am. Chem. Soc. 141 (2019) 8482–8488, https://doi.org/10.1021/jacs.9b01555.

[157] J. Ye, Q. Ge, C.-j Liu, Effect of PdIn bimetallic particle formation on CO_2 reduction over the Pd–In/SiO_2 catalyst, Chem. Eng. Sci. 135 (2015) 193–201, https://doi.org/10.1016/j.ces.2015.04.034.

[158] B. Lu, K. Kawamoto, Preparation of mesoporous CeO_2 and monodispersed NiO particles in CeO_2, and enhanced selectivity of NiO/CeO_2 for reverse water gas shift reaction, Mater. Res. Bull. 53 (2014) 70–78, https://doi.org/10.1016/j.materresbull.2014.01.043.

[159] Q. Zhang, L. Pastor-Pérez, W. Jin, S. Gu, T.R. Reina, Understanding the promoter effect of Cu and Cs over highly effective β-Mo_2C catalysts for the reverse water-gas shift reaction, Appl. Catal. B: Environ. 244 (2019) 889–898, https://doi.org/10.1016/j.apcatb.2018.12.023.

[160] K. Xiao, Z. Bao, X. Qi, X. Wang, L. Zhong, K. Fang, M. Lin, Y. Sun, Advances in bifunctional catalysis for higher alcohol synthesis from syngas, Chin. J. Catal. 34 (2013) 116–129, https://doi.org/10.1016/S1872-2067(11)60496-8

[161] K. Fang, D. Li, M. Lin, M. Xiang, W. Wei, Y. Sun, A short review of heterogeneous catalytic process for mixed alcohols synthesis via syngas, Catal. Today 147 (2009) 133–138, https://doi.org/10.1016/j.cattod.2009.01.038.

[162] D. Damma, P.G. Smirniotis, Recent advances in the direct conversion of syngas to oxygenates, Catal. Sci. Technol. 11 (2021) 5412–5431, https://doi.org/10.1039/D1CY00813G.

[163] J. Yu, D. Mao, L. Han, Q. Guo, G. Lu, CO hydrogenation over Fe-promoted Rh–Mn–Li/SiO_2 catalyst: The effect of sequences for introducing the Fe promoter, Fuel Process. Technol. 112 (2013) 100–105, https://doi.org/10.1016/j.fuproc.2013.03.004.

[164] T.-W. Kim, M.-J. Kim, H.-J. Chae, K.-S. Ha, C.-U. Kim, Ordered mesoporous carbon supported uniform rhodium nanoparticles as catalysts for higher alcohol synthesis from syngas, Fuel 160 (2015) 393–403, https://doi.org/10.1016/j.fuel.2015.07.062.

[165] Y. Liu, K. Murata, M. Inaba, I. Takahara, K. Okabe, Synthesis of ethanol from syngas over Rh/$Ce_{1-x}Zr_xO_2$ catalysts, Catal. Today 164 (2011) 308–314, https://doi.org/10.1016/j.cattod.2010.10.087.

[166] J.-J. Wang, J.-R. Xie, Y.-H. Huang, B.-H. Chen, G.-D. Lin, H.-B. Zhang, An efficient Ni–Mo–K sulfide catalyst doped with CNTs for conversion of syngas to ethanol and higher alcohols, Appl. Catal. A: Gen. 468 (2013) 44–51, https://doi.org/10.1016/j.apcata.2013.08.026.

[167] X. Xi, F. Zeng, H. Cao, C. Cannilla, T. Bisswanger, S. de Graaf, Y. Pei, F. Frusteri, C. Stampfer, R. Palkovits, H.J. Heeres, Enhanced C_{3+} alcohol synthesis from syngas using $KCoMoS_x$ catalysts: effect of the Co-Mo ratio on catalyst performance, Appl. Catal. B: Environ. 272 (2020) 118950, https://doi.org/10.1016/j.apcatb.2020.118950.

[168] S.F. Zaman, K.J. Smith, Synthesis gas conversion over a Rh–K–MoP/SiO_2 catalyst, Catal. Today 171 (2011) 266–274, https://doi.org/10.1016/j.cattod.2011.02.017.

[169] A. Cao, G. Liu, L. Wang, J. Liu, Y. Yue, L. Zhang, Y. Liu, Growing layered double hydroxides on CNTs and their catalytic performance for higher alcohol synthesis from syngas, J. Mater. Sci. 51 (2016) 5216–5231, https://doi.org/10.1007/s10853-016-9823-9.

[170] T.-y Chen, J. Su, Z. Zhang, C. Cao, X. Wang, R. Si, X. Liu, B. Shi, J. Xu, Y.-F. Han, Structure evolution of Co–CoO_x interface for higher alcohol synthesis from syngas over Co/CeO_2 catalysts, ACS Catal. 8 (2018) 8606–8617, https://doi.org/10.1021/acscatal.8b00453.

[171] S. Guo, G. Liu, Y. Zhang, Y. Liu, Oxygen vacancies boosted Co-Co_2C catalysts for higher alcohols synthesis from syngas, Appl. Surf. Sci. 576 (2022) 151846, https://doi.org/10.1016/j.apsusc.2021.151846.

[172] J. Sun, Q. Cai, Y. Wan, S. Wan, L. Wang, J. Lin, D. Mei, Y. Wang, Promotional effects of Cesium promoter on higher alcohol synthesis from syngas over Cesium-promoted Cu/ZnO/Al_2O_3 catalysts, ACS Catal. 6 (2016) 5771–5785, https://doi.org/10.1021/acscatal.6b00935.

[173] Y. Wu, H. Xie, S. Tian, N. Tsubaki, Y. Han, Y. Tan, Isobutanol synthesis from syngas over K–Cu/ZrO_2–La_2O_3(x) catalysts: Effect of La-loading, J. Mol. Catal. A: Chem. 396 (2015) 254–260, https://doi.org/10.1016/j.molcata.2014.10.003.

[174] Y. Liu, X. Deng, P. Han, W. Huang, Higher alcohols synthesis from syngas over P-promoted non-noble metal Cu-based catalyst, Fuel 208 (2017) 423–429, https://doi.org/10.1016/j.fuel.2017.07.043.

[175] J. Yu, D. Mao, L. Han, Q. Guo, G. Lu, The effect of Fe on the catalytic performance of Rh–Mn–Li/SiO_2 catalyst: A DRIFTS study, Catal. Commun. 27 (2012) 1–4, https://doi.org/10.1016/j.catcom.2012.06.010.

[176] J. Liu, R. Tao, Z. Guo, J.R. Regalbuto, C.L. Marshall, R.F. Klie, J.T. Miller, R. J. Meyer, Selective adsorption of manganese onto Rhodium for optimized Mn/Rh/SiO_2 alcohol synthesis catalysts, ChemCatChem 5 (2013) 3665–3672, https://doi.org/10.1002/cctc.201300479.

[177] G. Liu, H. Fang, G. Wang, N. Liu, J. Liu, L. Huang, X. Liang, Y. Yuan, Dispersion of Rh–W_xC nanocomposites on carbon nanotubes by one-pot carburization for synthesis of higher alcohols from syngas, Fuel 305 (2021) 121533, https://doi.org/10.1016/j.fuel.2021.121533.

[178] C. Wang, H. Yu, T. Lin, X. Qi, F. Yu, L. Zhong, Y. Sun, Direct synthesis of higher alcohols from syngas over modified Mo_2C catalysts under mild reaction conditions, Catal. Sci. Technol. 12 (2022) 1697–1708, https://doi.org/10.1039/D1CY02186A.

[179] M. Xiang, D. Li, W. Li, B. Zhong, Y. Sun, K/Fe/β-Mo_2C: A novel catalyst for mixed alcohols synthesis from carbon monoxide hydrogenation, Catal. Commun. 8 (2007) 88–90, https://doi.org/10.1016/j.catcom.2006.05.036.

[180] C.-H. Ma, H.-Y. Li, G.-D. Lin, H.-B. Zhang, MWCNT-supported Ni–Mo–K catalyst for higher alcohol synthesis from syngas, Catal. Lett. 137 (2010) 171–179, https://doi.org/10.1007/s10562-010-0343-y.

[181] G. Liu, D. Pan, T. Niu, A. Cao, Y. Yue, Y. Liu, Nanoparticles of Cu–Co alloy supported on high surface area $LaFeO_3$—preparation and catalytic performance for higher alcohol synthesis from syngas, RSC Adv. 5 (2015) 31637–31647, https://doi.org/10.1039/C5RA02433A.

[182] Y. Lu, B. Cao, F. Yu, J. Liu, Z. Bao, J. Gao, High selectivity higher alcohols synthesis from syngas over three-dimensionally ordered macroporous Cu-Fe catalysts, ChemCatChem 6 (2014) 473–478, https://doi.org/10.1002/cctc.201300749.

[183] A. Venugopal, J. Aluha, M.S. Scurrell, The water-gas shift reaction over Au-based, bimetallic catalysts. The Au-M (M=Ag, Bi, Co, Cu, Mn, Ni, Pb, Ru, Sn, Tl) on Iron (III) oxide system, Catal. Lett. 90 (2003) 1–6, https://doi.org/10.1023/A:1025872411739.

[184] J.C. Slaa, J.G. van Ommen, J.R.H. Ross, The synthesis of higher alcohols using modified Cu/ZnO/Al_2O_3 catalysts, Catal. Today 15 (1992) 129–148, https://doi.org/10.1016/0920-5861(92)80125-7.

[185] G. Natta, U. Colombo, I. Pasquon, Direct catalytic synthesis of higher alcohols from carbon monoxide and hydrogen, Catalysis 5 (1957) 131.

[186] D. Andriamasinoro, R. Kieffer, A. Kiennemann, P. Poix, Preparation of stabilized copper-rare earth oxide catalysts for the synthesis of methanol from syngas, Appl. Catal. A: Gen. 106 (1993) 201–212, https://doi.org/10.1016/0926-860X(93)80178-S.

[187] X. Xi, F. Zeng, H. Zhang, X. Wu, J. Ren, T. Bisswanger, C. Stampfer, J.P. Hofmann, R. Palkovits, H.J. Heeres, CO_2 hydrogenation to higher alcohols over K-promoted

bimetallic Fe–In catalysts on a Ce–ZrO_2 support, ACS Sustain. Chem. Eng. 9 (2021) 6235–6249, https://doi.org/10.1021/acssuschemeng.0c08760.
[188] R. Yao, J. Wei, Q. Ge, J. Xu, Y. Han, Q. Ma, H. Xu, J. Sun, Monometallic iron catalysts with synergistic Na and S for higher alcohols synthesis via CO_2 hydrogenation, Appl. Catal. B: Environ. 298 (2021) 120556, https://doi.org/10.1016/j.apcatb.2021.120556.
[189] Y. Wang, X. Zhang, X. Hong, G. Liu, Sulfate-promoted higher alcohol synthesis from CO_2 hydrogenation, ACS Sustain. Chem. Eng. 10 (2022) 8980–8987, https://doi.org/10.1021/acssuschemeng.2c02743.
[190] I.A. Bakare, O. Muraza, M.A. Sanhoob, K. Miyake, Y. Hirota, Z.H. Yamani, N. Nishiyama, Dimethyl ether-to-olefins over aluminum rich ZSM-5: The role of Ca and La as modifiers, Fuel 211 (2018) 18–26, https://doi.org/10.1016/j.fuel.2017.08.117.
[191] T. Ren, M. Patel, K. Blok, Olefins from conventional and heavy feedstocks: Energy use in steam cracking and alternative processes, Energy 31 (2006) 425–451, https://doi.org/10.1016/j.energy.2005.04.001.
[192] T. Numpilai, C.K. Cheng, J. Limtrakul, T. Witoon, Recent advances in light olefins production from catalytic hydrogenation of carbon dioxide, Process Saf. Environ. Prot. 151 (2021) 401–427, https://doi.org/10.1016/j.psep.2021.05.025.
[193] M. Ronda-Lloret, G. Rothenberg, N.R. Shiju, A critical look at direct catalytic hydrogenation of carbon dioxide to olefins, ChemSusChem 12 (2019) 3896–3914, https://doi.org/10.1002/cssc.201900915.
[194] Z. Zhang, H. Yin, G. Yu, S. He, J. Kang, Z. Liu, K. Cheng, Q. Zhang, Y. Wang, Selective hydrogenation of CO_2 and CO into olefins over Sodium- and Zinc-Promoted iron carbide catalysts, J. Catal. 395 (2021) 350–361, https://doi.org/10.1016/j.jcat.2021.01.036.
[195] N. Chaipraditgul, T. Numpilai, C.K. Cheng, N. Siri-Nguan, T. Sornchamni, C. Wattanakit, J. Limtrakul, T. Witoon, Tuning interaction of surface-adsorbed species over Fe/K-Al_2O_3 modified with transition metals (Cu, Mn, V, Zn or Co) on light olefins production from CO_2 hydrogenation, Fuel 283 (2021) 119248, https://doi.org/10.1016/j.fuel.2020.119248.
[196] W. Wang, X. Jiang, X. Wang, C. Song, Fe–Cu bimetallic catalysts for selective CO_2 hydrogenation to olefin-rich C_{2+} hydrocarbons, Ind. Eng. Chem. Res. 57 (2018) 4535–4542, https://doi.org/10.1021/acs.iecr.8b00016.
[197] Q. Xu, X. Xu, G. Fan, L. Yang, F. Li, Unveiling the roles of Fe-Co interactions over ternary spinel-type $ZnCo_xFe_{2-x}O_4$ catalysts for highly efficient CO_2 hydrogenation to produce light olefins, J. Catal. 400 (2021) 355–366, https://doi.org/10.1016/j.jcat.2021.07.002.
[198] J. Jiang, C. Wen, Z. Tian, Y. Wang, Y. Zhai, L. Chen, Y. Li, Q. Liu, C. Wang, L. Ma, Manganese-promoted Fe_3O_4 microsphere for efficient conversion of CO_2 to light olefins, Ind. Eng. Chem. Res. 59 (2020) 2155–2162, https://doi.org/10.1021/acs.iecr.9b05342.
[199] N. Chaipraditgul, T. Numpilai, C. Kui Cheng, N. Siri-Nguan, T. Sornchamni, C. Wattanakit, J. Limtrakul, T. Witoon, Tuning interaction of surface-adsorbed species over Fe/K-Al_2O_3 modified with transition metals (Cu, Mn, V, Zn or Co) on light olefins production from CO_2 hydrogenation, Fuel 283 (2021) 119248, https://doi.org/10.1016/j.fuel.2020.119248.
[200] I.A. da Silva, C.J.A. Mota, Conversion of CO_2 to light olefins over Iron-based catalysts supported on Niobium oxide, Front. Energy Res. 7 (2019), https://doi.org/10.3389/fenrg.2019.00049.
[201] L. Torrente-Murciano, R.S.L. Chapman, A. Narvaez-Dinamarca, D. Mattia, M. D. Jones, Effect of nanostructured ceria as support for the iron catalysed hydrogenation of CO_2 into hydrocarbons, Phys. Chem. Chem. Phys. 18 (2016) 15496–15500, https://doi.org/10.1039/C5CP07788E.
[202] J. Liu, A. Zhang, X. Jiang, M. Liu, J. Zhu, C. Song, X. Guo, Direct transformation of carbon dioxide to value-added hydrocarbons by physical mixtures of Fe_5C_2 and K-modified Al_2O_3, Ind. Eng. Chem. Res. 57 (2018) 9120–9126, https://doi.org/10.1021/acs.iecr.8b02017.
[203] M.V. Landau, N. Meiri, N. Utsis, R. Vidruk Nehemya, M. Herskowitz, Conversion of CO_2, CO, and H_2 in CO_2 hydrogenation to fungible liquid fuels on Fe-based catalysts, Ind. Eng. Chem. Res. 56 (2017) 13334–13355, https://doi.org/10.1021/acs.iecr.7b01817.
[204] Y. Zhang, C. Cao, C. Zhang, Z. Zhang, X. Liu, Z. Yang, M. Zhu, B. Meng, J. Xu, Y.-F. Han, The study of structure-performance relationship of iron catalyst during a full life cycle for CO_2 hydrogenation, J. Catal. 378 (2019) 51–62, https://doi.org/10.1016/j.jcat.2019.08.001.
[205] J. Liu, Y. Song, X. Guo, C. Song, X. Guo, Recent advances in application of iron-based catalysts for CO_x hydrogenation to value-added hydrocarbons, Chin. J. Catal. 43 (2022) 731–754, https://doi.org/10.1016/S1872-2067(21)63802-0.
[206] D. Peña, A. Cognigni, T. Neumayer, W. van Beek, D.S. Jones, M. Quijada, M. Rønning, Identification of carbon species on iron-based catalysts during Fischer-Tropsch synthesis, Appl. Catal. A: Gen. 554 (2018) 10–23, https://doi.org/10.1016/j.apcata.2018.01.019.
[207] E. de Smit, F. Cinquini, A.M. Beale, O.V. Safonova, W. van Beek, P. Sautet, B. M. Weckhuysen, Stability and reactivity of $\epsilon-\chi-\theta$ Iron carbide catalyst phases in Fischer−Tropsch synthesis: Controlling μ_C, J. Am. Chem. Soc. 132 (2010) 14928–14941, https://doi.org/10.1021/ja105853q.
[208] C. Wei, W. Tu, L. Jia, Y. Liu, H. Lian, P. Wang, Z. Zhang, The evolutions of carbon and iron species modified by Na and their tuning effect on the hydrogenation of CO_2 to olefins, Appl. Surf. Sci. 525 (2020) 146622, https://doi.org/10.1016/j.apsusc.2020.146622.
[209] X. Wang, J. Zhang, J. Chen, Q. Ma, S. Fan, T.-s Zhao, Effect of preparation methods on the structure and catalytic performance of Fe–Zn/K catalysts for CO_2 hydrogenation to light olefins, Chin. J. Chem. Eng. 26 (2018) 761–767, https://doi.org/10.1016/j.cjche.2017.10.013.
[210] N. Liu, J. Wei, J. Xu, Y. Yu, J. Yu, Y. Han, K. Wang, J.I. Orege, Q. Ge, J. Sun, Elucidating the structural evolution of highly efficient Co–Fe bimetallic catalysts for the hydrogenation of CO_2 into olefins, Appl. Catal. B: Environ. 328 (2023) 122476, https://doi.org/10.1016/j.apcatb.2023.122476.
[211] J.I. Orege, J. Wei, Y. Han, M. Yang, X. Sun, J. Zhang, C.C. Amoo, Q. Ge, J. Sun, Highly stable Sr and Na co-decorated Fe catalyst for high-valued olefin synthesis from CO_2 hydrogenation, Appl. Catal. B: Environ. 316 (2022) 121640, https://doi.org/10.1016/j.apcatb.2022.121640.
[212] Y. Liu, B. Chen, R. Liu, W. Liu, X. Gao, Y. Tan, Z. Zhang, W. Tu, CO_2 hydrogenation to olefins on supported iron catalysts: Effects of support properties on carbon-containing species and product distribution, Fuel 324 (2022) 124649, https://doi.org/10.1016/j.fuel.2022.124649.
[213] J. Huang, S. Jiang, M. Wang, X. Wang, J. Gao, C. Song, Dynamic evolution of Fe and carbon species over different ZrO_2 supports during CO prereduction and their effects on CO_2 hydrogenation to light olefins, ACS Sustain. Chem. Eng. 9 (2021) 7891–7903, https://doi.org/10.1021/acssuschemeng.1c01777.
[214] T. Numpilai, N. Chanlek, Y. Poo-Arporn, S. Wannapaiboon, C.K. Cheng, N. Siri-Nguan, T. Sornchamni, P. Kongkachuichay, M. Chareonpanich, G. Rupprechter, J. Limtrakul, T. Witoon, Pore size effects on physicochemical properties of Fe-Co/K-Al_2O_3 catalysts and their catalytic activity in CO_2 hydrogenation to light olefins, Appl. Surf. Sci. 483 (2019) 581–592, https://doi.org/10.1016/j.apsusc.2019.03.331.
[215] T. Witoon, N. Chaipraditgul, T. Numpilai, V. Lapkeatseree, B.V. Ayodele, C. K. Cheng, N. Siri-Nguan, T. Sornchamni, J. Limtrakul, Highly active Fe-Co-Zn/K-Al_2O_3 catalysts for CO_2 hydrogenation to light olefins, Chem. Eng. Sci. 233 (2021) 116428, https://doi.org/10.1016/j.ces.2020.116428.
[216] P. Zhang, F. Han, J. Yan, X. Qiao, Q. Guan, W. Li, N-doped ordered mesoporous carbon (N-OMC) confined Fe_3O_4-FeC_x heterojunction for efficient conversion of CO_2 to light olefins, Appl. Catal. B: Environ. 299 (2021) 120639, https://doi.org/10.1016/j.apcatb.2021.120639.
[217] J. Wang, Z. You, Q. Zhang, W. Deng, Y. Wang, Synthesis of lower olefins by hydrogenation of carbon dioxide over supported iron catalysts, Catal. Today 215 (2013) 186–193, https://doi.org/10.1016/j.cattod.2013.03.031.
[218] M. Alwin, P. Mathias, Synthetic manufacture of methanol, Google Patents, 1926.
[219] M. Bowker, Methanol synthesis from CO_2 hydrogenation, ChemCatChem 11 (2019) 4238–4246, https://doi.org/10.1002/cctc.201900401.
[220] M. Bowker, Chemisorption and industrial catalytic processes, Vacuum 33 (1983) 669–685, https://doi.org/10.1016/0042-207X(83)90591-2.
[221] S. Kattel, P.J. Ramírez, J.G. Chen, J.A. Rodriguez, P. Liu, Active sites for CO_{-2} hydrogenation to methanol on Cu/ZnO catalysts, Science 355 (2017) 1296–1299, https://doi.org/10.1126/science.aal3573.
[222] P. Schwiderowski, H. Ruland, M. Muhler, Current developments in CO_2 hydrogenation towards methanol: A review related to industrial application, Curr. Opin. Green. Sustain. Chem. 38 (2022) 100688, https://doi.org/10.1016/j.cogsc.2022.100688.
[223] X.-Y. Meng, C. Peng, J. Jia, P. Liu, Y.-L. Men, Y.-X. Pan, Recent progress and understanding on In_2O_3-based composite catalysts for boosting CO_2 hydrogenation, J. CO_2 Util. 55 (2022) 101844, https://doi.org/10.1016/j.jcou.2021.101844.
[224] Z. Shi, Q. Tan, D. Wu, Mixed-phase Indium oxide as a highly active and stable catalyst for the hydrogenation of CO_2 to CH_3OH, Ind. Eng. Chem. Res. 60 (2021) 3532–3542, https://doi.org/10.1021/acs.iecr.0c04688.
[225] C. Yang, C. Pei, R. Luo, S. Liu, Y. Wang, Z. Wang, Z.-J. Zhao, J. Gong, Strong electronic oxide–support interaction over In_2O_3/ZrO_2 for highly selective CO_2 hydrogenation to methanol, J. Am. Chem. Soc. 142 (2020) 19523–19531, https://doi.org/10.1021/jacs.0c07195.
[226] X. Jia, K. Sun, J. Wang, C. Shen, C.-j Liu, Selective hydrogenation of CO_2 to methanol over Ni/In_2O_3 catalyst, J. Energy Chem. 50 (2020) 409–415, https://doi.org/10.1016/j.jechem.2020.03.083.
[227] A. Pustovarenko, A. Dikhtiarenko, A. Bavykina, L. Gevers, A. Ramírez, A. Russkikh, S. Telalovic, A. Aguilar, J.-L. Hazemann, S. Ould-Chikh, J. Gascon, Metal–Organic Framework-derived synthesis of cobalt Indium catalysts for the hydrogenation of CO_2 to methanol, ACS Catal. 10 (2020) 5064–5076, https://doi.org/10.1021/acscatal.0c00449.
[228] J. Wang, G. Li, Z. Li, C. Tang, Z. Feng, H. An, H. Liu, T. Liu, C. Li, A highly selective and stable ZnO-ZrO_2 solid solution catalyst for CO_2 hydrogenation to methanol, Science Advances, 3 e1701290, ⟨https://doi.org/10.1126/sciadv.1701290⟩.
[229] Y. Wang, S. Kattel, W. Gao, K. Li, P. Liu, J.G. Chen, H. Wang, Exploring the ternary interactions in Cu–ZnO–ZrO_2 catalysts for efficient CO_2 hydrogenation to methanol, Nat. Commun. 10 (2019) 1166, https://doi.org/10.1038/s41467-019-09072-6.
[230] H. Chen, H. Cui, Y. Lv, P. Liu, F. Hao, W. Xiong, Ha Luo, CO_2 hydrogenation to methanol over Cu/ZnO/ZrO_2 catalysts: Effects of ZnO morphology and oxygen vacancy, Fuel 314 (2022) 123035, https://doi.org/10.1016/j.fuel.2021.123035.
[231] Z. Han, C. Tang, F. Sha, S. Tang, J. Wang, C. Li, CO_2 hydrogenation to methanol on ZnO-ZrO_2 solid solution catalysts with ordered mesoporous structure, J. Catal. 396 (2021) 242–250, https://doi.org/10.1016/j.jcat.2021.02.024.
[232] Y. Wang, W. Gao, K. Li, Y. Zheng, Z. Xie, W. Na, J.G. Chen, H. Wang, Strong evidence of the role of H_2O in affecting methanol selectivity from CO_2 hydrogenation over Cu-ZnO-ZrO_2, Chem 6 (2020) 419–430, https://doi.org/10.1016/j.chempr.2019.10.023.
[233] F.C.F. Marcos, L. Lin, L.E. Betancourt, S.D. Senanayake, J.A. Rodriguez, J. M. Assaf, R. Giudici, E.M. Assaf, Insights into the methanol synthesis mechanism via CO_2 hydrogenation over Cu-ZnO-ZrO_2 catalysts: Effects of surfactant/Cu-Zn-

Zr molar ratio, J. CO_2 Util. 41 (2020) 101215, https://doi.org/10.1016/j.jcou.2020.101215.
[234] X. Sun, Y. Jin, Z. Cheng, G. Lan, X. Wang, Y. Qiu, Y. Wang, H. Liu, Y. Li, Dual active sites over Cu-ZnO-ZrO_2 catalysts for carbon dioxide hydrogenation to methanol, J. Environ. Sci. 131 (2023) 162–172, https://doi.org/10.1016/j.jes.2022.10.002.
[235] C.D. Chang, W.H. Lang, Process for manufacturing olefins, Google Patents, 1977.
[236] C.D. Chang, C.T.W. Chu, R.F. Socha, Methanol conversion to olefins over ZSM-5: I. Effect of temperature and zeolite $SiO_2Al_2O_3$, J. Catal. 86 (1984) 289–296, https://doi.org/10.1016/0021-9517(84)90374-9.
[237] M. Guisnet, L. Costa, F.R. Ribeiro, Prevention of zeolite deactivation by coking, J. Mol. Catal. A: Chem. 305 (2009) 69–83, https://doi.org/10.1016/j.molcata.2008.11.012.
[238] P. Tian, Y. Wei, M. Ye, Z. Liu, Methanol to olefins (MTO): From fundamentals to commercialization, ACS Catal. 5 (2015) 1922–1938, https://doi.org/10.1021/acscatal.5b00007.
[239] S. Kvisle, T. Fuglerud, S. Kolboe, U. Olsbye, K.P. Lillerud, B.V. Vora, Methanol-to-Hydrocarbons, Handb. Heterog. Catal. (2008) 2950–2965, https://doi.org/10.1002/9783527610044.hetcat0149.
[240] M.R. Gogate, Methanol-to-olefins process technology: current status and future prospects, Pet. Sci. Technol. 37 (2019) 559–565, https://doi.org/10.1080/10916466.2018.1555589.
[241] A.J. Marchi, G.F. Froment, Catalytic conversion of methanol to light alkenes on SAPO molecular sieves, Appl. Catal. 71 (1991) 139–152, https://doi.org/10.1016/0166-9834(91)85011-J.
[242] L. Tan, P. Zhang, Y. Cui, Y. Suzuki, H. Li, L. Guo, G. Yang, N. Tsubaki, Direct CO_2 hydrogenation to light olefins by suppressing CO by-product formation, Fuel Process. Technol. 196 (2019) 106174, https://doi.org/10.1016/j.fuproc.2019.106174.
[243] M. Ghasemi, M. Mohammadi, M. Sedighi, Sustainable production of light olefins from greenhouse gas CO_2 over SAPO-34 supported modified cerium oxide, Microporous Mesoporous Mater. 297 (2020) 110029, https://doi.org/10.1016/j.micromeso.2020.110029.
[244] P. Wang, F. Zha, L. Yao, Y. Chang, Synthesis of light olefins from CO_2 hydrogenation over (CuO-ZnO)-kaolin/SAPO-34 molecular sieves, Appl. Clay Sci. 163 (2018) 249–256, https://doi.org/10.1016/j.clay.2018.06.038.
[245] X. Liu, M. Wang, H. Yin, J. Hu, K. Cheng, J. Kang, Q. Zhang, Y. Wang, Tandem catalysis for hydrogenation of CO and CO_2 to lower olefins with bifunctional catalysts composed of spinel oxide and SAPO-34, ACS Catal. 10 (2020) 8303–8314, https://doi.org/10.1021/acscatal.0c01579.
[246] J. Li, T. Yu, D. Miao, X. Pan, X. Bao, Carbon dioxide hydrogenation to light olefins over ZnO-Y_2O_3 and SAPO-34 bifunctional catalysts, Catal. Commun. 129 (2019) 105711, https://doi.org/10.1016/j.catcom.2019.105711.
[247] S. Dang, S. Li, C. Yang, X. Chen, X. Li, L. Zhong, P. Gao, Y. Sun, Selective transformation of CO_2 and H_2 into lower olefins over In_2O_3-$ZnZrO_x$/SAPO-34 bifunctional catalysts, ChemSusChem 12 (2019) 3582–3591, https://doi.org/10.1002/cssc.201900958.
[248] S. Wang, L. Zhang, W. Zhang, P. Wang, Z. Qin, W. Yan, M. Dong, J. Li, J. Wang, L. He, U. Olsbye, W. Fan, Selective conversion of CO_2 into propene and butene, Chem 6 (2020) 3344–3363, https://doi.org/10.1016/j.chempr.2020.09.025.
[249] W. Li, K. Wang, G. Zhan, J. Huang, Q. Li, Design and synthesis of bioinspired $ZnZrO_x$&Bio-ZSM-5 integrated nanocatalysts to boost CO_2 hydrogenation to light olefins, ACS Sustain. Chem. Eng. 9 (2021) 6446–6458, https://doi.org/10.1021/acssuschemeng.1c01384.
[250] A. Dokania, A. Dutta Chowdhury, A. Ramirez, S. Telalovic, E. Abou-Hamad, L. Gevers, J. Ruiz-Martinez, J. Gascon, Acidity modification of ZSM-5 for enhanced production of light olefins from CO_2, J. Catal. 381 (2020) 347–354, https://doi.org/10.1016/j.jcat.2019.11.015.
[251] W. Zhang, S. Wang, S. Guo, Z. Qin, M. Dong, J. Wang, W. Fan, Effective conversion of CO_2 into light olefins along with generation of low amounts of CO, J. Catal. 413 (2022) 923–933, https://doi.org/10.1016/j.jcat.2022.07.041.
[252] J. Wang, A. Zhang, X. Jiang, C. Song, X. Guo, Highly selective conversion of CO_2 to lower hydrocarbons (C_2-C_4) over bifunctional catalysts composed of In_2O_3-ZrO_2 and zeolite, J. CO_2 Util. 27 (2018) 81–88, https://doi.org/10.1016/j.jcou.2018.07.006.
[253] Y. Ni, Z. Chen, Y. Fu, Y. Liu, W. Zhu, Z. Liu, Selective conversion of CO_2 and H_2 into aromatics, Nat. Commun. 9 (2018) 3457, https://doi.org/10.1038/s41467-018-05880-4.
[254] W. Li, G. Zhan, X. Liu, Y. Yue, K.B. Tan, J. Wang, J. Huang, Q. Li, Assembly of ZnZrOx and ZSM-5 on hierarchically porous bio-derived SiO_2 platform as bifunctional catalysts for CO_2 hydrogenation to aromatics, Appl. Catal. B: Environ. 330 (2023) 122575, https://doi.org/10.1016/j.apcatb.2023.122575.
[255] S. Xing, S. Turner, D. Fu, S. van Vreeswijk, Y. Liu, J. Xiao, R. Oord, J. Sann, B. M. Weckhuysen, Silicalite-1 layer secures the bifunctional nature of a CO_2 hydrogenation catalyst, JACS Au 3 (2023) 1029–1038, https://doi.org/10.1021/jacsau.2c00621.
[256] K. Eguchi, T. Tokiai, H. Arai, High pressure catalytic hydration of olefins over various proton-exchanged zeolites, Appl. Catal. 34 (1987) 275–287, https://doi.org/10.1016/S0166-9834(00)82462-8.
[257] K. Weissermel, H.-J. Arpe, Industrial Organic Chemistry, John Wiley & Sons, 2008, https://doi.org/10.1002/9783527619191.
[258] G.J. Haining, Smith, Mark Royston, Turner, Malcolm John, Olefin hydration process EUROPEAN 1999. ⟨https://patentimages.storage.googleapis.com/34/d3/3c/ba604edcbaca74/EP0955284A1.pdf⟩.
[259] R.W. Cockman, Haining, Gordon John, Lusman, Philip, Melville, Archibald David, Olefin hydration process. EUROPEAN 1993.
[260] A. Isobe, Y. Yabuuchi, N. Iwasa, N. Takezawa, Gas-phase hydration of ethene over $Me(HPO_4)_2{\cdot}nH_2O$ (Me=Ge, Zr, Ti, and Sn), Appl. Catal. A: Gen. 194-195 (2000) 395–401, https://doi.org/10.1016/S0926-860X(99)00385-3.
[261] O. Kazuharu, I. Tokio, T. Kozo, Ethylene hydration over niobic acid catalysts, Chem. Lett. 13 (1984) 645–648, https://doi.org/10.1246/cl.1984.645.
[262] T. Kozo, I. Chijiko, M. Isao, I. Ichiro, H. Hideshi, Acidic property and catalytic activity of $TiO_2{\cdot}ZnO$, Bull. Chem. Soc. Jpn. 45 (1972) 47–51, https://doi.org/10.1246/bcsj.45.47.
[263] M. Iwamoto, M. Tajima, S. Kagawa, Gas-phase direct hydration of ethylene over proton-exchanged zeolite catalysts at atmospheric pressure, J. Catal. 101 (1986) 195–200, https://doi.org/10.1016/0021-9517(86)90243-5.
[264] O. Susumu, K. Masao, I. Tokio, T. Kozo, The effect of phosphoric acid treatment on the catalytic property of Niobic acid, Bull. Chem. Soc. Jpn. 60 (1987) 37–41, https://doi.org/10.1246/bcsj.60.37.
[265] F.P. Pruchnik, Organometallic Chemistry of the Transition Elements, Springer Science & Business Media,, 2013, https://doi.org/10.1007/978-1-4899-2076-8.
[266] N. Navidi, J.W. Thybaut, G.B. Marin, Experimental investigation of ethylene hydroformylation to propanal on Rh and Co based catalysts, Appl. Catal. A: Gen. 469 (2014) 357–366, https://doi.org/10.1016/j.apcata.2013.10.019.
[267] R. Franke, D. Selent, A. Börner, Applied hydroformylation, Chem. Rev. 112 (2012) 5675–5732, https://doi.org/10.1021/cr3001803.
[268] K. Jeske, T. Rösler, M. Belleflamme, T. Rodenas, N. Fischer, M. Claeys, W. Leitner, A.J. Vorholt, G. Prieto, Direct conversion of syngas to higher alcohols via tandem integration of Fischer–Tropsch synthesis and reductive hydroformylation, Angew. Chem. Int. Ed. 61 (2022) e202201004, https://doi.org/10.1002/anie.202201004.
[269] T.E. Kunene, P.B. Webb, D.J. Cole-Hamilton, Highly selective hydroformylation of long-chain alkenes in a supercritical fluid ionic liquid biphasic system, Green. Chem. 13 (2011) 1476–1481, https://doi.org/10.1039/C1GC15142H.
[270] O. Hemminger, A. Marteel, M.R. Mason, J.A. Davies, A.R. Tadd, M.A. Abraham, Hydroformylation of 1-hexene in supercritical carbon dioxide using a heterogeneous rhodium catalyst. 3. Evaluation of solvent effects, Green. Chem. 4 (2002) 507–512, https://doi.org/10.1039/B204822C.
[271] W. Zhou, D. He, A facile method for promoting activities of ordered mesoporous silica-anchored Rh–P complex catalysts in 1-octene hydroformylation, Green. Chem. 11 (2009) 1146–1154, https://doi.org/10.1039/B900591A.
[272] J.A. Bae, K.-C. Song, J.-K. Jeon, Y.S. Ko, Y.-K. Park, J.-H. Yim, Effect of pore structure of amine-functionalized mesoporous silica-supported rhodium catalysts on 1-octene hydroformylation, Microporous Mesoporous Mater. 123 (2009) 289–297, https://doi.org/10.1016/j.micromeso.2009.04.015.
[273] T. Wang, W. Wang, Y. Lyu, K. Xiong, C. Li, H. Zhang, Z. Zhan, Z. Jiang, Y. Ding, Porous Rh/BINAP polymers as efficient heterogeneous catalysts for asymmetric hydroformylation of styrene: Enhanced enantioselectivity realized by flexible chiral nanopockets, Chin. J. Catal. 38 (2017) 691–698, https://doi.org/10.1016/S1872-2067(17)62790-6.
[274] L. Yan, Y.J. Ding, L.W. Lin, H.J. Zhu, H.M. Yin, X.M. Li, Y. Lu, In situ formation of $HRh(CO)_2(PPh_3)_2$ active species on the surface of a SBA-15 supported heterogeneous catalyst and the effect of support pore size on the hydroformylation of propene, J. Mol. Catal. A: Chem. 300 (2009) 116–120, https://doi.org/10.1016/j.molcata.2008.10.050.
[275] C. Li, W. Wang, L. Yan, Y. Ding, A mini review on strategies for heterogenization of rhodium-based hydroformylation catalysts, Front. Chem. Sci. Eng. 12 (2018) 113–123, https://doi.org/10.1007/s11705-017-1672-9.
[276] M. Jiang, L. Yan, Y. Ding, Q. Sun, J. Liu, H. Zhu, R. Lin, F. Xiao, Z. Jiang, J. Liu, Ultrastable 3V-PPh_3 polymers supported single Rh sites for fixed-bed hydroformylation of olefins, J. Mol. Catal. A: Chem. 404-405 (2015) 211–217, https://doi.org/10.1016/j.molcata.2015.05.008.
[277] R.E. Brooks, Preparation of alcohols, Google Patents, 1951.
[278] E.L. John, A.L. Richard, S.M. Jay, W.V. Richard, Aldehyde hydrogenation catalyst and process, Google Patents, 1988.
[279] X. Wang, R.Y. Saleh, U.S. Ozkan, Reaction network of aldehyde hydrogenation over sulfided Ni–Mo/Al_2O_3 catalysts, J. Catal. 231 (2005) 20–32, https://doi.org/10.1016/j.jcat.2004.12.010.
[280] N. Yoneda, S. Kusano, M. Yasui, P. Pujado, S. Wilcher, Recent advances in processes and catalysts for the production of acetic acid, Appl. Catal. A: Gen. 221 (2001) 253–265, https://doi.org/10.1016/S0926-860X(01)00800-6.
[281] Z. Shen, Y. Zhang, F. Jin, From $NaHCO_3$ into formate and from isopropanol into acetone: Hydrogen-transfer reduction of $NaHCO_3$ with isopropanol in high-temperature water, Green. Chem. 13 (2011) 820–823, https://doi.org/10.1039/C0GC00627K.
[282] W. Ahmad, P. Koley, S. Dwivedi, R. Lakshman, Y.K. Shin, A.C.T. van Duin, A. Shrotri, A. Tanksale, Aqueous phase conversion of CO_2 into acetic acid over thermally transformed MIL-88B catalyst, Nat. Commun. 14 (2023) 2821, https://doi.org/10.1038/s41467-023-38506-5.
[283] T.V. Sagar, P. Kumar, B. Žener, A. Šuligoj, K. Kočí, U.L. Štangar, Effective production of formic and acetic acid via CO_2 hydrogenation with hydrazine by using ZrO_2 catalysts, Mol. Catal. 545 (2023) 113238, https://doi.org/10.1016/j.mcat.2023.113238.
[284] X. Liu, H. Zhong, C. Wang, D. He, F. Jin, CO_2 reduction into formic acid under hydrothermal conditions: a mini review, Energy Sci. Eng. 10 (2022) 1601–1613, https://doi.org/10.1002/ese3.1064.
[285] J. Wang, L. Zhang, F. Jin, X. Chen, Palladium nanoparticles on chitin-derived nitrogen-doped carbon materials for carbon dioxide hydrogenation into formic acid, RSC Adv. 12 (2022) 33859–33869, https://doi.org/10.1039/D2RA06462F.
[286] T. Yatabe, K. Kamitakahara, K. Higashijima, T. Ando, T. Matsumoto, K.-S. Yoon, T. Enomoto, S. Ogo, Synthesis of acetic acid from CO_2, CH_3I and H_2 using a water-

soluble electron storage catalyst, Chem. Commun. 57 (2021) 4772–4774, https://doi.org/10.1039/D1CC01611C.
[287] P. Duarah, D. Haldar, V.S.K. Yadav, M.K. Purkait, Progress in the electrochemical reduction of CO_2 to formic acid: a review on current trends and future prospects, J. Environ. Chem. Eng. 9 (2021) 106394, https://doi.org/10.1016/j.jece.2021.106394.
[288] K. Kamada, J. Jung, T. Wakabayashi, K. Sekizawa, S. Sato, T. Morikawa, S. Fukuzumi, S. Saito, Photocatalytic CO_2 reduction using a robust multifunctional iridium complex toward the selective formation of formic acid, J. Am. Chem. Soc. 142 (2020) 10261–10266, https://doi.org/10.1021/jacs.0c03097.
[289] K. Ding, Y. Le, G. Yao, Z. Ma, B. Jin, J. Wang, F. Jin, A rapid and efficient hydrothermal conversion of coconut husk into formic acid and acetic acid, Process Biochem. 68 (2018) 131–135, https://doi.org/10.1016/j.procbio.2018.02.021.
[290] X. Wang, Y. Yang, T. Wang, H. Zhong, J. Cheng, F. Jin, In Situ Formed Metal Oxide/Metal Interface Enhanced C–C Coupling in CO_2 Reduction into CH_3COOH over Hexagonal Closed-Packed Cobalt, ACS Sustain. Chem. Eng. 9 (2021) 1203–1212, https://doi.org/10.1021/acssuschemeng.0c06717.
[291] C. Tu, X. Nie, J.G. Chen, Insight into acetic acid synthesis from the reaction of CH_4 and CO_2, ACS Catal. 11 (2021) 3384–3401, https://doi.org/10.1021/acscatal.0c05492.
[292] W. Huang, K.C. Xie, J.P. Wang, Z.H. Gao, L.H. Yin, Q.M. Zhu, Possibility of direct conversion of CH_4 and CO_2 to high-value products, J. Catal. 201 (2001) 100–104, https://doi.org/10.1006/jcat.2001.3223.
[293] Y.-H. Ding, W. Huang, Y.-G. Wang, Direct synthesis of acetic acid from CH_4 and CO_2 by a step-wise route over Pd/SiO_2 and Rh/SiO_2 catalysts, Fuel Process. Technol. 88 (2007) 319–324, https://doi.org/10.1016/j.fuproc.2004.09.003.
[294] W. Huang, W.Z. Sun, F. Li, Efficient synthesis of ethanol and acetic acid from methane and carbon dioxide with a continuous, stepwise reactor, AIChE J. 56 (2010) 1279–1284, https://doi.org/10.1002/aic.12073.
[295] A.M. Rabie, M.A. Betiha, S.-E. Park, Direct synthesis of acetic acid by simultaneous co-activation of methane and CO_2 over Cu-exchanged ZSM-5 catalysts, Appl. Catal. B: Environ. 215 (2017) 50–59, https://doi.org/10.1016/j.apcatb.2017.05.053.
[296] R. Shavi, J. Ko, A. Cho, J.W. Han, J.G. Seo, Mechanistic insight into the quantitative synthesis of acetic acid by direct conversion of CH_4 and CO_2: An experimental and theoretical approach, Appl. Catal. B: Environ. 229 (2018) 237–248, https://doi.org/10.1016/j.apcatb.2018.01.058.
[297] G. Yao, F. Chen, H. Zhang, R. He, F. Jin, Hydrazine as a new and facile hydrogen source for hydrothermal reduction of CO_2 to formic acid. Advances in CO_2 Capture, Sequestration, and Conversion, American Chemical Society,, 2015, pp. 251–264, https://doi.org/10.1021/bk-2015-1194.ch010.
[298] M.I. Chinchilla, F.A. Mato, Á. Martín, M.D. Bermejo, Hydrothermal CO_2 reduction by glucose as reducing agent and metals and metal oxides as catalysts, Molecules 27 (2022) 1652. ⟨https://www.mdpi.com/1420-3049/27/5/1652⟩.
[299] L. Karam, C.N. Neumann, Heterogeneously catalyzed carboxylic acid hydrogenation to alcohols, ChemCatChem 14 (2022) e202200953, https://doi.org/10.1002/cctc.202200953.
[300] P.K. Rakshit, R.K. Voolapalli, S. Upadhyayula, Acetic acid hydrogenation to ethanol over supported Pt-Sn catalyst: Effect of Bronsted acidity on product selectivity, Mol. Catal. 448 (2018) 78–90, https://doi.org/10.1016/j.mcat.2018.01.030.
[301] G. Xu, J. Zhang, S. Wang, Y. Zhao, X. Ma, A well fabricated $PtSn/SiO_2$ catalyst with enhanced synergy between Pt and Sn for acetic acid hydrogenation to ethanol, RSC Adv. 6 (2016) 51005–51013, https://doi.org/10.1039/C6RA09199G.
[302] X. Dong, J. Tian, J. Lei, Y. Chen, Highly active and stable Cu-MnO/SBA-15 catalyst for hydrogenation of acetic acid to ethanol: Experimental and DFT studies, J. Environ. Chem. Eng. 10 (2022) 107517, https://doi.org/10.1016/j.jece.2022.107517.
[303] J. Du, P. Zhang, H. Liu, Electrochemical reduction of carbon dioxide to ethanol: an approach to transforming greenhouse gas to fuel source, Chem. – Asian J. 16 (2021) 588–603, https://doi.org/10.1002/asia.202001189.
[304] D. Li, C. Hao, H. Liu, R. Zhang, Y. Li, J. Guo, C.C. Vilancuo, J. Guo, Photocatalytic CO_2 conversion to ethanol: a concise review, Catalysts (2022), https://doi.org/10.3390/catal12121549.
[305] S. Wang, S. Yin, W. Guo, Y. Liu, L. Zhu, X. Wang, Influence of inlet gas composition on dimethyl ether carbonylation and the subsequent hydrogenation of methyl acetate in two-stage ethanol synthesis, N. J. Chem. 40 (2016) 6460–6466, https://doi.org/10.1039/C6NJ01109H.
[306] K. Cao, D. Fan, L. Li, B. Fan, L. Wang, D. Zhu, Q. Wang, P. Tian, Z. Liu, Insights into the pyridine-modified MOR zeolite catalysts for DME carbonylation, ACS Catal. 10 (2020) 3372–3380, https://doi.org/10.1021/acscatal.9b04890.
[307] Q. Wei, G. Yang, X. Gao, L. Tan, P. Ai, P. Zhang, P. Lu, Y. Yoneyama, N. Tsubaki, A facile ethanol fuel synthesis from dimethyl ether and syngas over tandem combination of Cu-doped HZSM35 with Cu-Zn-Al catalyst, Chem. Eng. J. 316 (2017) 832–841, https://doi.org/10.1016/j.cej.2017.02.019.
[308] P. Lu, Q. Chen, G. Yang, L. Tan, X. Feng, J. Yao, Y. Yoneyama, N. Tsubaki, Space-confined self-regulation mechanism from a capsule catalyst to realize an ethanol direct synthesis strategy, ACS Catal. 10 (2020) 1366–1374, https://doi.org/10.1021/acscatal.9b02891.
[309] C. Du, E. Hondo, L. Gapu Chizema, R. Hassan Ali, X. Chang, L. Dai, Q. Ma, P. Lu, N. Tsubaki, An efficient microcapsule catalyst for one-step ethanol synthesis from dimethyl ether and syngas, Fuel 283 (2021) 118971, https://doi.org/10.1016/j.fuel.2020.118971.
[310] X. Liu, F. Yuan, Y. Pan, S. Shi, N. Li, Z. Liu, Q. Liu, Direct synthesis of C_2-C_4 alcohols with methanol and CaC2 by tandem reactions, Chem. Eng. J. 475 (2023) 146250, https://doi.org/10.1016/j.cej.2023.146250.